FRACTURE CONDUCTIVITY OF A BAUXITE-PROPPED GEOTHERMAL SYSTEM

by

Trevor Ryan Stoddard

A thesis submitted to the faculty of
The University of Utah
in partial fulfillment of the requirements for the degree of

Master of Science

Department of Chemical Engineering

The University of Utah

December 2013

The University of Utah Graduate School

STATEMENT OF THESIS APPROVAL

The thesis of Trevor Ryan Stoddard

has been approved by the following supervisory committee members:

John McLennan	, Chair	**3/21/12** Date Approved
Joseph Moore	, Member	**3/21/12** Date Approved
Milind Deo	, Member	**3/21/12** Date Approved

and by **JoAnn Lighty** , Chair of

the Department of **Chemical Engineering**

and by David B. Kieda, Dean of The Graduate School.

ABSTRACT

Enhanced Geothermal Systems (EGS) are geothermal resources that are developed through hydraulic stimulation. Inadequate permeability and production from natural fractures and pores can be overcome via injection of cold water below fracturing pressure, by conventional hydraulic fracturing, or by some cyclic combination of these processes. At low injection rates or where thermal fracturing is being exploited, shearing of pre-existing weaknesses and potentially developing virgin fractures is envisioned to provide permeable, self-propped pathways. Alternatively, injection at pressures substantially above the minimum principal stress can also hydraulically connect, reopen, or create fractures and also possibly induce shearing (as known from microseismic monitoring). The heat from this artificially fractured reservoir is subsequently transferred to the injected fluid and extracted through a production well. Conventional steam turbines or a binary cycle power plants can be employed for electric generation.

The technical challenges in developing EGS reservoirs are substantial and include controlling fracture direction and morphology, establishing an adequate heat transfer surface area, and maintaining conductivity. The latter was the focal point of investigation. It is commonly assumed that that the induced fractures will fail by shear and be self-propping. If tensile fractures are generated, they need to be explicitly held open by proppant (and it needs to be ensured that the proppant is not produced back into the wellbore). The conductivity of bauxite-propped fractures over extended periods of time

and at elevated temperatures were measured in laboratory tests in order to assess the temporal and thermal dependency of conductivity in a typical surrogate fracture.

CONTENTS

ACKNOWLEDGEMENTS

I would like to thank Dr. John McLennan, Dr. Milind Deo, and Dr. Joseph Moore for their guidance and support over the past two years while I have been working on this project. I would also like to gratefully acknowledge the Department of Energy for funding the project "The Role of Geochemistry and Stress on Fracture Development and Proppant Behavior in EGS Reservoirs," grant DE-FG36-08GO18189. I must also thank my friends and colleagues from TerraTek, a Schlumberger Company for providing testing guidelines and helping with designing the pressure vessel that was fabricated – in particular Mr. Randy Nielson. I would also like to thank Kohle Hansen for helping with machine drawings.

My family is also due thanks for all their support while I have been working on this project, I wouldn't have been able to make it this far in my education without the love and support of my family. Also, I would like to thank my girlfriend, Kandace, for all her support in my studies. Also, I wouldn't have made it without the friends I have made in engineering during my college years.

CHAPTER 1

INTRODUCTION

1.1 EGS systems

Hydraulic fracturing has been the most efficient production technology in the oil and gas industry since it was first employed in 1947. It is a technology that is used in the recovery of oil, natural gas, or water from underground reservoirs. The process of hydraulic fracturing is used to stimulate areas in the reservoir of interest to increase production. Injection of a highly pressurized fracking fluid down the well induces or opens many channels in the reservoir rock. Fractures generated in hydraulic fracturing operations tend to open normal to the direction of the least principal stress and extend into the formation. At shallow depths, horizontal fractures may form but typical hydraulic fractures are oriented vertically. Independent of its specific orientation, hydraulic fractures will propagate perpendicular to the smallest principal stress unless in-situ discontinuities perturb this tendency.

In the process of hydraulic fracturing, certain materials such as sand, ceramics, or bauxite are pumped downhole in the fracturing fluid and are used as propping agents. This “proppant” is used to maintain fracture width downhole under in-situ stresses acting to close the created factures and enable and maintain production by preserving fracture conductivity. Fracture conductivity is the permeability of a downhole fracture multiplied by the corresponding width of the fracture. Fracture conductivity gives an indication as

to the ease with which fluid will flow through the fractures and can be recovered. Depending on depths and the associated in-situ stresses at those depths, sand is typically used under lower stress conditions whereas sintered bauxite is typically used when the far-field stresses acting to close the fracture are more extreme (greater depths and higher temperatures). High-strength sintered bauxite proppant was introduced to the petroleum industry in late 1976 (R.D. Atteberry et al., 1979).

Geothermal reservoir environments can be at depths in excess of 7000 ft and at temperatures greater than 200°C. Typical geothermal environments must be over 200°C in order to recover enough energy to be cost effective. At these elevated temperatures, sand is an insufficient proppant as it crushes at a lower stress and begins to dissolve at moderate temperatures. Maurer engineering (1981) found that 20/40 Ottowa sand retained 33% of the initial permeability at 350°F, with other sands losing approximately 85% of their permeability at this temperature and crushing at low stresses (2000-4500 psi). Knox et al. (1989) found that 77% of the mass of sand was dissolved at elevated temperature.

Sintered bauxite is a high-strength alumino-silicate formed by creating a fine alumino-silicate powder, creating small spherical pellets out of this powder, and then sintering of the pellets together to create larger pellets at high temperature. Typical sintered bauxite proppant ranges in composition from 85-90% Al_2O_3, 3-6% SiO_2, 4-7% Fe_2O_3 and 3-4% TiO_2 (Cobb et al., 1986). The higher alumina-to-silica ratio results in greater density of sintered bauxite particles than those of the intermediate strength ceramic proppants. There are two commercial processes that are typically used to manufacture alumino-silicate proppants. Both of the commercial processes involve

grinding the raw materials to a fine powder, forming spherical pellets from the powder, and final densification (sintering) of the pellets (Cobb et al., 1986). The two processes for pelletization that are typically used are a fluidized bed agglomeration technique (Lunghofer, 1984) and high speed rotary mixing (Fitzgibbon, 1984). Typically, the densification occurs in a rotary kiln at a sintering temperature of 1500°C. "The major crystalline phase after processing is Corundum (alpha-alumina) with minor amounts of mullite and glassy phase also present" (Cobb et al., 1986).

Conventional geothermal reservoirs are drilled into formations with sufficient temperature, permeability, and naturally occurring water. The connate water is extracted as pressurized hot water or steam and sent directly to a turbine to generate electricity or to a heat exchanger system in a binary power plant. Conventional geothermal wells are limited by downhole resources and the limiting amount of naturally occurring water as well as permeability therefore limit the quantity and duration that energy can be extracted from these conventional wells. A newer envisioned technology, enhanced geothermal systems (EGS), can create geothermal resources wherever temperatures can be obtained at reasonable drilling depths. EGS technologies enhance permeability and create production zones in hot and dry impermeable reservoirs. An injection well is drilled into the hot rock and high pressure water is injected to create tensile hydraulic fractures and to mobilize existing planes of weakness producing allegedly-self-propped shear fractures. Heat transferred from the rock to the water creates hot water that is extracted through a production well that is directionally drilled to intersect the created fracture system. The heated water is sent to a steam or binary power plant for electricity generation. After the energy from the hot water has been extracted at the surface, the now cooled water is

reinjected downhole in a nominally closed loop system. The best locations for these EGS reservoirs have been generally considered to be in deep igneous formations covered by multiple kilometers of insulating sediments. The literature review that follows will cover asperity-dominated fractures and will then move into proppant testing procedures. Asperity-dominated fractures are fractures whose conductivity is maintained by the asperities of displaced fracture faces propping off of one another and holding the fracture open. Conductivity can be asperity dominated even in fractures containing proppant. If the proppant begins to crush or is inadequately dispersed in the fracture, the conductivity will be asperity dominate. After proppant testing procedures are reviewed, data from a previous study on proppant use in geothermal developments conducted by Geothermal Republic, Inc. will be presented, followed by other more general literature describing proppant conductivity at elevated temperature and stress.

CHAPTER 2

LITERATURE REVIEW

2.1 Proppant Use in Geothermal Systems- Case Studies

There are few literature sources that describe proppant use in geothermal hydraulic fracturing operations. One of the first geothermal proppant case studies was reported in 1981, by Campbell et al. Campbell et al. (1981) described early work that occurred at geothermal wells at the Raft River site at Raft River, Idaho. The Raft River geothermal resource area is a naturally fractured, hard rock reservoir at a relatively low geothermal resource temperature (149°C). Two stimulations experiments were performed in late 1979- a conventional hydraulic fracturing treatment was completed in Well RRGP-5 and a "Kiel dendritic fracturing" technique was used in Well RRGP-4 (low proppant concentrations and flow back cycles are typical of Kiel fracturing). Dendritic fractures are caused by pulsing the formation with reverse flow to cause spalling and diversion of the fracture wings by in-situ stress modification (Campbell et al., 1981). Multiple pumping periods are used with each stage using low-viscosity fluid, sand slugs, and several flowback periods. RRGP-4 and RRGP-5 were selected due to their limited production and proximity to the Bridge and Narrows Faults. Due to the close proximity to these faults, it was determined that it was likely that high productive fractures existed near the wells.

Previous to stimulation, RRGP-4 was nonproductive; RRGP-5 was capable of flowing at 140 gallons per minute and up to 600 gallons per minute with a pump, though the produced fluid came from the upper portion of the completion interval so the produced fluid temperature of 107°C was undesirably low. A total of 59 meters of open hole were available in Well RRGP-4.

The technique employed was a four-stage dendritic fracture treatment. The main concern was that a single, planar fracture might only parallel and not intersect the principal natural fractures. The injection rates were relatively high and friction reduction was used with a low concentration hydroxypropyl guar carrying a relatively low concentration of proppant. 50,400 lb_m of 100-mesh sand was pumped for leak-off control in addition to 58,000 lb_m of 20/40 sand to prop the fractures. Sand was used as the propping agent due to the relatively low resource temperature.

The created fracture extended the full 59.4 meter height of the open interval and was oriented approximately east-west, parallel to the Narrows Fault (from televiewer information). After stimulation, a rate of 0.33 m^3/minute (60 gallons per minute) was sustained with a downhole fluid temperature of 132°C – five times the prestimulation rate (Campbell et al., 1981). Though the production had increased, it still remained below commercial values.

The produced fluid temperature is significantly higher than before the treatment - likely producing fluid from a deep zone not open previously. Type curve analysis suggested a fracture length of approximately 102 meters and transmissibility (kh) of 800 mD-feet.

Well RRGP-5 had a 65.8 meter barefoot section. It was similarly treated with proppant and sand- 1208 m^3 (7,600 barrels) of a relatively low viscosity HPG with 84,000 lb_m of 100-mesh sand and 347,000 lb_m of 20-40 mesh sand were pumped. Estimates of the late time transmissibility (k_h) were large, and determined to be greater than 100 Darcy-feet. Pressure-rate and televiewer analysis indicated that communication with the major natural fracture system had been successfully achieved (Campbell et al., 1981).

In summary, there was no noticeable increase in temperature from any of the water produced from the stimulated wells. Also, productivity indices only increased slightly from before the hydraulic fracturing treatment; neither well reached commercial levels after stimulation.

Also reported by Campbell et al. (1981) of the Geothermal Reservoir Well Stimulation Program were two stimulation experiments in East Mesa, California in 1980. Stimulation of Well 58-30 provided the first geothermal well fracture experiment at a moderate geothermal temperature (177°C). The two hydraulic stimulation treatments were a conventional hydraulic fracturing experiment in the deep, low-permeability zone and a "Kiel" dendritic fracture treatment in the shallow, high-permeability zone.

The East Mesa field in Imperial Valley, California, is a moderate temperature (160-177°C) reservoir producing from sandstone and siltstone. Well 58-30 was completed with a cemented and perforated liner. The first treatment was in a 76.2-meter thick, low-permeability, carbonate-cemented, sandstone interval. 2800 barrels of crosslinked fluid were pumped at 40 barrels per minute with 163,000 lb_m of sand to hydraulically fracture the interval.

Next, a Kiel fracture was pumped in a shallower and cooler zone predominantly composed of sand with a high porosity and permeability. The zone was however mud-damaged; a 300 foot (91.4 meters) interval was selected for dendritic fracturing in the same well. 10,300 barrels of linear polymer (HPG) were injected at 48 barrels per minute with 44,000 lb_m of 100-mesh sand (five stages).

From July 25 to August 2 in 1980, the well was production tested to evaluate the fracture experiment on the upper zone. The lower section of the well, from 1995.5 meters to TD, was sanded to prevent flow from the lower frac zone. The well flowed at an average of (135,000 lb_m) per hour. Reservoir pressure buildup data show the total open interval permeability-thickness was 9,881 md-ft. This is equivalent to a 2.5-fold increase in productivity within the upper frac zone. This analysis indicated that the shallow hydraulic stimulation treatment of the high permeability upper interval was very successful. The upper zone treatment to correct near wellbore damage is of particular importance because such mud and cement damage is typically a primary production impairment cause of impairment within Imperial Valley wells (Campbell et al., 1981).

Morris and Sinclair (1984) documented a hydraulic fracturing operation in New Mexico conducted by the Department of Energy's Geothermal Reservoir Well Stimulation Program in 1980. The well selected for hydraulic stimulation was Baca 20, located in north-central New Mexico in the Redondo Project area.

A nonproductive 240-ft [73-m] openhole interval at 4880-5120 feet in depth with a formation temperature of 271°C was selected and isolated for the job. Due to the elevated temperature of the reservoir, 16/20 and 12/20 sintered bauxite proppants were used in high concentrations. Transient pressure analysis methods yielded a reservoir

permeability-thickness value of about 3,000 md-ft, suggesting that this well may have been in a less productive area (Morris et al., 1984). The well produced approximately 110,000 lb_m/hr initially but declined to a final rate of roughly 50,000 lb_m/hr due to two-phase flow conditions in the formation (Morris et al., 1984). The low productivity was attributed to the relative permeability reduction associated with the two-phase flow effects in the formation.

More recent geothermal treatments where proppant has been pumped have been described by Huenges (Heunges, 2010) at Groβ Schönebeck. Groβ Schönebeck 3/90 was previously an exploratory gas well that was drilled in 1990. It was deepened in 2000 to a depth of 4294 meters to serve as an "in-situ geothermal laboratory".

Treatments were carried out in 2002 and 2003 (GrSk3/90) and in 2007 (GrSk4/05), targeting the Rotliegendes Formation in northeastern Germany. In GrSk3/90, the target formations were high-permeability sedimentary formations and the treatments were in openhole. The treatment intervals of GrSk3/90 were located at depths of 4130-4190 meters and 4078-4118 meters, and at temperatures of about 140°C. More than 11 tonnes of proppants (20/40 high-strength ceramic proppant and sand) and 200 m^3 of frac fluid (crosslinked gel or slickwater) were injected into the formation.

Interpretation of the transient production periods within the GrSk3/90 well indicated a significant increase in productivity, approximately by a factor of 1.8 (Legarth et al., 2003). The authors found that the transmissibility of the production zones remained relatively unchanged, indicating that the increase in productivity was a result of skin reduction, (as described by Cinco et al., 1977), caused by artificial fractures rather than high-permeability zones being connected to the wellbore. Two explanations posed

by the authors with regard to the low and unchanging transmissibilities is that a frac was created without properly connecting the productive zones to the well (Tischner et al., 2002) and that the conductivity may have declined as a consequence of proppant crushing, embedment, and proppant flow-back (Legarth et al., 2003). Modelling of the system indicated an approximate monolayer of proppant in the fractures, which increases the proppant crushing and embedment. Legarth also notes that proppant flow-back also occurred during the production tests. Proppant volume was further diminished and the concentration of proppant in the vicinity of the well-bore was also decreased, leading to a loss in expected conductivity (Legarth et al., 2003). Also it was found that non-Darcy flow effects deteriorated the effective well productivity by reducing the effective fracture conductivity through the proppant pack (Legarth et al., 2005).

2.2 Asperity Dominated Fractures

In 1994, Moore et al. measured the reduction of permeability associated with hydrothermal conditions in granite fractures at elevated temperatures. Fractured Westerly Granite cylinders were tested at 150 MPa confining pressure and 100 MPa pore pressure and 2.0 MPa differential pore pressure across the samples. The core samples were tested in increments of 50°C from 300°C to 500°C. Moore et al. (1994) found that at 300°C, the permeability in the fracture was reduced from 166×10^{-21} m^2 to 56×10^{-21} m^2 and the reduction in permeability only increased with increasing temperature, as the fracture permeability at 500°C was reduced from 330 to $19.4 \times 10^{-21} m^2$. They attributed the extreme loss of permeability to dissolution of the asperities and filling of the pores and fracture with dissolved materials. Although the temperatures are substantial, they are

encountered in-situ, indicating that concepts of self-propping because of asperities (roughness) keeping a fracture open should be carefully considered.

Yasuhara et al. (2006) also looked at the evolution of fracture permeability through fluid-rock reactions under hydrothermal conditions. Systems under hydrothermal conditions are pressurized by the vapor pressure of water at the given temperature. The difference in pressure across the samples is maintained using back pressure regulators to ensure flow. The sample evaluated was a cylinder of Arkansas novaculite, which is more than 99.5% quartz, which was 50 mm diameter by 89.5 mm in length. Testing was conducted at a net effective stress of 200 psi (250 psi confining stress and 50 psi pore pressure) at ambient and elevated temperatures. The overall experiment conducted by Yasuhara et al. comprised two stages; "the first over 1494 hours at constant temperature (20°C) but varying flow rate (1-0.125 mL/min and a reversed flow of 0.125 mL/min), and the second over 1656 hours at fixed flow-rate (in two sequential stages 0.0625 and 0.125 mL/min) but with stepped temperatures (20, 40, 80, 120°C)" (Yasuhara et al., 2006, p. 189). During the first stage, the fracture aperture was measured continuously. During the second stage, 120 fluid samples were collected at the outlet to monitor silicon concentration in the flow through fluid at various temperatures.

Yasuhara et al. found that the hydraulic aperture decreased monotonically from 18.5 to 10.3 μm during the first 860 hours of the test, with a reduction in the flow rates from 1 to 0.25 mL/min. After a 72-hour shutdown, flow was resumed at a rate of 0.25 mL/min and the aperture increased slightly to 10.6 μm, followed by a consistent reduction in aperture. After the flow direction was reversed at 1292 hours, the aperture reduced to 7.5μm during 1292-1494 hours (Yasuhara et al., 2006). This amounts to a

60% reduction in fracture aperture after 1500 hours of testing and can be attributed to mass removal from bridging asperities. Si concentrations in the effluent fluid were much lower than equilibrium conditions at all temperatures due to their short residence time in the fracture. Si concentrations under these conditions showed an Arrhenius-type dependence. "Concentrations measured at 20°C were in the range 0.13 to 1.20 ppm with a mean of 0.76 ppm, and showed slight fluctuations. Si concentration values at 40, 80, and 120°C were 1.30, 2.96, and 8.10 ppm, respectively" (Yasuhara et al., 2006, p. 191).

Using a standard fracture conductivity measurement cell, Fredd et al. (2000) studied conductivity at various proppant concentrations, including unpropped fractures and aligned versus displaced fracture faces (simulating shearing). The conductivity was measured after 18 to 22 hours of flowback at effective closure stresses ranging from 1,000 to 7,000 psi. The first two cases that were assessed were unpropped fractures at 250°F; the first with the faces aligned and the second where the faces were shifted slightly and the fracture was initially propped open by asperities overriding one another.

In the first case, the fracture conductivity at 1000 psi was 7.8 md-ft. Fracture conductivity dropped to 0.11 md-ft at 3,000 psi which strongly indicates that hydraulic fractures do not provide significant conductivity when the fracture faces are aligned.

In the second case, the conductivity varied from as high as 1,200 md-ft at 1,000 psi to values as low as 0.5 md-ft at 7,000 psi. Not surprisingly, at an effective closure stress of 7,000 psi, the asperities were crushed by approximately 0.01 inches or about 9% of their original average value of 0.1 in. In the absence of proppants, the conductivity varied by about two orders of magnitude (Fredd et al., 2000); at a confining pressure of 2,000 psi, the displaced fracture faces had conductivity values between 10 md-ft and 100

md-ft. The conductivity was as much as four orders of magnitude lower than the cases studied with 0.1 lbm/ft^2 proppant (Fredd et al., 2000). From these articles, it is apparent that crushing of asperities at high overburden stress is capable of closing the fracture and dissolution of propping asperities at elevated temperature will degrade fracture conductivity through dissolution of fractures asperities and precipitation in the fracture pore spaces. Inadequate fracture conductivity of self-propped fractures at geothermal conditions prompts considering proppant that can perform at high stress and temperature conditions and maintain fracture permeability.

2.3 Proppant Testing Procedures

The conductivity of a fracture is calculated by multiplying the fracture width by the fracture permeability. In 1989, the America Petroleum Institute (API) standardized procedures for measuring the conductivity of proppant in the laboratory using what is colloquially known as a Cooke conductivity cell (API RP-61, 1989). The Cooke conductivity cell consists of two metal plates between which proppant is placed and held under applied normal stress. Single phase brine is typically flowed at room temperature through the proppant pack (generally only applied for 15-30 minutes prior to testing) at rates of 1-10 mL/min - rates low enough to ensure Darcy flow (Cooke, 1973). The proppant is typically loaded to a concentration of 2 lb/ft^2 between the metal plates and tested for "short" periods of time (Palisch, 2007). RP-61 was created to provide a means to compare the performance of proppants in a way that was reasonable and repeatable within all proppant experiments (Palisch, 2007). In 1989, a proppant industry consortium recommended that minor changes to the API test could result in substantial improvements in testing accuracy. In the modified RP-61, it was decided that the steel

pistons would be replaced with Ohio sandstone; the testing temperature range was increased to 150-250°F, and some protocols mandated maintaining the stress constant for at least 50 hours. Using Ohio sandstone wafers ensures that proppant embedment is accounted for. The increase in temperature and length of time the proppant is maintained under stress is intended to capture any stress-intensified corrosion of the proppant which is expedited under increased temperature. Also, the 2% KCl brine water used in standard flow-through tests is fully saturated with silica to avoid leaching silica from the surface of the sandstone wafers. Duenckel et al. (2011) observed that:

> generally the formation waters that are in contact with the proppant have been present within the formation for millions of years and therefore are fully saturated with alumina and silica. When water is injected into the formation this is not the case as the water injected is typically not saturated with minerals of the like which will have a drastic impact on the proppant as etching may occur. RP-61 comes with a disclaimer that the testing procedures presented within the publication are not meant to give absolute down hole proppant conductivity measurements and that time, elevated temperature, fracturing fluid residues, embedment, and formation fines may ultimately reduce proppant pack conductivity by up to 90% ormore. (API RP-61, 1989)

Changes to RP-61 to account for elevated temperature and more realistic downhole conditions (though increased stress and temperature over longer periods of time) have had the effect of reducing the measured conductivity by as much as 85% depending on the quality of the proppant and the testing conditions (Palisch, 2007). The International Organization for Standardization has adopted this "long-term conductivity test" as its standard for proppant testing, as prescribed in ISO 13503-5 (ISO, 2006). While the modified API tests are a good indicator of how proppant behaves under laminar flow conditions, it drastically overestimates the conductivity of proppant when it is placed in actual fractures. Laboratory conductivity measurements do not account for effects such as non-Darcy flow, multiphase flow, fines migration, proppant crushing,

proppant flowback, proppant crushing and reservoir spalling, or proppant diagenesis. The first tests on proppant to be applied in a geothermal setting were conducted in 1979 by Republic Geothermal, Inc.

2.4 Republic Geothermal Studies

In 1979, Republic Geothermal, Inc. executed four experimental fracture stimulation treatments under the Department of Energy (DOE) funded Geothermal Reservoir Well Stimulation Program (GRWSP), DOE contract W-7404-ENG. 36. Maurer Engineering was the company hired to do the proppant testing portion under the Republic Geothermal DOE grant. In 1981, Maurer Engineering published a full report on their findings for proppants under geothermal conditions. Maurer Engineering tested various proppant types between hydraulic metal plates at temperatures of 350°F and 500°F and closure stress ranging from 2700 to 9700 psi and 2200 to 9200 psi, respectively, at these temperatures. It was concluded that sand does not hold up well under elevated stress or even moderate stresses under temperature and is not a viable option for propping geothermal systems. McDaniel found 50% reduction in conductivity at 250°F. Maurer Engineering found crushing of sand at elevated temperatures to occur at 2000 or 3000 psi. Resin-coated sand can withstand the elevated temperatures and maintain conductivity but still crushes at relatively low stresses (Maurer Enginering, 1981).

Premium proppants showed substantially less conductivity degradation. For example, based on short-term, 350°F tests of 20/40 sintered bauxite, there was an 82.5% permeability retention under 5000 psi closure stress. At 500°F, there was 90% retention of permeability. For the sintered bauxite tested, Maurer Engineering found that temperature sensitivity could not be proven; there was some loss of permeability due to

loose particle repacking and slight crushing of the proppant (Maurer Engineering, 1981). The study also justified the use of sintered bauxite in geothermal application if the economical considerations can justifity its high cost per pound (Maurer Engineering, 1981). Other testing has been done on various proppants at elevated temperature and stress for oil and gas well considerations; those findings can be extended to geothermal scenarios. These papers will be presented in the next section. Since sand can be considered to be a poor proppant at elevated temperature and stress, only data for ceramic proppants and sintered bauxite are presented in the following section.

2.5 Proppant Testing at Elevated Temperature and Stress

Cooke (1973) was the first to address the effect of environment (both the fluid present and the temperature) on the conductivity of a brittle proppant under stress, and the effect of the flow rate and non-Darcy flow resistance of proppants. To assess these variables Cooke placed 0.5-inch wide 10/20 sand proppant packs in a heated hydraulic press and flowed 250°F brine through the packs, both continuously and intermittently. After 10 days of flow through the sand packs, Cooke found a permeability reduction of nearly 30%. Cooke concluded that non-Darcy flow had a drastic impact on lowering the permeability of the proppant pack. Cooke's primary recommendation was that the industry needs sufficient proppants to maintain higher pemeabilities so as to diminish the pressure gradient associated with non-Darcy flow. All future proppant testing at elevated temperature and stress has been based on the experiments by Cooke in 1973.

The majority of factors that have hindered most experimenters since Cooke's work were reported by McDaniel in 1986 to which he also offered some solutions (McDaniel, 1987). McDaniel studied the effects of extended time at different test

conditions; variation between ambient and elevated temperature testing; and effects of brine flow at high temperature and closure stress. Experiments were conducted in both a linear testing cell and a radial testing cell (for comparison). McDaniel found that all loss of conductivity due to temperature increase was permanent and could not be recovered during test cool-down. During the extended time experiments at 275°F, 20/40 high strength bauxite proppant fracture conductivity decreased by 20% after 1 day and decreased by 30% after 300 hours. At 8000 psi simulated closure stress the temperature was increased from 75°F to 275°F the conductivity dropped by 25% from 4.95 to 3.73 D-ft. After these baseline measurements, brine at 275°F was flowed through a proppant pack of high strength bauxite proppant for 10 to 14 days and conductivity decreased by 46%, from 4.95 D-ft to 2.7 D-ft.

McDaniel made the claim that the early proppant experiments during the 1980s that found between 90 and 99% conductivity losses for many of the manufactured proppants were believed to have been due to faulty procedural errors (McDaniel, 1986). McDaniel claimed that the early experiments in the 1980s did not presaturate the testing brine with silica and minimize oxygen content. Oxygen in the brine could have led to multiple phases in the fractures and reduced the conductivity significantly and leeching of the sandstone surface of the brine would have generated fines in the frature, leading to non-Darcy flow and diminished conductivity. To comprehend the effect of silica saturation McDaniel obtained results for both silica saturated and unsaturated fluids. There was a substantial difference in retained fluid conductivity for intermediate strength bauxite proppant -75% conductivity was retained with presaturated fluid compared to 48% conductivity retained in the unsaturated case after 150 hours of testing.

In 1987, McDaniel noticed a lack of proppant conductivity data at elevated temperatures and stresses. To create a data base of realistic fracture conductivity as a function of temperature, he compiled over one hundred tests where the stress was varied and held at values between 2,000 psi and 13,000 psi for extended times and for simulated formation temperatures between 70°F and 325°F.

McDaniel observed that when a proppant is held at a particular closure stress and temperature for a significant amount of time, stress corrosion weakens the grains and increases the degree of proppant crushing. The chemical composition, crystal structure, and the presence of surface flaws were identified as the primary factors controlling the degree of additional crushing that results from stress-intensified corrosion at a given closure stress and temperature.

McDaniel's work also demonstrated that averaged conductivity values for high strength and ceramic 20/40 proppants (all at 20/40 mesh) at 4,000 psi confining stress showed a decrease by approximately 20% with a temperature increase from 150°F to 325°F. At a confining stress of 8,000 psi, the conductivity dropped an additional 25%. McDaniel also pointed out that the "effect of using realistic conductivity data in fracturing design is that, given the same design criteria, higher proppant concentrations are necessary than would be predicted if short-time conductivity data were used in the design simulation" (McDaniel, 1987, p. 4).

In addition to McDaniel's compilation of dozens of tests at elevated temperatures and normal stresses, other researchers also carried out testing under extreme conditions. Hahn (1986) showed that two ceramic proppants subjected to a normal stress of 8500 psi lost between 20% and 50% of their flow capacity over 50 days. Montgomery (1984)

showed that two high strength bauxite packs between steel plates at 5,000 psi lost approximately 50% of their flow capacity over 9 months. Hahn and Montgomery used testing fluids that were not presaturated with silica. Cobb (1986) wanted to isolate the contribution associated with stress corrosion and designed a test to eliminate all other failure mechanisms. Cobb isolated the proppant in a deformable Teflon tube and placed it in a pressure vessel at 10,000 psi and 93°C. This isolated the proppant from the steel plates and assessed stress corrosion in the middle of the proppant pack. Over 70 days of testing at these conditions, conductivity of high strength ceramic proppants reduced by 20%. Cobb (1986) concluded that the ceramic proppant tested did not show large enough declines in performance over time to account for the large discrepancies that had been found before in laboratory and field measurements (Cobb et al., 1986).

In 1989, Whitney argued that generation of fines and lack of edge effects due to proppant embedment significantly reduces the fracture flow capacity of the fracture in comparison to published data (Whitney, 1989). Whitney's experimental results showed that the conductivity for a sintered bauxite proppant at 2000 psi confining stress at 200°F (93°C) was reduced from 7000 md-ft to 3000 md-ft. In the same year, Knox et al. found that high-strength, alumina-based proppants were not stable under the test conditions of 1200 psi, and at a fluid temperature of 550°F and a pH of 11. The tested proppants lost 37-60% of their weight in three days. Severe permeability damage to the pack was observed that was attributed to large amount of fines generated (Knox et al., 1989). Fines generation was one of the first proposed hypotheses in fracture conductivity decline over time and at elevated temperature; since 1989, several other mechanisms have been found that can also drastically decrease in-situ proppant pack permeability.

Barree et al. (2003), Palisch et al. (2007), and Vincent (2009) affirmed that the cumulative effects of damage factors such as non-Darcy flow, multiphase flow, fines migration, proppant crushing, proppant flowback, proppant crushing and reservoir spalling, or proppant diagenesis can reduce effective flow capacity by 95% to 99.9% below values measured in API proppant conductivity reference tests. These damaging factors will be described below, beginning with non-Darcy flow.

Darcy's law predicts a linear relation between pressure gradient and flow rate. At higher flow rates, a deviation from this linear relationship is observed and a second-order term is used to account for the nonlinearity; the second term depends on a tortuosity constant and superficial velocity to the second power. This term reflects inertial losses and accounts for non-Darcy pressure drops across the system. As proppant grains are crushed or the formation spalls and decreases the porosity of the pack with fines intrusion, the probability for non-Darcy flow increases (more tortuous). Non-Darcy flow is seen when the pack is not adequately wide, the porosity is low, and velocity is substantial; this can be the case in an actual reservoir as fines are generated or the proppant was not dispersed well enough in the fractures. A typical fracture will likely have a much lower proppant concentration—more often on the order of 1 lb/ft^2 (Palisch et al., 2007). A 50% reduction fracture width reduction has the potential to nearly double the superficial velocity in the fracture, generating a large non-Darcy pressure drop through the proppant pack particularly for gas flow. Barree et al. (2003), Palisch et al. (2007), and Vincent (2009) found that non-Darcy effects can effectively reduce conductivity by 25-60%.

When there is insufficient pressure or when there are high levels of dissolved oxygen in the fluid in contact with the proppant, multiphase flow in the fracture becomes a concern. Palisch et al. (2007) claims that when both liquid and gas phases are mobile within a fracture, the pressure losses within that fracture may increase by at least an order of magnitude (Palisch et al., 2007). It has been determined in the field that at least three phenomena contribute to multiphase pressure drops. The first is alteration of fluid saturation. This first phenomena occurs when as the saturation of one phase (i.e., liquid) increases, it reduces the flow area available to the other phase (gas). As an example, if 20% of the pore volume is occupied by water, then the flowing gas has only 70% of its original flow area available. The second factor is relative permeability changes. It is well known that as the saturation of one phase (i.e., liquid) increases, the permeability relative to the other phase (i.e., gas) decreases. The third phenomena is typically the most significant - phase interaction between the fluids. Phase interaction means that as two phases move through a porous media at drastically different velocities (due to mobility differences), they begin to interfere with the flow paths of one another. Phase interation is particularly evident in gas-liquid flow (Palisch et al., 2007). Barree et al. (2003), Palisch et al. (2007), and Vincent (2009) found that multiphase flow can reduce effective conductivity by as much as 60-70%.

During fracturing or during production, flow through a proppant pack can vary. Wells may be shut in and brought back on line frequently, cycling the effective stress acting on the proppant. Laboratory testing has shown that the cycling of proppant in a conductivity cell will damage the conductivity (Palisch et al., 2007). These authors demonstrated that cycling sand and ceramic proppant from 4000 to 8000 psi net effective

stress 25 times caused a 25% reduction in conductivity for ceramic proppant and 35% reduction in conductivity for the resin-coated sand. The bulk of the conductivity losses were seen in the first cycle.

Palisch looked at an extensive well testing program in the Wamsutter field, and found that even in a tight gas reservoir, the hydraulic conductivities are finite and indicated over 99% reduction from lab measurements (Palisch et al., 2007). Palisch et al. (2007) indicated as much as 98% cumulative conductivity loss from the three phenomena as described above. Similarly, Barree et al. (2003) forecasted as much as a 97% reduction in conductivity from cumulative permeability diminishing effects.

Recently, diagenesis has been studied as another permeability damaging effect in proppant packs. Diagenesis is the dissolution of proppant mass and mass transfer to highly concentrated areas between grains where the mass reprecipitates. Yasuhara et al. (2003) was the first to consider diagenetic alteration of proppants. One view is that "Diagenesis refers to a dissolution and reprecipitation process that may reduce the porosity, permeability, and strength of the proppant pack as precipitants are deposited" (Duenckel et al., 2011, p. 1). Diagenesis acts according to LeChatelier's principle much like galvanic corrosion. Le Chatelier's principle states that if stress is applied to a system in equilibrium, the system will respond to lower that stress to reach a new equilibrium. Stresses that may be applied to a system in equilibrium can be pressure, temperature, and/or species concentrations.

> Very high stress exists at the contact points of the granular material, and the effective solubility of the quartz is increased, resulting in a higher silica concentration in the inter-grain region. As the silica from this region diffuses to the pore space where there is no mechanical stress, the solution becomes supersaturated and precipitates silica. This process acts like a material pump, moving material from high-stress regions to low-stress

> regions. This mechanism is often called pressure solution. (Weaver et al., 2009, p. 3)

In the case of mixed metal oxide proppants (such as sintered bauxite), all of the same forces of pressure solution are acting on the sintered bauxite pellets to increase the solubility of the aluminum and other various metal ions. The contact area between sintered bauxite pellets becomes super saturated with metal ions and silica from the formation to form aluminosilicates. Typically during manufacture, the sintering process will expose reactive surface. Any proppant crushing in the fracture can also create/expose additional highly reactive sites on the assumed unreactive surfaces of sintered bauxite proppants.

Yashuara et al. (2003) reported that at an effective stress of 5,000 psi with temperatures in the range 170-570°F the rates of porosity reduction and ultimate magnitudes of porosity reduction increase with increased temperature. Effective porosity was diminished between 15% (570°F) to 25% (170°F) of the original porosity after completion of the dissolution-mediated compaction observed in these experiments (Yashuara et al., 2003). These findings indicate that for reservoirs near 390°F and 7,000 psi (typical of a good geothermal well), only 17% of the initial pack porosity (for quartz proppant in a silica-based fracture) would be expected after a mere 10 days postfracturing (Weaver et al., 2006). Weaver et al. (2006) reported static test results from frac sand and ceramic proppant held at 250°F and 10,000 psi closure stress between Ohio sand cores in 2% KCL. Crystal growth was observed in both cases. No such growth was documented on proppant samples coated with nonhardening resin, possibly showing that the hydrophobic resin surface can slow diagenetic reactions.

Later, in 2009, Weaver et al. placed coarse-ground formation material in closed 3 in. diameter vessels with deionized water in an oven at 500°F. The vessels were left in the oven for 1 to 12 months to observe the effect of diagenesis on the proppant particles. "Evidence of diagenetic reactions were observed at all temperatures at high stress, but these reactions appear to be dramatically accelerated as temperature was increased. Frequently loss of more than half of the initial permeability of the pack was observed" (Weaver et al., 2009, p. 4). Crystalline precipitates were observed on all the proppants tested. Weaver saw almost a 70% reduction in permeability from one of the bauxite proppants with extensive diagenetic reactions. In addition to the static tests, Weaver performed conductivity and strength testing on the proppant grains that had undergone diagenetic reactions. After 9 days of testing, flowing at 1-2 mL/min at 550°F, the Weibull probability plot for the bauxite proppant showed a strength decrease from an average of 310 MPa to 180 MPa.

Dueneckel et al. (2011) criticized Weaver's results, claiming that the posttest conductivities were compared to the reported API baseline conductivities of differing bauxites, which makes it impossible to tell if the effects were attributed to lower quality bauxites, particle weakening, presence of crystalline deposits, or less desirable packing arrangements that were achieved through the use of previously used samples that could have contributed to loss of flow capacity compared to the original published expectations (Duenckel et al., 2011).

Factors that contribute to diagenesis include closure stress, reservoir temperature, proppant type, and mineralogy of the rock formation (Duenckel et al., 2011). Duenckel et al. (2011) demonstrated that crystalline precipitates can be formed on the surface of all

proppant types- including ceramic, sand, resin-coated materials, and even inert steel balls or glass rods when subject to the appropriate conditions. Duenckel classified the precipitates as zeolites, and concluded that "there is not yet evidence that zeolite precipitation poses significant concern in actual propped fractures, or that chemical treatment of the proppant surface is justified or effective at mitigating zeolite precipitation" (Duenckel et al., 2011, p. 1).

Duenckel et al. (2011) conducted additional static diagenetic testing to determine the effects of zeolite precipitation on performance. He used vessels that were 29 cm in length with an internal diameter of 4.6 cm and a volume of 450 mL, filled with approximately 400 mL of proppant (including glass rods and inert materials) and crushed formation and the remainder with deionized water was sealed in an oven at 400°F from 7 to 154 days.

Duenckel et al. (2011) found that:

- After 14 days of exposure to Pinedale shale, diagenetic material formed extensively on all types of proppant samples (including inert steel balls and glass rods) tested.
- On the Steamboat Mountain cores, some diagenesis was present after 14-21 days on the 20/40 light weight ceramic (LWC) and resin-coated sand (RCS), but no precipitates were observed in any of the high-strength ceramic tests.
- Testing done with the Haynesville/Bossier shales showed no precipitation after 14 days. Moderate to extensive diagenetic materials were observed 42 to 154 days later, even on the stainless steel balls and glass rods. The diagenetic material heavily coated these proppants after 154 days.

In all of Duenckel's static testing, in no case did a diagenetic precipitant form when shale was not present in the cell (Duenckel et al., 2011). Further, "To date, the authors are unaware of any proppant samples that have been recovered from actual wells with evidence of zeolite precipitation" (Duenckel et al, 2011, p. 23). Duenckel concludes with "It does not appear that diagenesis involving zeolite precipitation is a primary concern in most reservoirs" (Duenckel et al., 2011, p. 25).

2.6 Varying Concentration and Displaced Fracture Faces

One aspect of fracture conductivity that has been understudied relates to the specific morphology of the surfaces of the rock in contact with the proppant. One of the few studies considering this was published by Fredd et al. in 2000. They used a standard fracture conductivity measurement cell and measured conductivity at various proppant concentrations and discerned the differences between precisely aligned and displaced fracture faces. 20/40 sintered bauxite and Jordan sand were evaluated at 250°F at concentrations of 0, 0.1, or 1.0 lb_m/ft^2. Conductivity was measured after 18 to 22 hours of flowback at effective closure pressures ranging from 1,000 to 7,000 psi. They describe four cases:

- Case 1: Aligned fracture faces, no proppant
- Case 2: Displaced fracture faces, no proppant
- Case 3: Aligned fracture faces, 0.1 lbm/ft^2 proppant
- Case 4: Displaced fracture faces, 0.1 lbm/ft^2 proppant.

The results of these four cases were then compared with data for conventional proppant fracturing treatments with 1.0 lbm/ft^2 proppant. The results were as follows:

- Case 1: Aligned fracture faces, no proppant: The conductivity at

1000 psi was 7.8 md-ft and it fell to 0.11 md-ft at 3,000 psi, suggesting that hydraulic fractures may not provide significant conductivity when the fracture faces are aligned.

- Case 2: Displaced fracture faces, no proppant: The conductivity varied from as high as 1,200 md-ft at 1,000 psi to as low as 0.5 md-ft at 7,000 psi. "At a normal stress of 7,000 psi asperities were apparently crushed by approximately 0.01 in., or about 9% of their original average value of 0.1 in." (Fredd et al., 2000, p. 4). At a confining pressure of 2,000 psi, the displaced fracture faces had conductivity values between 10 md-ft and 100 md-ft. "Furthermore the conductivity was as much as four orders of magnitude lower than the cases studied with 0.1 lbm/ft^2 proppant" (Fredd et al., 2000, p. 6).

- Case 3: Aligned fracture faces, 0.1 lbm/ft^2 proppant: The sintered bauxite had conductivity values of approximately 1,000 md-ft up to a normal stress of approximately 5,000 psi, beyond which it decreased as the proppant began to crush. At 7,000 psi, approximately 35% of the proppant had been crushed to smaller than 300 μm from the original size of 20/40 mesh. It was found that low-strength proppant will not provide significant conductivity above about 2,000 psi, whereas low concentrations of high-strength proppant will provide significant conductivity up to at least 5,000 psi. Since this behavior depends on how completely the fracture surface is covered in proppant, these trends may not be representative. Conductivity was compared between hydraulically fractured and flat, parallel cores (cores that were saw cut with the faces aligned) and it was found that both were consistent with one another, showing that conductivity is not a strong function of surface roughness if the fracture faces are aligned.

- Case 4: Displaced fracture faces, 0.1 lbm/ft^2 proppant: It was found that the sintered bauxite had conductivity values degrading from 2,000 to 1,000 md-ft for normal stress increasing from 1,000 to 7,000 psi closure stress. Approximately 7% of the sintered bauxite was crushed at 7,000 psi. The amount of crushing was lower than that observed with the fracture faces aligned. To look at asperitiy/proppant dominated conductivity at 4,500 psi, the sintered bauxite was removed and the system reloaded; the conductivity immediately decreased from 2,500 to 575 md-ft. Over the next 20 hours of flowback, the conductivity of the asperity dominated fracture decreased to about 180 md-ft.

These results indicate that strong proppants such as sintered bauxite dominate the conductivity in fractures, whereas weaker proppants such as Jordan sand are more likely to be crushed and allow for the asperities of the fracture to coincide with one another to prop the fracture and dominate the maintained conductivity of the fracture.

In comparing the tests with field data at 1.0 lbm/ft^2 concentrations of proppant, it was found that high strength proppant or conventional concentrations of proppant are required to achieve at least 50 md-ft at closure pressures greater than 2,000, presuming that 50 md-ft is a reasonable conductivity requirement for an effective stimulation. In comparing the 1.0 lbm/ft^2 data (obtained in PredictK) to the four cases presented, it was found that flat, parallel core (saw cut) fracture faces tend to overestimate the conductivity that would be achieve in actual hydraulic fractures.

2.7 Summary

In summary, testing of granite at hydrothermal conditions by Yasuhara et al. (2006) showed that over 1500 hours of flow, there was a 60% reduction in aperture

height. Moore et al. (1994) showed that under similar hydrothermal conditions, there was a 66% reduction in permeability at a temperature of 300°C. Knox et al. (1989) found that at 1200 psi with 60 psi across the system, Bauxite lost 37-60% of its weight when it came into contact with fluid at 550 °F and a ph of 11. Fredd et al. (2000) showed that under asperity dominated conditions, the conductivity may vary by at least two orders of magnitude and that proppant concentrations generally dominate the conductivity and differ from unpropped systems by three to four orders of magnitude. Cooke (1973) was the first to perform experiments under elevated temperature and stress and hypothesized that non-Darcy effects have a large contribution to lowering the effective conductivity in proppant filled fractures. McDaniel (1987) continued with the hypothesis of Cooke and found that conductivity was reduced by 25% at 4000 psi from increasing temperature from 150 to 325°F. McDaniel (1986) also found that at 275°F 20/40 sintered bauxite conductivity decreased 46% over two weeks of testing at 5000 psi confining stress. McDaniel (1986) also noted that conductivity was not well retained when fluids not presaturated with silica were used in the fracture. Hanh (1986) and Montgomery (1984) found that flow capacity decreased 20-50% at 8500 psi and 5000 psi, respectively. Both Hanh and Montgomery used fluids that were not presaturated with silica, so their results may be reduced more than silica saturated fluids would indicate.

Proppant under geothermal conditions was first performed by Maurer Engineering in 1981. Maurer Engineering found 82.5% permeability retention at 350°F and 90% permeability retention at 500°F at 5000 psi for 20/40 sintered Bauxite. Cobb (1986) attempted to look at the influence of only stress corrosion in the proppant pack in terms of conductivity losses by testing proppant in a Teflon tube at 93°C and 10,000 psi. Cobb

(1986) found that 20/40 sintered bauxite lost 20-30% of its conductivity at these conditions. Whitney et al. (1989) found that at 2000 psi and 93°C sintered bauxite conductivity decreased from 7000 to 3000 md-ft.

Barree et al. (2003), Palisch et al. (2007), and Vincent (2009) found that non-Darcy flow can reduce conductivity by 25-60%, multiphase flow can reduce conductivity by 60-70%, and stress cycling can reduce conductivity by as much as 25% after only one cycle.

Weaver et al. (2006) was the first to hypothesize that proppant diagenesis has a drastic influence on reducing the conductivity of proppants. Weaver et al. (2006) showed that at 10,000 psi and 250°F, there was no diagenetic growth on resin coated proppants. All other proppants tested in closed vessels at 500°F over 1-12 months showed diagenetic growth and loss of over half of the initial permeability of the proppant pack. Weibull crush analyses after the testing saw a decrease in crush from 310 to 180 MPa. Dueneckel et al. (2011) showed that even inert materials such as glass rods and steel balls can have diagenetic growth when placed in static test vessels at elevated temperature with formation material (shale in the Dueneckel et al. (2009) paper). Dueneckel et al. (2011) concluded that diagenetic zeolite formation does not have a drastic impact on fracture conductivity.

CHAPTER 3

TESTING MATRIX AND MOTIVATION

3.1 Baseline Testing Matrix

Initial testing of 1.5" diameter saw cut and wedge split samples was used as baseline testing for the entire project. In the initial set up of the system, it was determined that a confining pressure of 3000 psi (corresponding to an approximate depth of 3000 ft) would be used. Initial testing was to be completed at ambient temperature to determine if the testing system would be adequate for the project; later testing would be completed at 200°C to correspond more closely with temperatures at the depth ranges being tested. Though 200°C is not the optimal temperature for geothermal production, the upper temperature limit on most testing materials (such as o-rings) is around 204°C.

Initial testing of the saw cut sample over a week of time showed that the system had some leaks in the tubing or jacket. Following this, the wedge split sample was also attempted at 3000 psi. The wedge split test failed due to bending and closure of the tubing used to transport the fluid through the sample fracture. The confining pressure of 3000 psi was found to be over the safety limit of the o-rings used and several sets of o-rings were ruptured during the first set of tests. The failure of the o-rings prompted reduction of the testing confining pressure to 2000 psi for the remainder of the testing.

A new pressure transducer, with a factory calibration, was obtained and testing of the wedge-split sample resumed with the third set of tests. An initial pressure of 200 psi

was tested and then ramped to 2000 psi. During the ramp of the pressure to 2000 psi, the Teflon jacket on the sample ruptured and the pressure transducer was over pressurized, leading to inaccurate readings of the fourth test (2000 psi test).

Another pressure transducer was then used for the remainder of the testing. It was calibrated using a nitrogen cylinder and calibrated pressure gauge. The fifth and sixth tests (1.5" diameter saw cut and wedge-split at ambient temperature) showed great agreement in terms of permeability and were successfully completed. The results presented in the testing matrix begin with the fifth and sixth tests as the previous data were inaccurate and only obtained through troubleshooting the testing system. After successful completion of a saw cut and wedge split set, a test at elevated temperature was attempted on the wedge-split sample. The attempted temperature was 95°C; without a back pressure regulator there was some vaporization of the pore fluid, leading to a reduced relative permeability due to two phases being present in the fracture. All later experiments incorporated a back pressure regulator.

Using the knowledge of what caused test failures in the initial vessel, a new vessel was designed with modifications to avoid some of the pitfalls of using the first vessel for testing. The newly manufactured vessel could accommodate 2.5" diameter samples. Ambient tests were completed on both a saw cut and wedge split 2.5" diameter sample for comparison with the 1.5" diameter baseline tests. The 2.5" diameter sample tests are presented in the initial baseline testing matrix in Table 3.1. Testing resumed with tests at temperature on the 2.5" diameter sample, which are presented in Table 3.2.

Experiments were run at 90°C, 150°C, and 200°C to determine the effect that temperature had on fracture conductivity and to simulate fluid flow through a fracture at

Table 3.1- Initial Ambient Baseline Testing Matrix

Test Number	Diameter & Sample Type	Confining Pressure (psi)	Temperature	Average Permeability
1	1.5” Saw Cut	3000	Ambient (~23°C)	---
2	1.5” Wedge Split	3000	Ambient (~23°C)	---
3	1.5” Wedge Split	200	Ambient (~23°C)	---
4	1.5” Wedge Split	2000	Ambient (~23°C)	Over pressured
5	1.5” Saw Cut	2000	Ambient (~23°C)	120 Darcy
6	1.5” Wedge Split	2000	Ambient (~23°C)	110 Darcy
7	1.5” Wedge Split	2000	95°C	---
8	2.5” Saw Cut	2000	Ambient (~23°C)	143 Darcy
9	2.5” Wedge Split	2000	Ambient (~23°C)	185 Darcy

Table 3.2- 2.5” Diameter Samples Testing Matrix

Test Number	Diameter & Sample Type	Effective Confining Pressure (psi)	Temperature	Average Permeability
8	Saw Cut	2000	Ambient (~23°C)	143 Darcy
9	Wedge Split	2000	Ambient (~23°C)	185 Darcy
10	Saw Cut	2000	90°C	---
11	Saw Cut	2000	150°C	82 Darcy
12	Saw Cut	2000	200°C	91 Darcy
13	Wedge Split	2000	90°C	96 Darcy
14	Wedge Split	2000	150°C	132 Darcy
15	Wedge Split	2000	200°C	50 Darcy
16	Wedge ½ Concentration	2000	Ambient (~23°C)	220 Darcy
17	Wedge Self-Prop	2000	Ambient (~23°C)	3000-2000 Darcy
18	Wedge Self-Prop	2000	90°C	500-120 Darcy
19	Wedge Self-Prop	3000	90°C	120-40 Darcy

downhole geothermal conditions. The 90°C temperature tests on the 2.5" diameter sample were lowered from the 95°C tests on the 1.5" sample to avoid possible multiphase effects. Although a BPR was employed and the temperature lowered, the low flow rates indicated vaporization of the water in the proppant pack as the permeability was much lower than the ambient baseline experiments.

Tests at temperature were first run on the 2.5" diameter saw cut sample and then on the 2.5" diameter wedge-split sample. Following the suite of tests at temperature, half of the proppant pack was removed from the wedge-split (rough surface) sample and saved for SEM analysis and the other half of the proppant was retested to compare permeability through the fracture with varying concentrations of proppant. Following this set of tests, all of the proppant pack was removed from the 2.5" wedge-split sample and the fracture faces were shifted 0.375" and the fracture was tested to compare the permeability of a self-propped fracture to that of a proppant filled fracture. The self-propped fracture test was run to determine the effect that proppant has on maintaining fracture conductivity as compared to fractures that are not propped. On the final day of testing of the self-propped fracture, the confining pressure was increased in an attempt to see what effect a greater principal stress had on the self-propped fracture. An overall summary of all of the 2.5" diameter sample tests is presented in Table 3.2. Confining pressure, temperature, and average permeability are presented in Table 3.2 to give an indication of average values obtained from the various tests within the testing matrix.

CHAPTER 4

EXPERIMENTAL SET-UP

4.1 General Set Up

A basic schematic for the experimental set up is shown in Figure 4.1. One pump was used for the confining pressure and a factory calibrated pressure transducer was placed in line between the pump and vessel and near to the inlet on the vessel to ensure accurate confining pressure was maintained. The confining pressure acts hydrostatically around the radius of the sample being testing. The other pump pumped water through the fracture to determine the permeability through the sample. The controller on the pump ensured a highly accurate volumetric flow rates, ISCO pumps are well known for their accurate volumetric flow rates. On the outlet of the system that flows through the fracture, a back pressure regulator was implemented to ensure that the water going through the system was not vaporized. A differential pressure transducer was plumbed at the inlet and outlet of the fracture flow through line to determine pressure drop and the corresponding permeability of the fracture.

Both ISCO 500D pumps were equipped with high-temperature seals. The original plan had been to heat the water as it was being pumped into the vessel. It was later decided to preheat the flowing water inside the oven. A coil was constructed from 1/8" OD Swagelok tubing in order to heat the water in the tubing as it entered the oven and before it entered the vessel containing the propped fracture. The pumps and differential

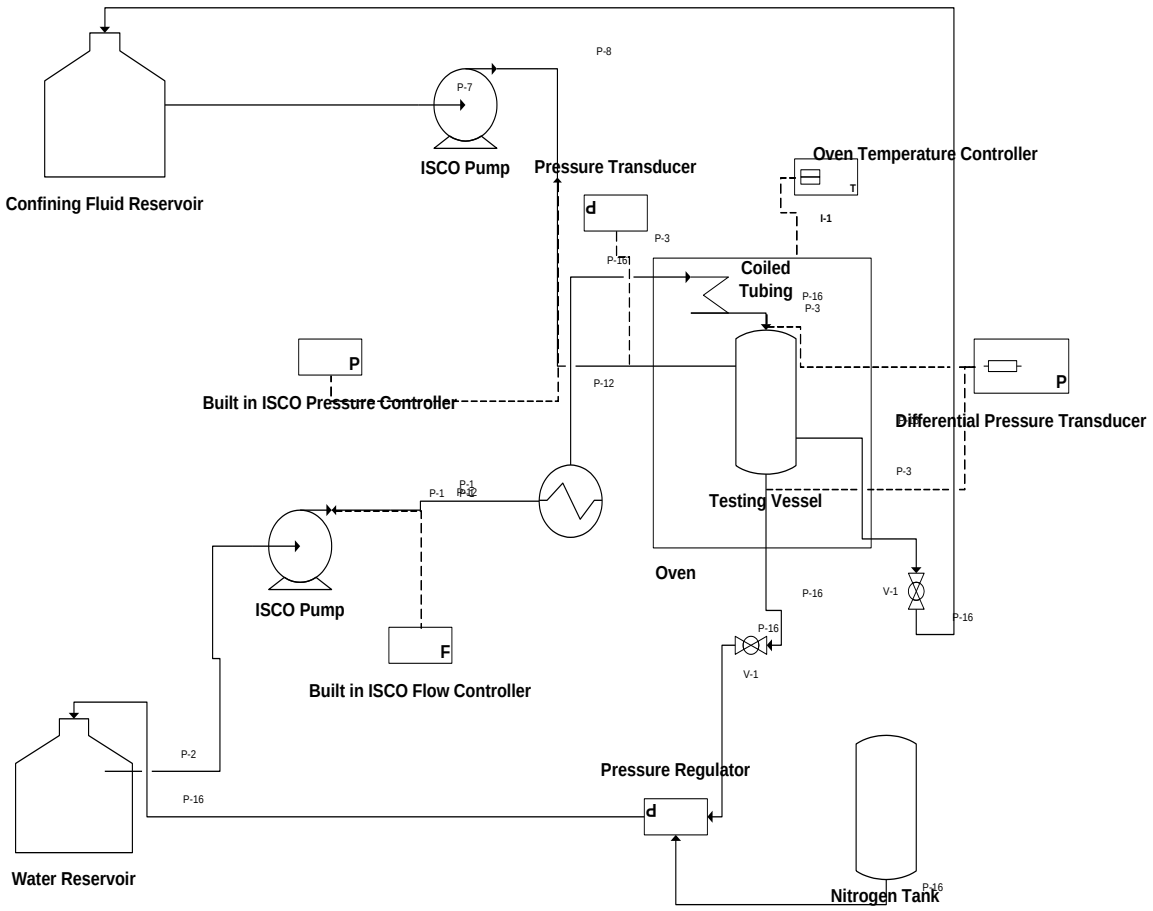

Figure 4.1. Schematic of testing apparatus

pressure transducer were plumbed with 1/8" NPT to 1/8" Swagelok fittings and 1/8" OD Swagelok tubing was used on the entire system.

LabView™ software along with a National Instruments NI CDAQ-9172 control board was used for all data acquisition. The pressure vessel was contained in a Binder FP Series forced convection oven, capable of a maximum temperature of 300 °C. Figure 4.2 shows the external pumping and measurement components.

Figure 4.2 shows the two ISCO pumps used for confining pressure and flow through. In addition to the pumps, the back pressure regulator and pressure transducers are shown as they were plumbed in the system. The confining pressure, differential

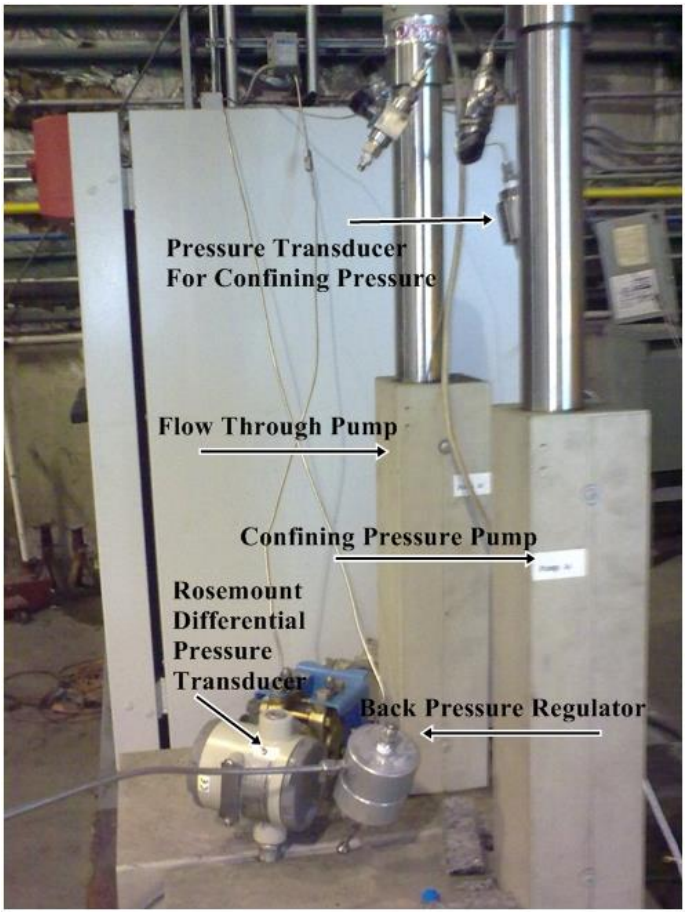

Figure 4.2. System outside of the oven

pressure transducer, and back pressure regulator were placed away from the oven so as to ensure that they did not overheat. The differential pressure transducer shown in Figure 4.2 was connected across the inlet and outlet of the vessel (inside the oven) and the difference in pressure was sent to the National Instruments control board for acquisition at one second intervals. Both ISCO pumps were calibrated using a graduated cylinder method for all flow rates used.

Flow rates through the sample were varied at 1, 2, 3, 4, 5, 10, 15, 20, 25, and 30 mL/min. The API standard, as specified in API RP-60, states that the standardized flow rates through the sample are between 1 and 10 mL/minute. The flow rate is kept at low

rates so as to ensure Darcy flow (laminar flow, linear flow, and single phase flow) which allows for easy permeability and conductivity calculations. The slow flow rate ensures that the tortuosity in the system remains low and non-Darcy effects do not need to be accounted for. Non-darcy effects are squared in terms of the specific discharge (whereas the pressure drop through the system only depends on the specific discharge to the first power) so the low flow rate ensures that the non-Darcy terms go to zero.

The 30/60 sinterball bauxite proppant was packed in the fracture to the standard value of 2.74 lbf/ft^2 of area on each side of the sample (Andrews, 1987). Typically, when sandstone wafers are used in the system, the standard packing value is 2 lbf/ft^2, but this number was corrected for the use of granite slabs in the testing vessel. The proppant was placed in the fracture by holding the faces open a standard width using spacers and slowly removing the spacers as proppant was poured into the fracture. On the ends of the sample, 100 mesh screens were used to prevent proppant from plugging the flow lines.

A back pressure regulator was installed on the outlet line of the pressure vessel to ensure that the water entering the system did not have regions of water vapor and condensed liquid, as two phases will create a relative permeability of one phase with respect to another. A nitrogen tank was connected to the back pressure regulator. This maintained a pressure of 165 psi (the maximum pressure from the regulator on the nitrogen tank).

At the conclusion of the testing, the proppant pack was sieved (to determine the particle sizes) and analyzed using SEM (scanning electron microscope) as well as optical microscopy.

4.2 Theory-Darcy's Law

Henry Darcy was a French hydraulic engineer interested in purifying water supplies using sand filters. In 1856, Henry Darcy derived a phenomenological constitutive equation from his experiments with these sand filters known as Darcy's law. Darcy's law describes the flow of a fluid through a porous medium and is commonly used in hydrogeology and in the oil and gas industry to calculate the flow of oil, gas, and water flows in reservoirs.

The permeability of the propped fracture in all experiments was calculated using

Darcy's law, given in Equation (4.1).

$$k = \frac{Q\mu L}{A\Delta p} \tag{4.1}$$

where k is the fracture permeability, [Darcy or m^2]; Q is the flow rate through the fracture [m^3/s]; μ is viscosity of the fluid [Pa-s]; L is the length of the fracture [m]; A is the cross-sectional area of the fracture [m^2], and Δp is the pressure difference through the fracture [psi or Pa].

Darcy's law is only valid for slow (low Reynold's number) flow where viscous effects dominate. The Reynold's number is the dimensionless ratio of inertial effects to viscous effects; for porous media flow it is expressed as

$$Re = \frac{\rho v d}{\mu} \tag{4.2}$$

where ρ is the fluid density, v is the specific discharge, d is the diameter of the proppant particles, and μ is the viscosity of the fluid. Standard proppant tests ensure slow enough

flow rates to keep the Reynold's number below one so that non-Darcy effects are not present.

Conductivity through the fractures was calculated by multiplying the permeability by the fracture aperture, as is shown in Equation (4.3).

$$C = kW_f \tag{4.3}$$

where C is the conductivity of the propped fracture [mD-ft or mD-m] and W_f is the width of the fracture [ft or m].

CHAPTER 5

SAW CUT VS. WEDGE-SPLIT

5.1 1.5" Results

Averaged typical values calculated for flow through the propped saw cut sample tested at a confining pressure of 2000 psi are shown in Table 5.1. Averaged typical values calculated through the wedge-split sample tested at a confining pressure of 2000 psi are shown in Table 5.2.

The pressure drop through the proppant pack in the wedge split sample is marginally greater than the pressure drop across the saw cut sample. While there may be some influence from the added friction of the surface asperities, Fredd et al. (2000) showed that for any sample with the rock faces aligned to one another at adequate proppant concentrations, such as the ones at the standard 2 lb/ft^2, the pressure drop is "not a strong function of the surface asperities" (Fredd et al., 2000).

Because of the reduced effective width and increase in tortuosity from the surface asperities on the wedge-split sample, the injectivity indices at all of the various flowrates are higher for the saw cut tests than the wedge-split cases.

The differences between average permeability and conductivity values obtained in the saw cut and wedge split tests are highlighted in Figures 5.1-5.2. Absolute permeability inferred from Darcy's law in Equation (4-1) is lower for the rough sample

Table 5.1. Summary of Saw Cut Sample Tested at 2000 psi- Average Values

Flowrate (mL/min)	**ΔP (Pa)**	**k(m^2 x 10^{-10})**	**k(Darcy)**	**Conductivity (mD*ft)**	**Q/ΔP (mL/Pa*min x10^{-3})**
1	220	1.07	109	1268	4.55
2	339	1.33	135	1575	5.90
3	529	1.25	127	1476	5.67
4	714	1.23	125	1456	5.60
5	908	1.21	122	1428	5.51
10	1959	1.13	114	1335	5.10
15	2874	1.15	116	1359	5.22
20	3775	1.16	118	1376	5.30
30	5465	1.20	122	1422	5.49

Table 5.2. Summary of Wedge-Split Sample Tested at 2000 psi- Average Values

Flowrate (mL/min)	**ΔP (Pa)**	**k(m^2 X10^{-10})**	**k(Darcy)**	**Conductivity (mD*ft)**	**Q/ΔP (mL/Pa*min x10^{-3})**
1	164	1.44	145	1688	6.09
2	372	1.21	122	1429	5.37
3	615	1.19	121	1413	4.88
4	836	1.17	118	1380	4.79
5	1217	0.98	100	1162	4.11
10	2187	1.05	107	1244	4.57
15	3452	0.99	100	1167	4.35
20	4044	1.12	114	1328	4.95
30	6158	1.08	110	1280	4.87

(wedge-split) than for the relatively smooth, saw cut sample. At low flow rates (API's RP-61 which is the API standard for testing proppant), the permeability of the proppant differs by 5-10 Darcies. This shows a slight influence of surface asperities on pressure drop through the fracture but not of noticable magnitude, confirming the findings by Fredd et al. (2000). Although this may suggest that the difference is slight, the friction in fractures is higher in actual hydraulic fracturing operations due to inadequate proppant concentration, fines in the fracture, and consequently non-Darcy effects, as described by

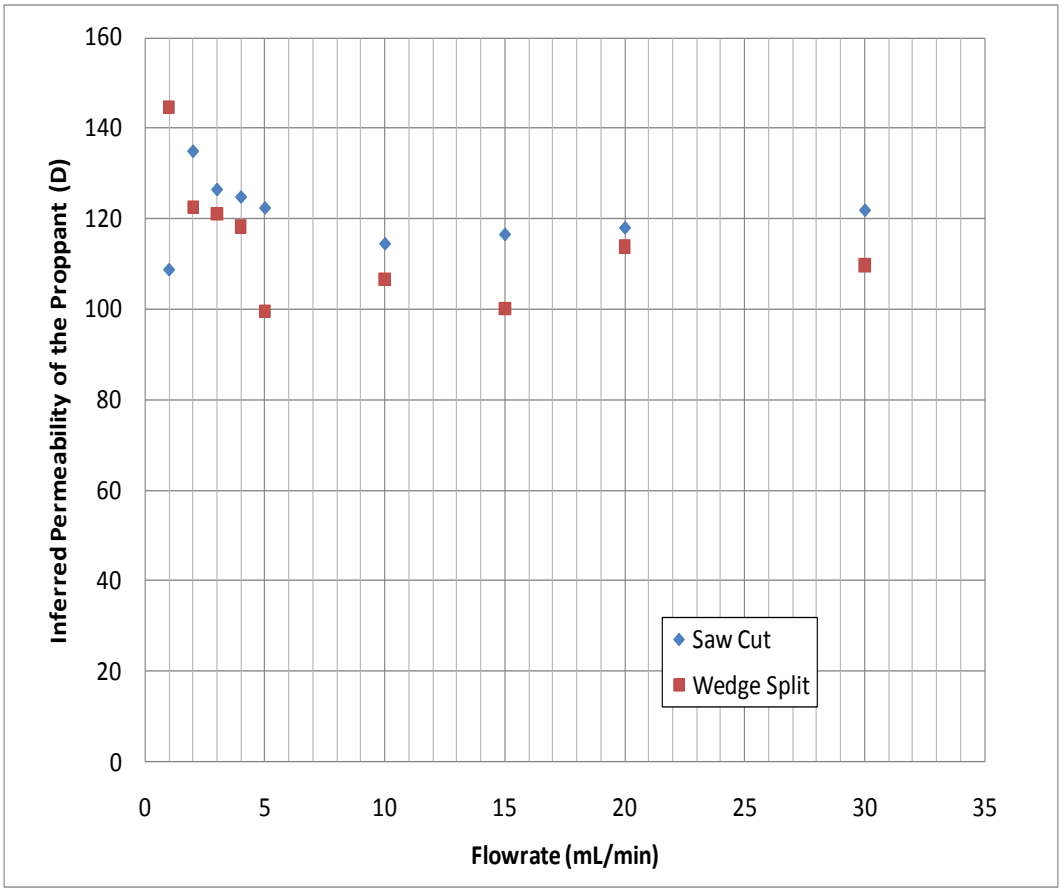

Figure 5.1. Permeability summary plot

Barree et al. (2003), Palisch et al. (2007), and Vincent (2009). Downhole conditions and fracture asperities will increase the likelihood of permeability decreasing mechanisms. While the higher flow rates in both the saw cut and wedge-split cases showed comparable trends to the literature values of permeability and conductivity through the sample, they are still lower than reported values. The main cause of this might be accounted for by the increased flow path and associated increased in pressure drop from the surface asperities on each face of the sample. Even in the case of the saw cut sample, there is enough friction from the granite face to lower the permeability and conductivity values below the literature values reported using the standardized methods in API's RP-61.

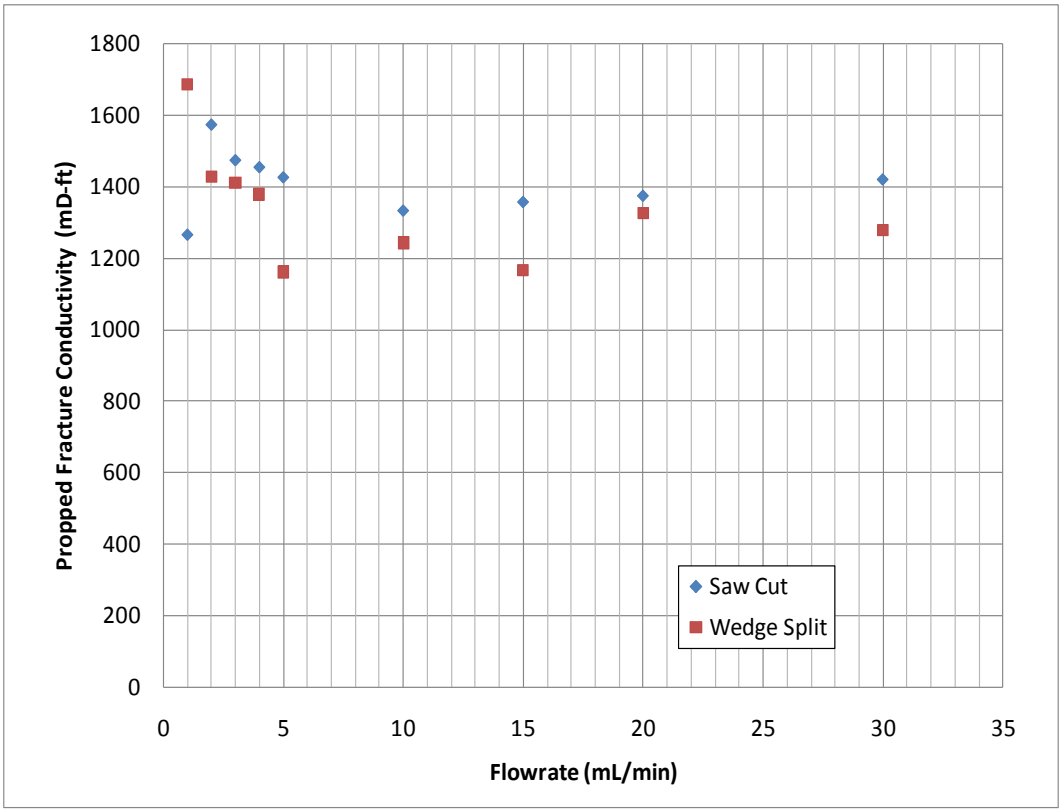

Figure 5.2. Conductivity summary plot

5.2 2.5" Results

Several tests were run at the elevated temperatures. Table 5.3 shows averaged permeability values for tests at elevated temperature on the saw cut sample.

Permeabilities of the 90°C saw cut tests were the lowest values seen in all of the tests. One of the reasons that these values were so low can be attributed to the fact that a back pressure regulator was not used on this set of tests. Vaporization of the water must have occurred and the relative permeability of the two phases reduced the effective permeability of the water flowing through the sample (Palisch, 2007).

Permeability values of the tests at 150°C were approximately one-half of those at the baseline ambient temperature. It appears that vaporization of the water may have also

Table 5.3: Average Saw Cut Permeability Summary Table

	Temperature			
	Ambient (~22°C)	**90°C**	**150°C**	**200°C**
Flow Rate (mL/min)	**Permeability (Darcy)**			
1	110.0	9.2	50.0	6.1
2	123.3	16.9	54.1	16.0
3	125.0	20.0	185.5	44.1
4	133.4	27.8	85.2	32.0
5	163.2	21.3	88.9	53.2
10	160.5	24.8	85.2	68.8
15	150.4	25.1	74.7	158.6
20	176.3	43.2	68.3	123.3
25	146.4	40.8	64.2	143.9
30	145.9	37.2	63.6	107.3

occurred at the lower flow rates of the 200°C test, as in the 90°C case, leading to a relative permeability of the water flowing through the proppant pack being established, despite application of back pressure to maintain single phase conditions.

The permeability values were also averaged over multiple runs at the various temperatures in the wedge-split sample; the results are presented in Table 5.4.

Permeability values at 90°C were again approximately one-half those for the baseline ambient permeability conditions. It also appears that vaporization of the water may have occurred in the wedge sample at the lower flow rates at 200°C, leading to a low relative permeability. Although there was a back pressure regulator on the tests at 200°C, the flow rates may have been low enough to allow for some water vaporization to occur, leading to both a gas and liquid phase in the pack, reducing the relative permeability. McDaniel (1986) found permeability decreases on the order of 46% after two weeks of

Table 5.4: Average Wedge-Split Permeability Summary Table

	Temperature			
	Ambient (~22°C)	**90°C**	**150°C**	**200°C**
Flow Rate (mL/min)	**Permeability (Darcy)**			
1	66.6	101.5	111.5	6.0
2	154.1	104.3	129.1	34.3
3	193.8	97.6	294.7	9.3
4	269.8	109.4	134.4	39.8
5	236.7	106.0	134.7	17.4
10	215.6	93.6	136.8	76.8
15	193.4	89.6	130.6	56.1
20	183.2	88.1	96.6	49.0
25	172.2	84.8	82.3	98.7
30	162.7	85.8	73.0	61.4

testing at 275°F, which agree with the findings presented for both the saw cut and wedge split cases. McDaniel (1987) also showed that without presaturation of silica, the permeability is decreased to approximately half of the initial values, but with presaturation of silica, the permeability was retained by 75%; from these findings, the permeability could be higher than found. Montgomery (1984) found a 50% reduction in flow capacity over 9 months of testing at 5000 psi confining stress. Although the length of testing and confining stress were higher, the results presented are not out of the realm of other experimentally obtained values. Barree et al. (2003), Palisch et al. (2007), and Vincent (2009) found that multiphase flow can reduce conductivity by 60-70% and this is the dominate factor that ultimately reduced permeability in the fracture in the results presented.

Figure 5.3 shows a comparison plot of the averaged permeability values at all of the temperatures for the saw cut case. Error bars were incorporated into the

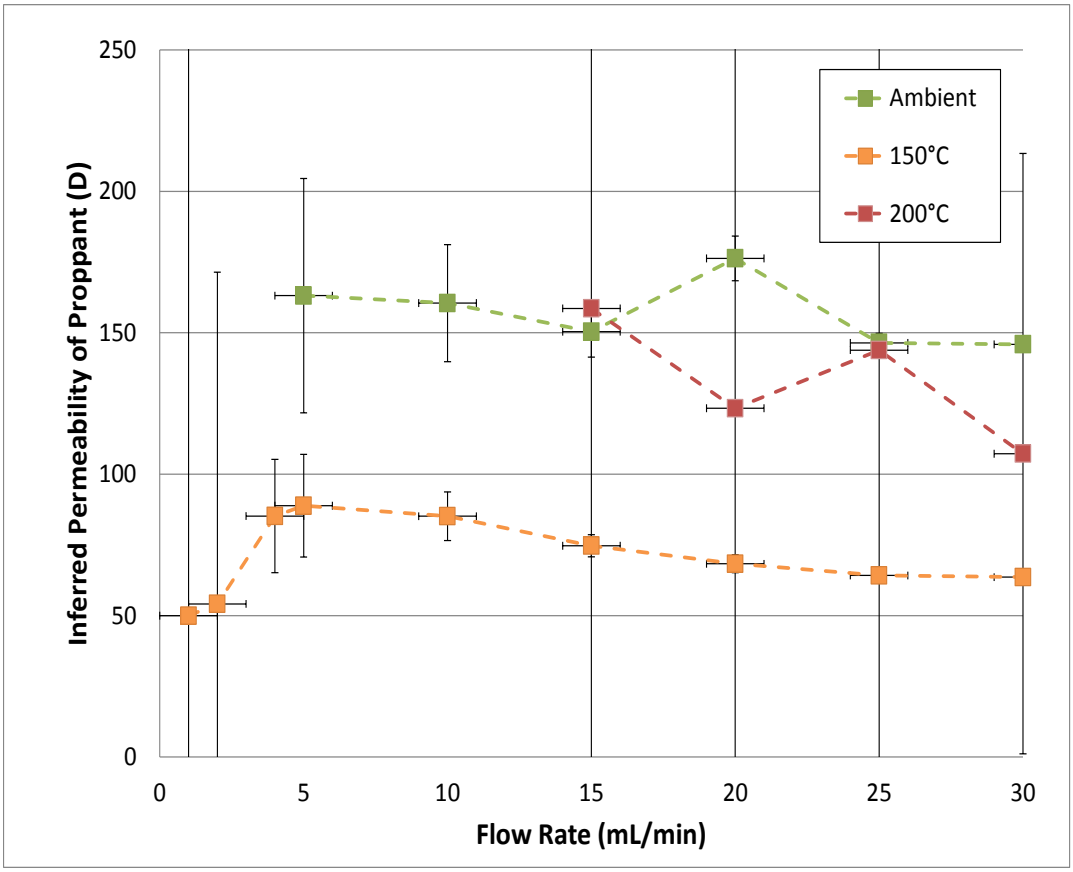

Figure 5.3: Saw cut permeability summary plot

measurements to give a true depiction of how variable the presented results may have been, the error bars were created using the variation between all runs. Ambient permeability and the permeability of the higher flow rates at 200°C for the saw cut sample approach the values in the published literature for the bauxite proppant used in the testing, although they are still well below them. Interestingly, the permeability around the boiling point of water stays at a constant low value. At the intermediate temperatures of 90°C and 150°C and even the lower flow rates at 200°C, temperature appears to have an effect on the permeability of the proppant pack in the saw cut tests. A comparison of the averaged permeability values at all the temperatures for the wedge-split case is presented in Figure 5.4.

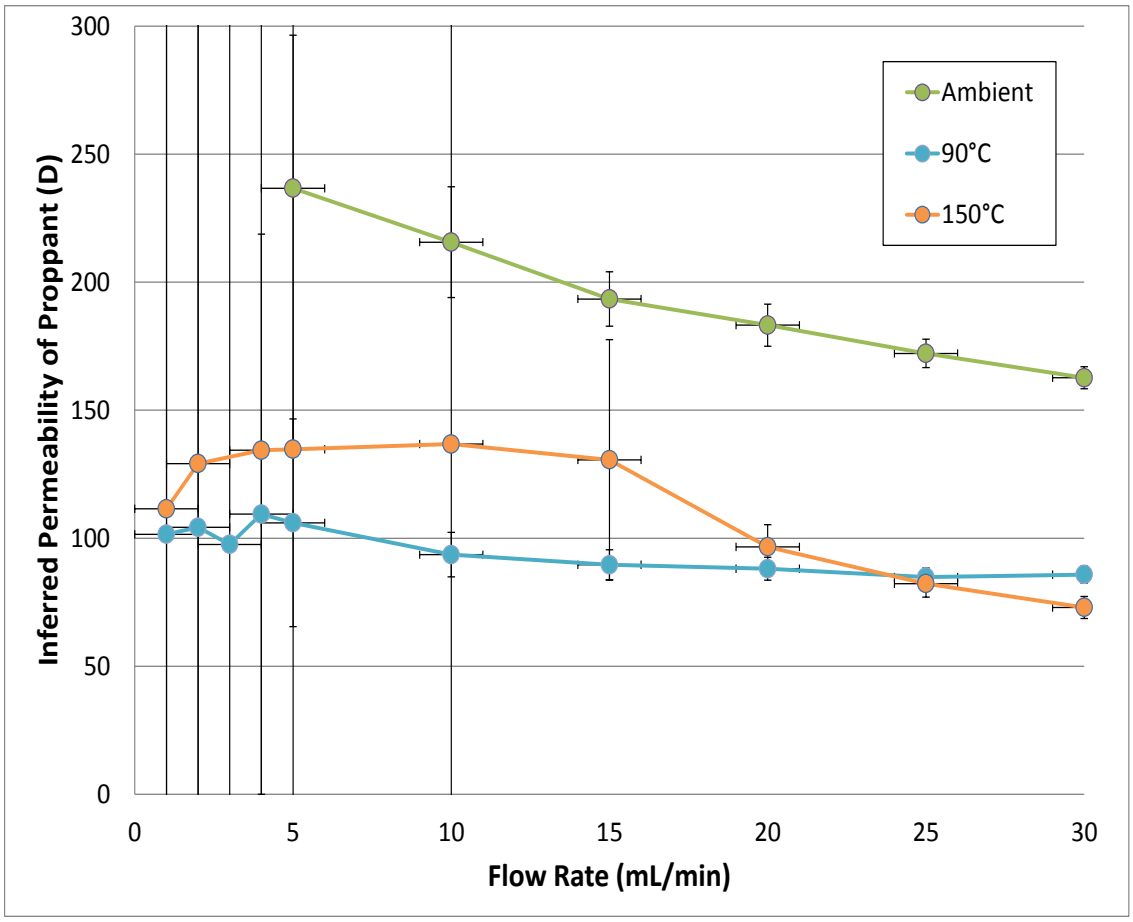

Figure 5.4: Wedge-split permeability summary plot

As with the saw cut tests, the ambient permeability approaches the published literature values. In the wedge-split cases, the permeability for 90°C and 150°C approach nearly constant values of approximately 100 Darcy and 120 Darcy, respectively. Permeability values at 200°C are lowest in the wedge-split case; at higher flow rates, they appear to rise to just below the permeability values of the other temperature tests. A back pressure regulator was used for the wedge-split tests at 90°C, and while the values are higher than in the saw cut case, they are still low compared to the baseline ambient test. In the wedge-split tests, the measurements at temperature appear to show that there may be temperature effect on the permeability of the proppant pack.

Figure 5.5 is a comparison of the averaged permeability values for saw cut and wedge split scenarios. In the 200°C temperature set, the saw cut sample had higher permeability values than in the wedge-split case; in all other temperature sets, the wedge-split sample averaged higher permeability values than the corresponding temperature saw cut test. These findings are in agreement with the findings by Fredd et al. (2000) that stated that permeability "is not a strong function of surface asperities when the fracture faces are aligned". Alternative hypotheses were also formulated for these findings.

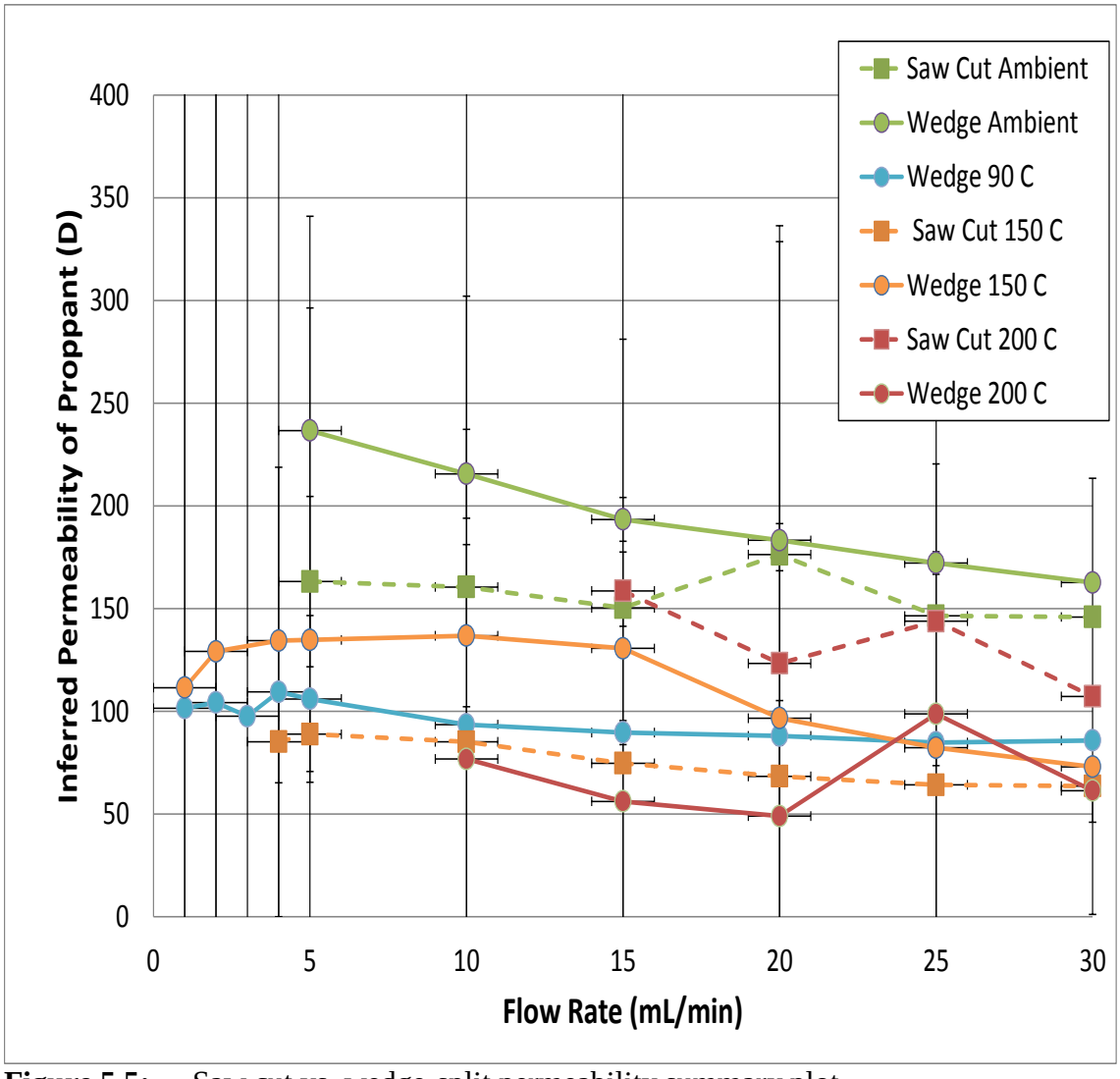

Figure 5.5: Saw cut vs. wedge-split permeability summary plot

Another potential reason that the permeability of the wedge-split tests was greater than the saw cut tests can be attributed to the difference in the width of the fracture in the wedge-split tests. The width of the gasket material that was placed in the saw cut edges on the wedge-split faces held the fracture open approximately 1.5 mm more than in the saw cut case. This would have increased the number of pathways that water could take through the proppant, limiting exposure to the apertures on the faces of the wedge-split sample. Fredd et al. (2006) found in a similar study that the higher the proppant concentration, the less the fracture relies on aperture effects in maintaining permeability and conductivity. Aperture vs. proppant dominated conductivity scenarios are presented in Figure 5.6.

Temperature, even at the low scenario of 90°C appears to have a great effect on lowering the permeability of the system; all of the permeabilities measured at temperature are much lower than the baseline permeabilities found at ambient temperature. Whitney et al. (1989) observed a decrease in conductivity from 7000 to 3000 md-ft for sintered bauxite at 2000 psi confining stress after increasing the temperature from ambient to 93°C.

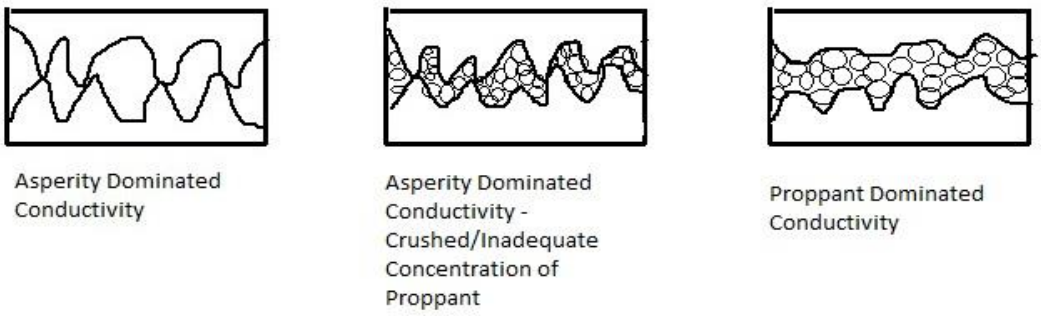

Figure 5.6. Aperture vs. proppant dominated conductivity scenarios

One of the reasons the permeability may decrease with an increase in temperature from ambient could be attributed to the thermal expansion of the rock and proppant, decreasing some of the void space that was available in the ambient testing. A more likely scenario is that in running the tests they were run in order of increasing temperature. During any one of the tests, the proppant pack may have compacted and prevented flow in the manner that it was flowing in the previous tests. Restarted tests (after reloading of the proppant following a jacket failure) did appear to have higher permeability values than the later tests run. Though that may be one of the main reasons for the decrease in permeability through the sample, at increasing temperature, it is still believed that temperature has an effect on the permeability of the sample, though the extent of this is not known.

Average conductivity values obtained in the saw cut tests at the various temperatures is presented in Table 5.5. Average conductivity values at the various temperatures for the wedge-split case are presented in Table 5.6. A summary plot comparing the saw cut and wedge-split conductivity values is presented in Figure 5.7.

Of note in Figure 5.7 is the widening gap in conductivity values between the saw cut and wedge-split samples. This is attributed to the wider fracture gap of the wedge-split sample. The conductivity of the ambient baseline wedge-split test is much greater than all of the other average conductivity values obtained (~1000 mD-ft greater than the next closest values at all flow rates), which intuitively makes sense.

Cobb et al. (1986) found that stress corrosion in a proppant pack of sintered bauxite contributes a loss of 20-30% of conductivity in the pack. Whitney et al. (1989) found at 93°C and 2000 psi (similar scenario to tested) that conductivity of 20/40

Table 5.5: Average Saw Cut Conductivity Summary Table

	Temperature			
	Ambient (~22°C)	**90°C**	**150°C**	**200°C**
Flow Rate (mL/min)	**Conductivity (mD-ft)**			
1	1787	300	812	99
2	2004	274	880	260
3	2032	325	3014	716
4	2168	452	1384	521
5	2651	345	1444	864
10	2608	403	1384	1118
15	2444	408	1214	2578
20	2865	702	1110	2004
25	2379	663	1043	2338
30	2371	605	1033	1743

Table 5.6: Average Wedge-Split Conductivity Summary Table

	Temperature			
	Ambient (~22°C)	**90°C**	**150°C**	**200°C**
Flow Rate (mL/min)	**Conductivity (mD-ft)**			
1	1073.0	1587.6	1672.5	98.2
2	2410.6	1624.0	1937.2	558.1
3	3017.7	1511.2	4420.9	150.5
4	4157.4	1700.1	2015.3	646.7
5	3657.6	1658.7	2020.8	283.4
10	3343.9	1443.8	2051.7	1247.7
15	3009.5	1382.1	1959.1	912.3
20	2853.8	1356.2	1449.4	795.8
25	2683.5	1306.7	1233.8	1604.2
30	2537.3	1325.3	1094.6	997.2

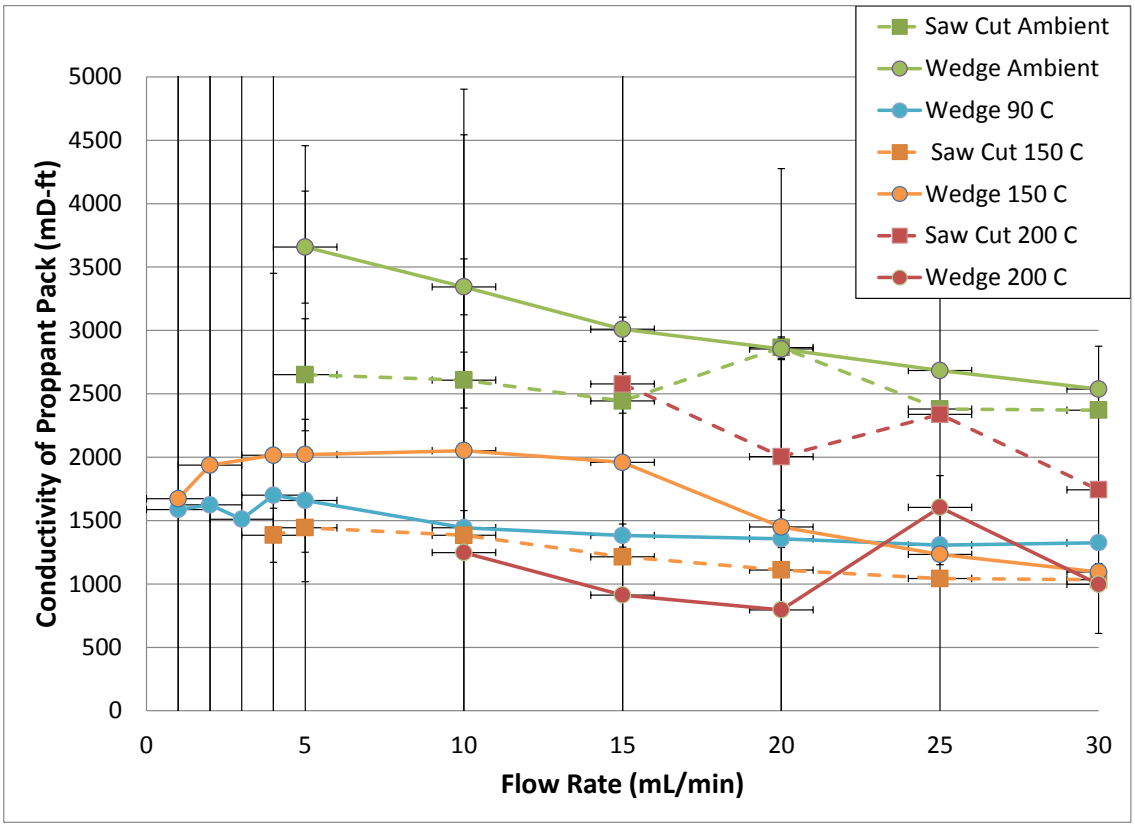

Figure 5.7: Average saw-cut vs. wedge-split conductivity summary plot

sintered bauxite decreased 57% -- from 7000 md-ft to 3000 md-ft. Again, while literature indicates that the results obtained are comparable to other experiments obtained in the scientific world, multiphase flow in the fracture was the dominate factor that ultimately reduced conductivity.

Other studies on proppant in hydraulic fractures at extreme conditions have concluded that geochemical reactions occur to both the rock and proppant pack under extreme temperature, the effect of which is lowering of conductivity and porosity. McDaniel (1987) found that permeability does not rebound after cool down once the proppant pack has experienced elevated temperatures, suggesting that temperature is a factor in lowering proppant pack conductivity. Weaver et al. (2006), in a study on sustaining fracture conductivity, found that

> Geochemical reactions can lead to rapid, dramatic loss of porosity of proppant packs exposed to high temperature and stress conditions, leading to significant loss of fracture conductivity. This mechanism is functional at lower temperatures and closure stresses, but may be sufficiently slow to not be a significant factor in production. The use of high-strength proppants may actually exacerbate porosity filling reactions by forming clay-like minerals. This may partially mitigate the advantage of using stronger proppants. (Weaver et al., 2006)

Weaver et al. (2008) found that static testing of proppant and formation material at 500°F over the course of 1 to 12 months showed extensive diagenetic activity on the proppant surfaces, which ultimately reduced permeability in the pack by 50%. Dueneckel (2011) also observed diagentic reactions at elevated temperatures on even inert materials in static vessels with formation material present. Geochemical reactions within the fracture may have attributed to the decrease in permeability and conductivity with increase in temperature (Palisch et al., 2007).

CHAPTER 6

RESIDUAL CONDUCTIVITY- INFLUENCE OF SELF-PROPPING, CONCENTRATION, TIME, AND CLOSURE STRESS

6.1 Self-Propping and Closure Stress

In order to determine the effect that proppant has on maintaining fracture conductivity if shear displacement has occurred, a baseline set of tests were run with the fracture faces shifted 0.375". This was intended to simulate a fracture subjected to shearing and propped only by asperities on the face of the fracture.

Initially, a test was run at ambient temperature. To ensure isothermal testing at 90°C, the oven was set at 90°C and left overnight, with flow through the fracture set at 0.1 mL/min to ensure that the pump would not need refilling overnight. After the system had equilibrated, 5 liters of water were pumped through the fracture at various flow rates, with an average flow rate of approximately 30 mL/min.

Initial measurements at 90°C indicated that with an increase in temperature, the permeability of the fracture did not drastically decrease – i.e., conductivity was unchanged due to a modest change in temperature in an unpropped fracture. Previous testing completed under similar conditions with proppant in the showed that fracture conductivity was diminished at elevated temperature (Stoddard et al., 2011).

Throughout the remainder of the testing, the temperature was maintained at 90°C. Several liters of water were flowed through the fracture every day, usually at a rate of 30 mL/min - but sometimes less or more - with flow rates no higher than 50 mL/min and no lower than 10 mL/min during the day. For overnight testing, the flow rate was left at 0.1-0.5 mL/min to maintain flow through the fracture without needing to refill the pump until morning. Before testing, the shifted fracture was approximately 0.057" in thickness. After final unloading, the measured fracture width averaged 0.0398". Since fracture width was not measured in-vessel during the tests that were run, the results presented in the permeability summary plot incorporate error. All permeability values until the last two days were calculated using the initial fracture width, and the last two days use the final fracture width. Naturally, this uncertainty will not be an issue if one only compares conductivity (product of permeability and fracture aperture).

After the testing campaign, granite fines were removed. After cleaning the fracture surfaces of granite fines generated as contacting asperities were crushed, the rock was aligned. Some asperities had been altered enough that the realigned faces did not conform to one another. When the realigned faces were mated together posttest, the fracture was open 0.020", compared to flush with one another previous to testing.

Tables 6.1 and 6.2 summarize the tests run without proppant. Testing conditions are presented in terms of effective normal stress (Pc'). Effective normal stress is the difference between confining pressure and pore pressure; all experiments were run with a pore pressure of 165 psi which has been subtracted out to present effective confining stress under testing conditions (e.g., the tests up until 164 hours were run at 2165 psi confining pressure and 165 psi pore pressure).

Table 6.1. Summary of Corrected ΔP Values for Fracture without Proppant

	Differential Pressure (Pascal)				
Testing Conditions	**23°C, Pc'=2000 psi**	**90°C, Pc'= 2000 psi**			**90°C, Pc'=3000 psi**
Elapsed Time, Flow Rate (mL/min)	**24 Hours**	**43 Hours**	**72 Hours**	**144 Hours**	**164 Hours**
5	194	133	520	314	1555
10	154	216	768	686	4683
15	158	335	1229	1299	9169
20	257	493	1858	2088	14293
25	482	732	2622	3039	21303
30	748	986	3420	4090	23798

Table 6.2. Average Permeability Values for Fracture without Proppant

	Permeability (Darcy)				
Testing Conditions	**23°C, Pc'=2000 psi**	**90°C, Pc'= 2000 psi**			**90°C, Pc'=3000 psi**
Elapsed Time, Flow Rate (mL/min)	**24 Hours**	**43 Hours**	**72 Hours**	**144 Hours**	**164 Hours**
5	1580	475	117	195	56
10	3021	589	158	175	40
15	3897	543	147	138	29
20	2324	490	129	114	25
25	1682	410	114	98	21
30	1266	366	105	88	22

Averaging of experiments conducted at ambient data was conducted over the initial 24 hours of testing. After temperature equilibrium was established (19 hours later), the experiments at 90°C were conducted. As shown in Tables 6.1 and 6.2, the initial averaged values at 90°C saw a large increase in pressure drop, indicating closure of the fracture or some other conductivity change. Experiments conducted at the elapsed 72-hour mark indicate further closure of the fracture as potential asperity crushing or shifting were occurring to effectively decrease fracture width.

Average pressure drops between the experiments done at elapsed times of 43 hours and 144 hours remained relatively stable, indicating that the asperities on the fracture faces had shifted to find equilibrium locations or that the asperities that could not withstand the normal stress had been crushed.

After the experiments were completed at the elapsed 144-hour mark, the effective normal stress was increased to 3000 psi. Experiments conducted after 164 hours of testing and the increase in normal stress showed the average pressure drop increased by a factor of 6 from the experiments completed at the 144-hour mark.

Screens were not used on the end caps in the self-propped testing. This may have led to fines from asperity crushing plugging the tubing and contributing to the drastic increase in pressure drop on the final day of testing. Even with the possibility of fines plugging the tubing, it is apparent that the increase in stress led to additional generation of granite fines which led to further "effective fracture closure" (i.e., beyond closure due strictly to aperture reduction) at the final stress conditions. Also, the closure stresses were relatively modest- 2000 to 3000 psi effective closure stress.

Approximate permeability values obtained over the 164 hours of testing are presented in Table 6.2. The values presented in Table 6.2 are approximate due to the inability to measure fracture width in-vessel under stress. Figure 6.1 shows graphical representation of the permeability data over time.

Figure 6.1 indicates that at 90°C, the permeability drops to less than 25% of the values obtained at ambient temperature during the first 24 hours of testing. In addition to this, after 72 hours of testing at 90°C, the permeability drops to less than 25% of the permeability values obtained after the initial 90°C values obtained at the 43-hour mark of testing. Permeability values obtained after the stress increase (after 164 hours of testing) indicate near closure of the fracture or fracture width filled with granite fines. In addition to the possibility of granite fines in the fracture, there may have been granite fines blocking the tubing at the outlet of the fracture where the outlet pressure was measured.

Since the initial and final unstressed fracture widths are accurate, it is anticipated that comparison between early permeability values and the final permeability values obtained validate fracture closure (although width change due to stress is an issue). The presumption of width-related permeability degradation assumes that no granite fines influence the differential pressure existing through the fracture over the duration of the testing.

The best factor to compare the results for flow through a fracture where the stressed fracture width is unknown is conductivity. Because the denominator of Darcy's law contains the cross-sectional area of the fracture and the conductivity is calculated by multiplying the permeability by the fracture width, the fracture width cancels out and does not influence the values obtained.

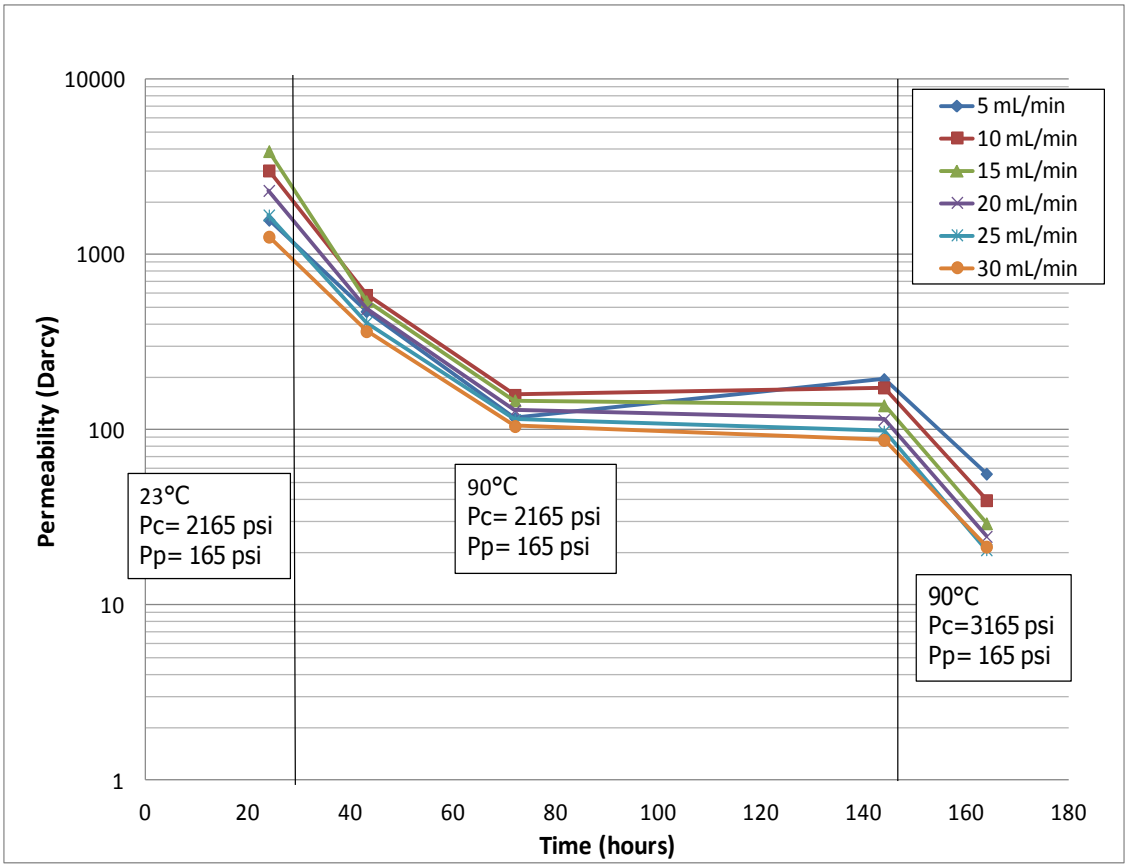

Figure 6.1. Permeability variation with time, temperature, and normal stress for the self-propped fracture. The zones are divided by testing conditions, which are specified in the boxes between lines.

Conductivity values for the flow through experiments on the fracture that did not contain proppant are presented in Table 6.3. Graphical representation of Table 6.3 is presented in Figure 6.2.

As with the permeability values presented, the conductivity values presented were also multiplied by the corresponding unstressed fracture widths. Conductivity values at 90°C between 72 and 144 hours indicate an equilibrium scenario where the fracture asperities had been crushed to an extent and the fracture faces had shifted to an equilibrium state.

Table 6.3. Summary of Conductivity Values for Fracture without Proppant

	Conductivity (mD-ft)				
Testing Conditions	**23°C, Pc'=2000 psi**	**90°C, Pc'= 2000 psi**			**90°C, Pc'=3000 psi**
Elapsed Time, Flow Rate (mL/min)	**24 Hours**	**43 Hours**	**72 Hours**	**144 Hours**	**164 Hours**
5	7856	2256	555	926	186
10	17145	2796	752	829	132
15	20504	2577	700	656	97
20	13046	2330	614	544	82
25	9466	1948	543	467	69
30	7295	1737	499	416	72

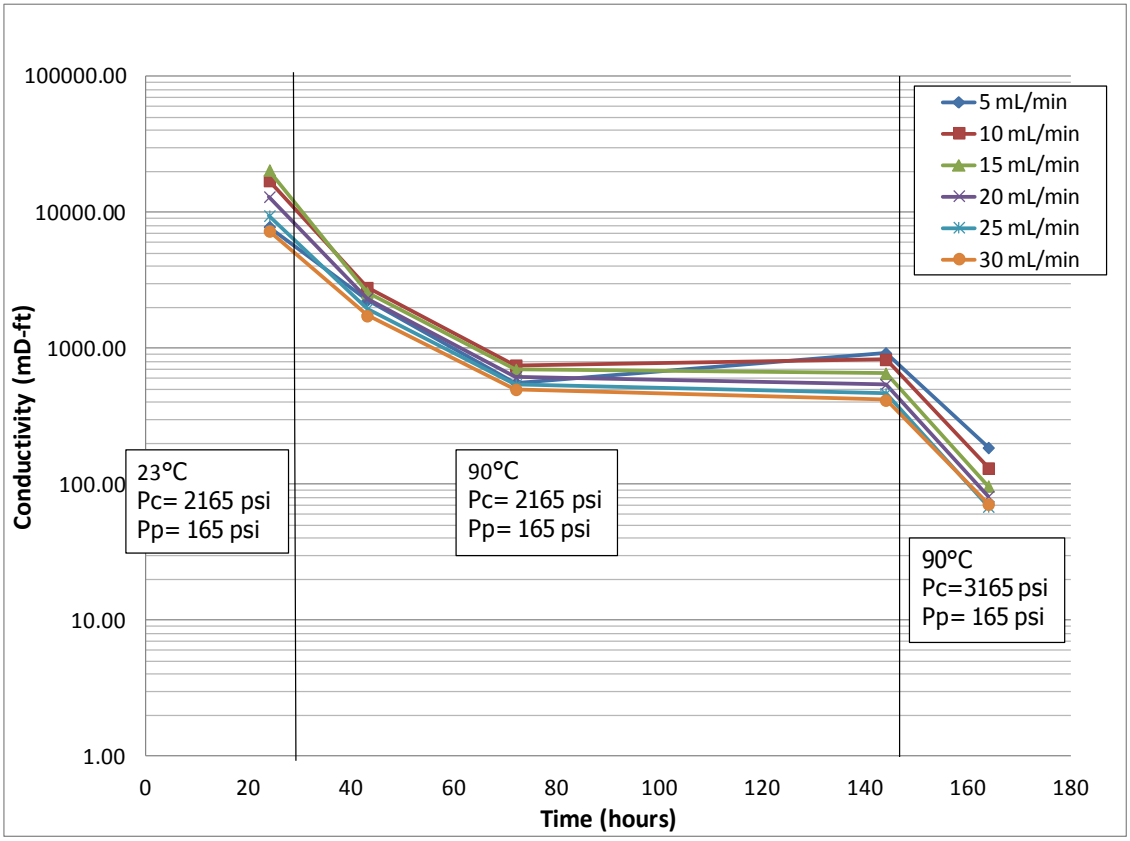

Figure 6.2. Conductivity variation with time, temperature, and normal stress for the self-propped fracture. The zones are divided by testing conditions, which are specified in the boxes between lines.

The increase in normal stress on the sample further shifted the fracture faces and more crushing of fracture asperities was observed as the conductivity dropped substantially.

These conductivity values presented at 90°C are the most accurate for the self-propped scenario under the conditions presented as the self-propped fracture at ambient temperature is an unrealistic scenario. Self-propped fractures will be at elevated temperatures downhole, and thus, the ambient case is only presented as a baseline to compare conductivity with time and also as a baseline to compare to proppant-filled fractures in a later section of this paper.

6.2 Conductivity-Time Relationships

As shown previously, the fracture conductivity of the test without any proppant has a drastic time-stress-conductivity dependence, whereas the conductivity of fractures filled with proppant are less time-sensitive.

For the case of the self-propped fracture, the pressure drop increased greatly after 72 hours of testing (48 hours of testing at 90°C, 24 hours of testing at 23°C). Over the course of the next three days, the pressure drop through the self-propped fracture increased only gradually, consistent with creep deformation. After 144 hours of testing the self-propped fracture, the confining stress was increased by 1000 psi to 3165 psi. The increase in stress led to further fracture surface degradation as well as closure. Presuming that more granite fines filled the fracture (even though there were more granite fines available for “self-propping”), flow paths were eliminated and this drastically decreased fracture conductivity. The pressure drop increased more drastically at higher flow rates (suggesting non-Darcy behavior). This apparent inertial resistance is not surprising

because of the tortuous and changing flow paths – with fines accumulation. If proppant testing is performed at the rate specified by the American Petroleum Institute (API) for proppant conductivity testing - 1 mL/minute (API, 1989), this behavior may be under-represented.

The permeability values for the self-propped fracture decline substantially during the first day. Although inferred permeability reduces drastically over the first day of loading, the degradation may not be as extreme since only unstressed aperture could be measured. While unstressed, posttest aperture was available for the self-propped testing, reductions in conductivity were compounded by granite fines - certainly in the fracture and possibly even downstream of that.

Propped testing of this sample showed the average permeability is relatively independent of the injection rates used, indicating Darcy behavior (McDaniel, 1987). Though propped fracture conductivity has been shown to decline over time (McDaniel, 1987; Cobb et al., 1986; Knox et al., 1989), the corresponding fracture permeability of sintered bauxite remains relatively stable over long periods of time at elevated temperature and stress (Maurer Engineering Inc., 1981).

These observations make the case for using proppant because permeability degradation with time is impeded. The self-propped data shown indicate the substantially higher compressibility of the self-propped fracture, which is a reflection on the sensitivity to closure stress. It is a very important observation suggesting that self-propping may not be a realistic conductivity preservation technique. More testing would be required to be definitive, particularly situations where the shearing was done under in-situ conditions and the shear deformation was smaller than implemented in this testing program.

6.3 Postmortem Examination of the Self-Propped Sample

After the testing program, the sample was dismantled. Recall that there was no proppant present. The mated fracture faces created by splitting the core along its axis were kept apart by applying a small axial translation before jacketing the sample and installing it in the vessel. This simulated asperity override during shear displacement – argued to be a self-propping mechanism. Figures 6.3 through 6.5 are photographs taken after the testing program and document the fracture and the fracture faces.

The most surprising observation was that the fracture itself was filled with granite fines, as shown in Figure 6.4. This is anticipated to be one of the reasons that conductivity was nearly completely lost. This degradation dominantly happened when closure stress was raised to 3165 psi. This in itself is possible rationale for using proppant that can tolerate higher normal stresses than this.

In Figure 6.4, the sample had been opened up (still with the offset) and photographed. The majority of fracture surface in the figure is covered with wetted granite grains. After initial observations of the fracture faces, the granite debris was removed. Figure 6.5 shows the fracture faces with most of the granite fines removed by gentle sweeping. It is apparent that the surface of the "sheared" fracture had been degraded after only five days of exposure to stress and moderate temperature. Based on conductivity measurements, it appears that most of the conductivity loss occurred at the increased normal stress – at a value which is easily within the effective normal stress range that would be experienced in current geothermal operations.

Figure 6.3. This is a view of the outlet of the fracture- after testing of a proppant-free, translated fracture – tested to simulate what has been alleged to result as shear-induced self-propping due to asperity override at low normal stress. The orange strip is a flexible membrane installed along saw cut grooves (sawn to guide the fracture when the sample was mechanically split).

Figure 6.4. Granite fines – caused by fracture face degradation – are visible on the fracture surface (all dark areas encompassing nearly the entire fracture surface area). The sample has been removed from its jacket and rotated open.

Figure 6.5. Proppantless fracture after granite fines were removed, posttesting. Comparing the fracture face above to another similarly wedge-split sample by touch indicated that most of the bridging asperities during testing were fractured, creating the granite fines in the fracture that diminished conductivity.

6.4 Variable Proppant Concentration

Previous to the self-propped fracture experiments, the fracture had been filled with 2.74 lb_f/ft^2 of 30/60 sintered bauxite proppant and tested at temperature. Upon completion of this testing, the sample was taken from the vessel and the proppant in the middle of the pack was removed and saved for SEM analysis. The remaining proppant (which was still wet and adhering to the fracture surfaces) was left in place and the sample was reassembled – faces put back together – no offset, jacketed, installed in the vessel, replumbed, and tested. The new fracture width (unstressed) was approximately 0.07". The original unstressed fracture width (before removal of proppant) was 0.125", or 36% greater. The proppant concentration in the fracture was reduced from 2.74 lb_f/ft^2 to approximately 1.2 lb_f/ft^2.

Figure 6.6 is a permeability summary plot comparing the permeability of these proppant concentrations to the self-propped fracture at temperatures of ambient (~23°C) and 90°C.

All experiments presented in Figure 6.6 were tested at the temperatures and proppant concentrations shown. In addition to this, all experiments were performed at 2165 psi confining pressure and 165 psi pore pressure. As seen in Figure 6.6, the 1.2 lb_f/ft^2 proppant concentration permeability values does not deviate much from the values obtained for the proppant concentration of 2.74 lb_f/ft^2 (more than a monolayer present). The permeability of the experiment without proppant at ambient conditions, as anticipated, shows the highest permeability, an order of magnitude higher than the other experiments.

The 90°C test presented without any proppant was taken to be the data 72 hours after testing had begun, from the previous section. These data were selected as being representative due to similar normal stress conditions to the proppant filled fracture experiments and that it had settled after 72 hours of testing, as the values did not change much over an additional 72 hours of testing.

Because of the difference in proppant concentrations in the tests presented in this section, it is important to show a summary of the conductivity of the fractures due to the differing fracture widths. Figure 6.7 summarizes conductivity values for the differing proppant concentration tests – conductivity being the product of permeability and width. The majority of the error in the observed error bars occurs only on the proppantless fracture test, as any error incorporated in the conductivity was given by a slight variation in fracture width during testing.

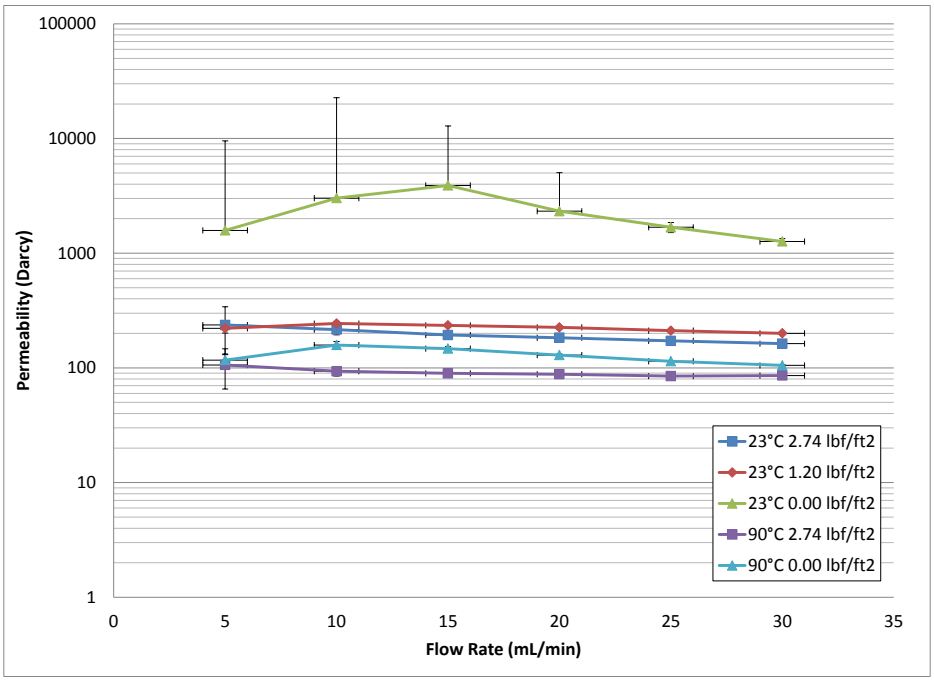

Figure 6.6. Permeability vs flow rate plot for various proppant concentrations. Conditions are noted in the legend, temperature is given first and then concentration of proppant in the fracture. 0.00 lb_f/ft^2 corresponds to the fracture that did not contain proppant.

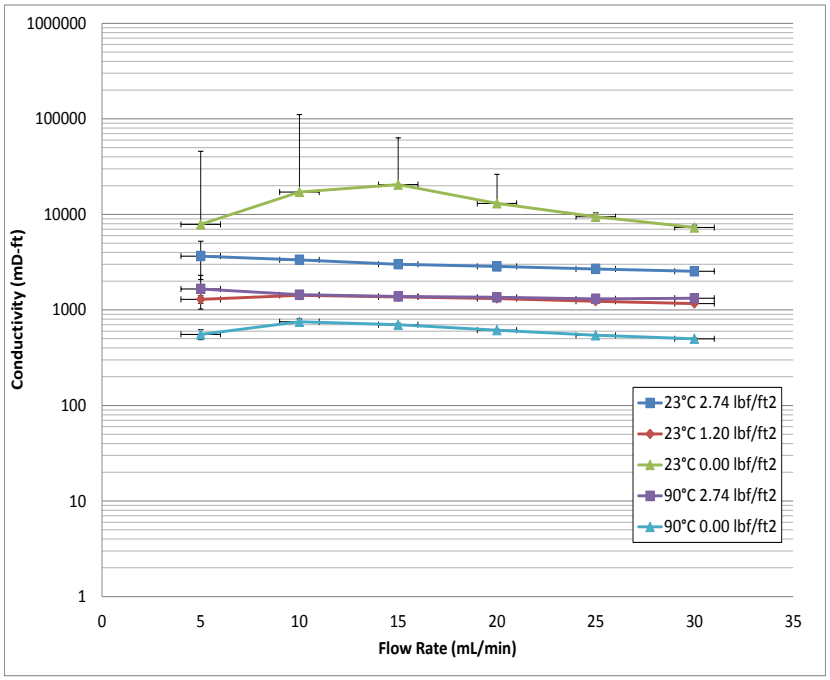

Figure 6.7. Conductivity (permeability multiplied by width) as a function of width for various proppant concentrations and temperatures.

Figure 6.7 shows:

- At ambient conditions and 2000 psi effective normal stress, the conductivity of the fracture that did not contain proppant is much higher than the proppant-filled fractures at the same stress and ambient or 90°C. This is an unrealistic scenario; however, all self-propped fractures will be near in-situ temperatures which will be much higher than 23°C.
- The conductivity of the lower concentration proppant test (reduced proppant concentration, rough surface) at ambient temperature conditions is comparable to the conductivity of the rough surface, at the higher proppant concentration (2.74 lbm/ft^2) at 90°C, showing that when a fracture contains more than a monolayer, the fracture conductivity is dominated by the porosity and strength of the proppant.
- The similar conductivity values for the proppant filled fractures indicates that even at lower proppant dispersion in the fractures in the reservoir, the fracture conductivity will be maintained as long as the concentration is greater than a minimum concentration that is determined by the conditions of the reservoir.
- Literature has shown that the fracture conductivity of fractures containing proppant reduced at higher temperature. This is seen by comparing the conductivity at ambient temperature and at 90°C at a concentration of 2.74 lbm/ft^2.
- The self-propped fracture at 90°C has lower conductivity values than all of the proppant filled fracture conductivities. Realistically, a self-propped fracture will be at elevated temperature; this result argues that proppant must be used to maintain fracture conductivity in a geothermal scenario.

6.5 Summary

At an effective confining stress of 2000 psi and 90°C, it was found that in the case of asperity dominated conductivity in a self-propped fracture, the stress was high enough to crush asperities and cause shifting of the fracture faces to reach an equilibrium fracture width. Over the initial 72 hours of testing (24 hours at 23°C and 48 hours at 90°C) the equilibrium permeability and conductivity values of the self-propped fracture were less than 10% of the values obtained after 24 hours of testing at 23°C. After an additional increase of effective normal stress to 3000 psi, the fracture asperities further crushed and the fracture reached a smaller equilibrium width. The result of which was further reduction in permeability and conductivity through the fracture. Postmortem examination of the fracture indicated extensive granite fine generation, which contributed to the large increases of differential pressure across the fracture. The granite fines in the fracture greatly reduced the permeability and conductivity through the fracture. Results of the self-propped fracture conductivity experiments argue that proppant is necessary for maintaining fracture conductivity in EGS systems.

Experimental results using different proppant concentrations indicate that as long as more than a monolayer of 30/60 sintered bauxite proppant was present in the fracture, the permeability was less sensitive to stress over time and maintained higher conductivity values than a self-propped fracture at elevated temperature. Though temperature effects and granite fines generation affect propped fracture conductivity, the conductivity of propped fractures is less susceptible to increases in stress and temperature over time and maintains adequate conductivity for geothermal energy production.

CHAPTER 7

POSTFRACTURE CONDUCTIVITY TESTING MEASUREMENTS AND ANALYSES

7.1 Optical Profilometry

A Zygo® optical profilometer was used to determine the roughness of the asperities on the samples tested. The optical profilometer uses scanning white-light interferometry to determine a 3D profile of the surface being analyzed. Scanning white-light interferometry combines a microscope and an interferometer to make roughness estimates over a surface area. A beam of white light passes through a filter and then a microscope objective lens to the sample surface. The white light is also sent to a beam splitter which is sent to a reference mirror which reflects the undisturbed white light to which the light reflected from the sample surface is compared. The light reflecting back to the surface is recombined with the reference beam and light and dark bands show up on the interferogram. The sample surface is then tilted slightly to create the largest, most visible bands in the area being analyzed. Once this is completed, a camera at the top of the microscope scans the surface and software interprets the peaks and valleys of the sample. Some filling information is usually incorporated in the gaps of data on the sample surface. Gaps arise from inadequate spacing of the fringes seen by the camera. Once the gaps had been filled in over the surface area, Metropro® software was used to

determine the average roughness over each spot tested on the samples. Metropro® analyzes roughness using both a root-mean-squared roughness and an arithmetic mean roughness. R_a is the arithmetical mean deviation of roughness from a standard calibrated plane. R_a is the calculated average roughness of all points deviating from a central line that goes through the middle of the data over the test length. Rms is the average of the measured height deviations taken within the evaluation length or area and measured from the mean linear surface. PV is the absolute value of the maximum peak to valley height over the sample area. A typical surface generated by the Metropro® software is presented in Figure 7.1.

Typically, the apertures on the sample that were not worn down by shearing were too large for the optical profilometer to interpret all of the gaps. While adequate fringes were obtained over the majority of the sample area, some areas could not be interpreted; an example of this is shown in Figure 7.2.

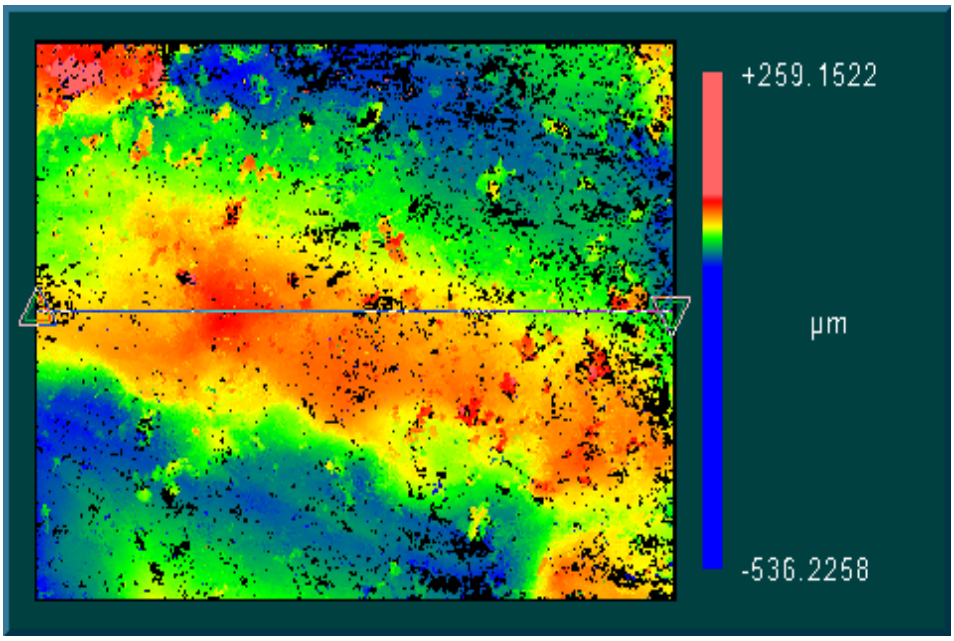

Figure 7.1. Surface from sample "2" Worn Down

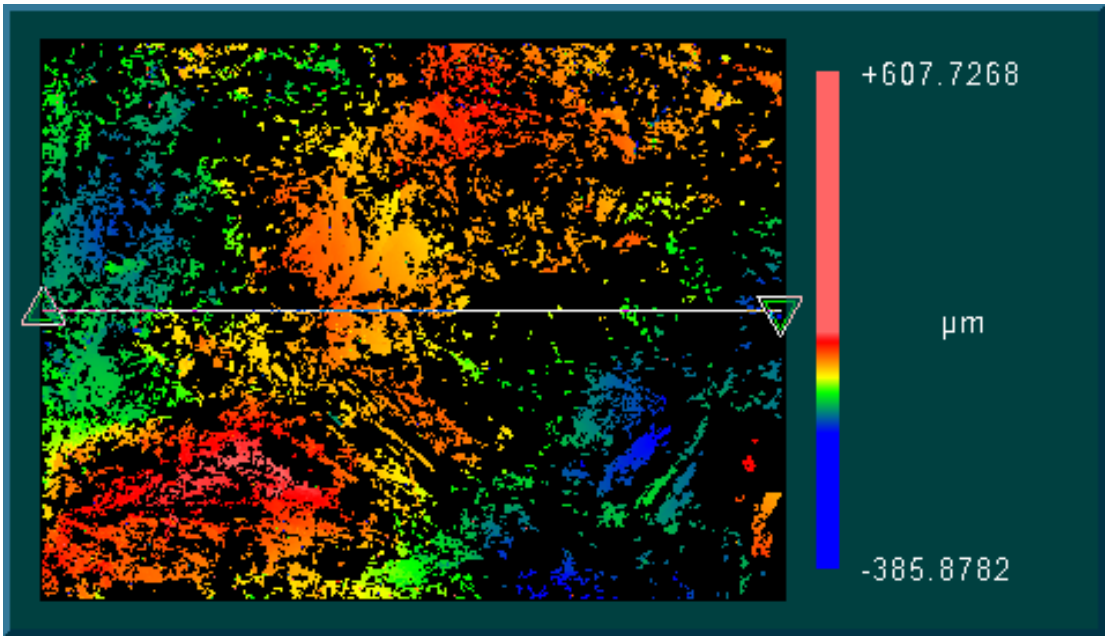

Figure 7.2. Sample 1, typical rough sample

Figure 7.2 has many more black areas where the surface roughness could not be interpreted by the software. In choosing the lines of interpretation across the area of the sample, lines were placed over the areas where more data were available.

A typical topography of the 1.5" sample is shown in Figure 7.3. The areas interpreted on the surface of the 1.5" sample were not as rough as in the 2.5" sample case, and looked more similar to the topography of the worn down 2.5" sample faces. Across the top of Figure 7.3 is what appears to be a band of static where individual points were interpreted to be much higher or lower than the surrounding points; this occurred in several of the samples taken and may have influenced the average PV values reported. Due to the manner in which the roughness parameters were calculated, a handful of these individual points did not drastically influence the roughness parameter results. In all sample cases, a line was drawn between the lowest and highest points on the sample in an effort to get the most accurate PV values, though in some of the other results, the

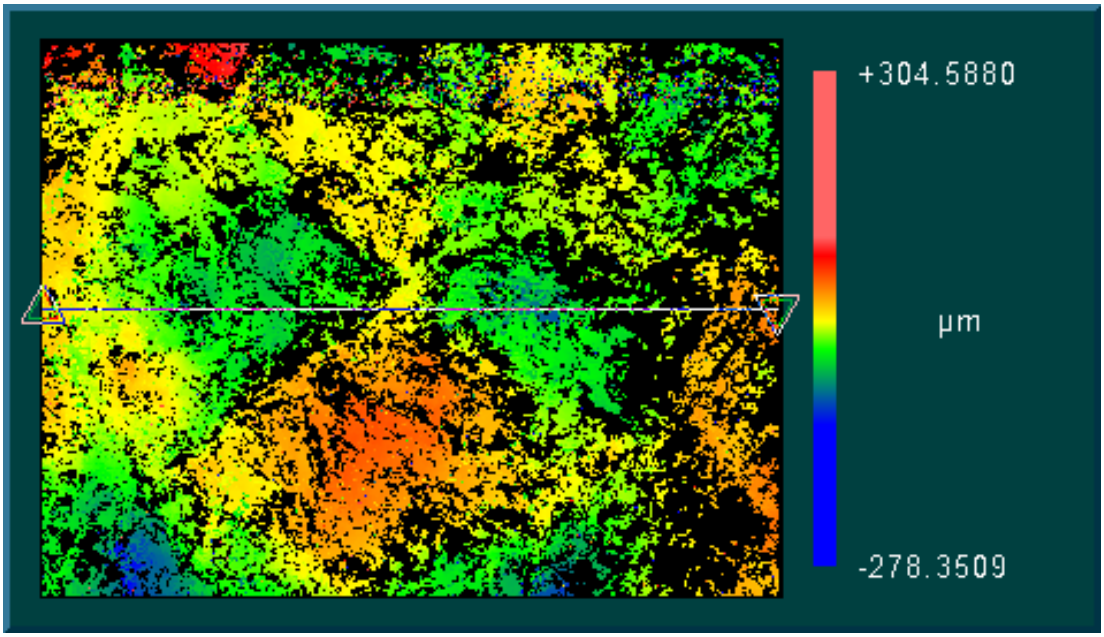

Figure 7.3. Typical topography of the 1.5" sample

individual high or low points may have been included in the interpretations and influenced the final average for PV. In addition to the high to low line, four more interpretations were drawn across each sample face.

Most of the areas of roughness interpreted on the samples were approximately 0.36 mm x 0.27 mm in area. Only twelve to fourteen samples were taken per core, six to seven samples per side. The samples could only be interpreted when reflectance of the white light on the sample was adequate to obtain well-spaced fringes on the sample face. All roughness interpretations were averaged per core and the results compared. The averaged results are presented in Table 7.1.

As shown in Table 7.1, the peaks and roughness were greater in the rough 2.5" diameter sample case than in the worn down or 1.5" diameter sample. The worn down 2.5" diameter sample refers to the sample used in all testing, including the testing without proppant which crushed many of the asperities off the face of the sample. The rough 2.5"

Table 7.1. Average Roughness Results from Optical Profilometry

Sample	PV (µm)	Rms (µm)	Ra (µm)
rough 2.5	201.2613	32.9294	25.47783
worn 2.5	182.5086	24.48512	18.82693
1.5 rough	151.7717	24.26965	19.69257

sample was a sample that was used as a baseline test as it was never used for proppant testing. As shown in Table 7.1, the 1.5" diameter sample is approximately as rough as the 2.5" diameter sample that was worn down, though the average height from the valley to peaks was higher for the 2.5" diameter sample.

The peak to valley values presented are much lower than the actual peak to valley height should be. Because the optical profilometer was limited to a height range on the order of a couple hundred micrometers, it could not read the resolution of the actual peaks to valleys. The values presented in the table are averages obtained over samples taken on the sample that contained operator bias in that the profilometer could not obtain any images on any areas that contained the larger asperities. Although there is bias in these results, it does indicate that the 2.5" sample that was tested and had asperities crushed did see a decrease in roughness and asperity height.

At the standard proppant concentrations tested, it is apparent that roughness of the fracture face does little to influence the conductivity values in the fracture. At proppant concentrations greater than 1 lb_m/ft^2, the proppant pack conductivity is dominated by the porosity and packing of the pack. Asperities on the fracture face contribute a higher probability of granite fines invading the pack and clogging the pore spaces in the proppant pack. Also, asperities are more likely to be dissolved over time as fluid comes in contact; this ultimately can reduce the conductivity by contributing silica to diagenetic reactions.

Posttest CT scanning of the sample did not reveal any additional microfractures or any compromising of the sample. Although additional microfractures did not form, the confining stress on the sample during the self propping testing was adequate to wear down the asperities on the face of the fracture.

7.2 CT Scanning

Some CT scanning was performed on the 2.5" diameter sample before it was tested without a proppant pack, the results show a microfracture that was probably created when the sample was split using a wedge. Figure 7.4 shows a top view of the sample, and Figure 7.5 shows a side view of the sample.

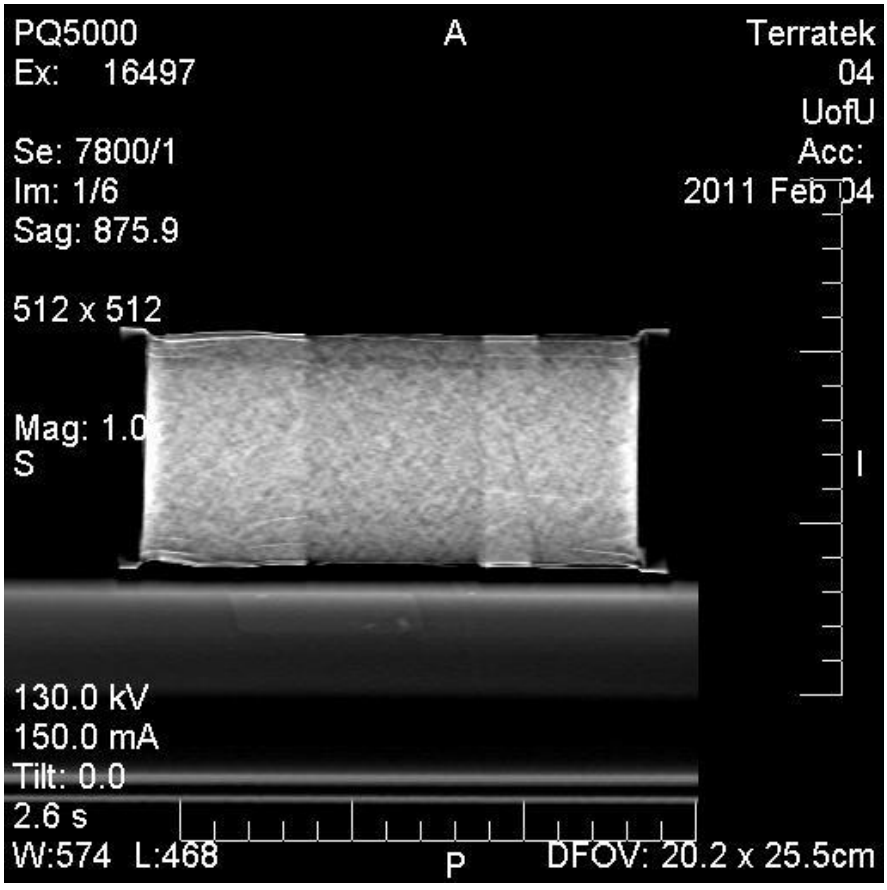

Figure 7.4. CT scan (top view).

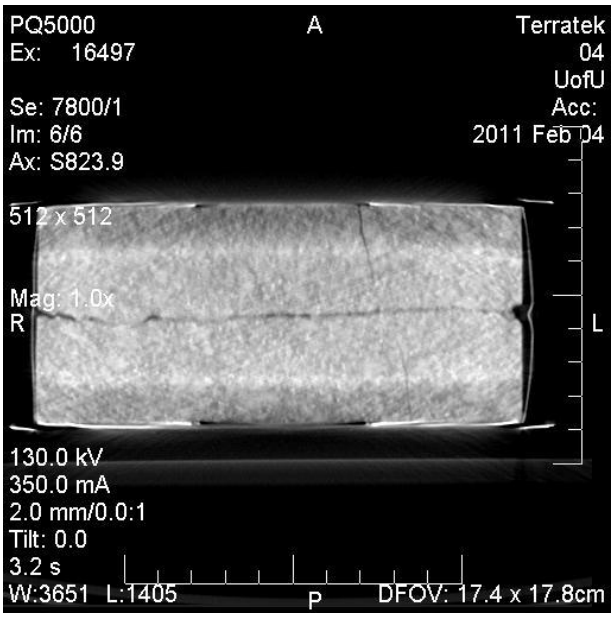

Figure 7.5. CT scan (side view).

7.3 Optical Microscope

The 30/60 Sinterball bauxite proppant was viewed under an optical microscope both before and after testing during one of the initial 1.5" saw cut experiments. Untested proppant is shown in Figure 7.6 followed by posttest images of granite fines and broken pieces of proppant.

The most notable posttest observation was chips of granite from the sample mixed in with the bauxite proppant. Figure 7.7 shows what appears to be one of these rock chips.

Figure 7.7 also shows close packed material, indicating the proppant particles were pressed together and clumped to a certain extent. The system did not appear to have been fully deoxygenated; rust formation was seen on a few of the proppant particles, as shown in Figure 7.8. Fractured proppant particles were also found under the microscope analysis; some of which are shown in Figures 7.9 and 7.10.

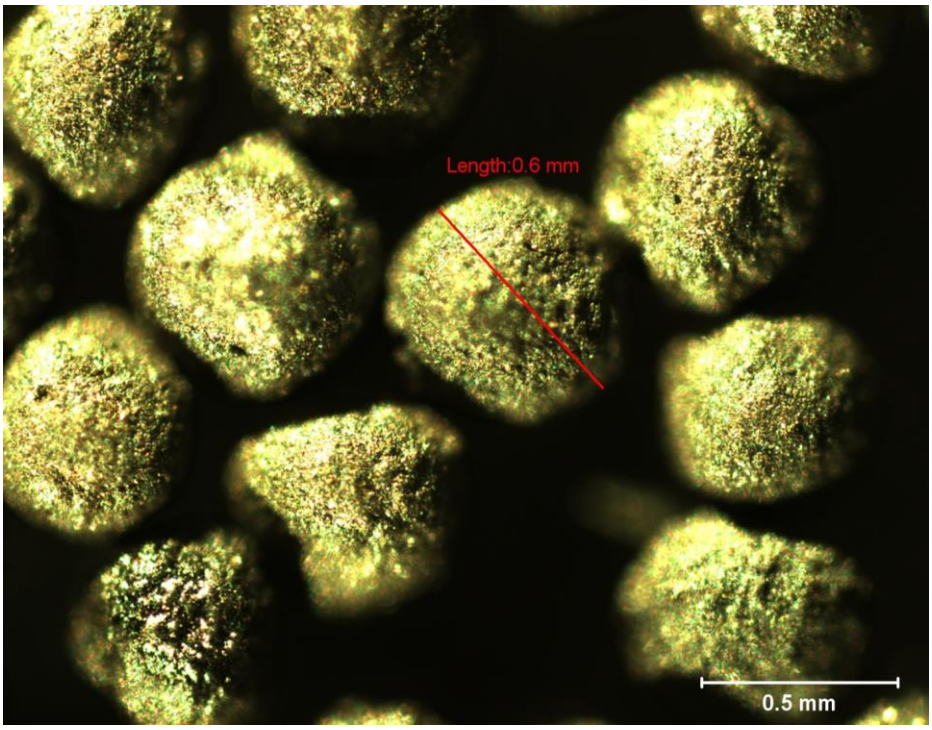

Figure 7.6. Untested Proppant 5x Magnification

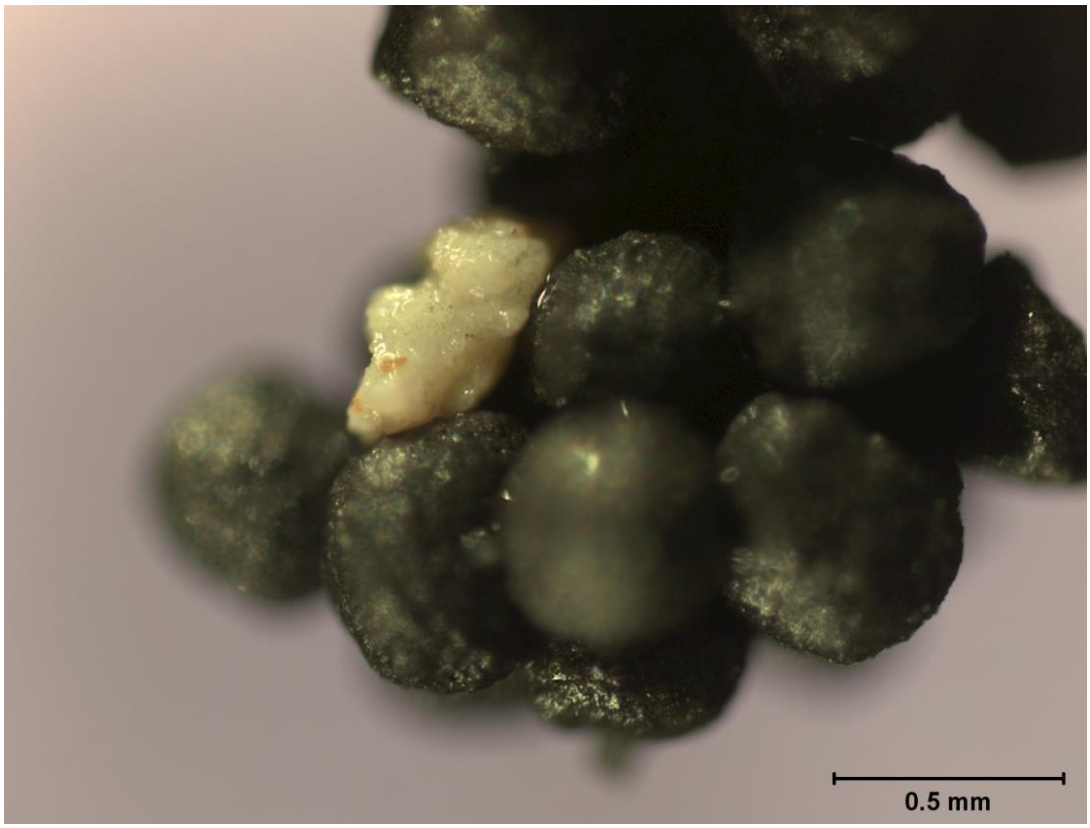

Figure 7.7. Rock Chip in Tested Proppant, 5x Magnification

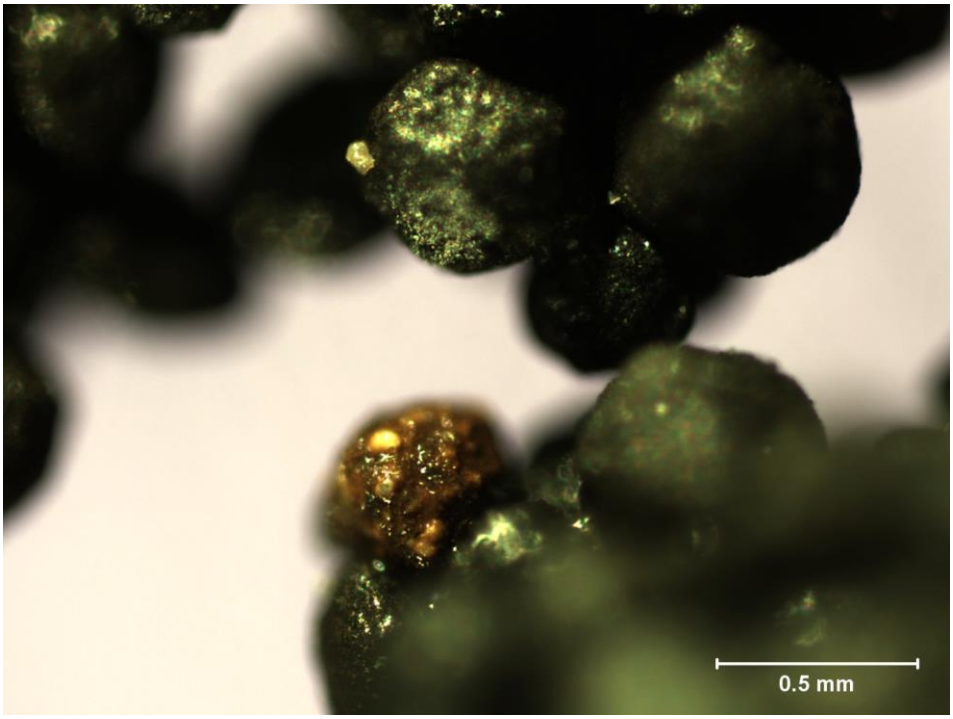

Figure 7.8. Rusted Proppant, 5x Magnification

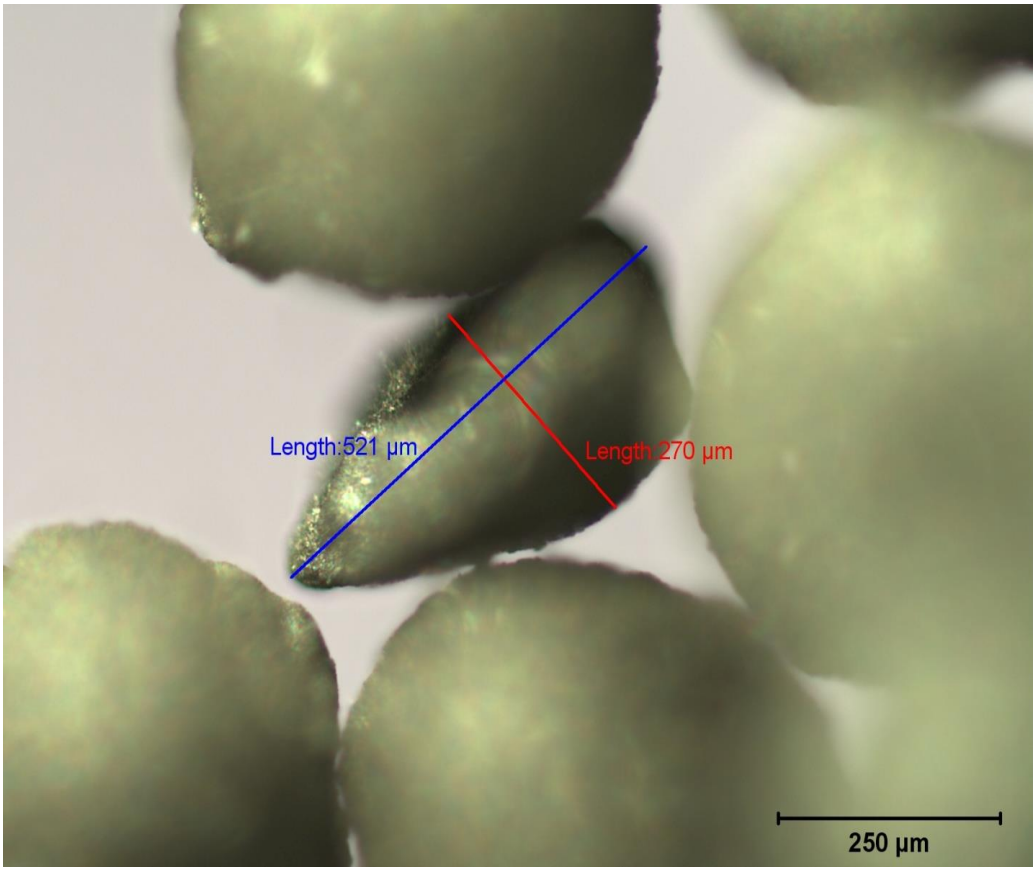

Figure 7.9. Fractured Proppant, 10x Magification

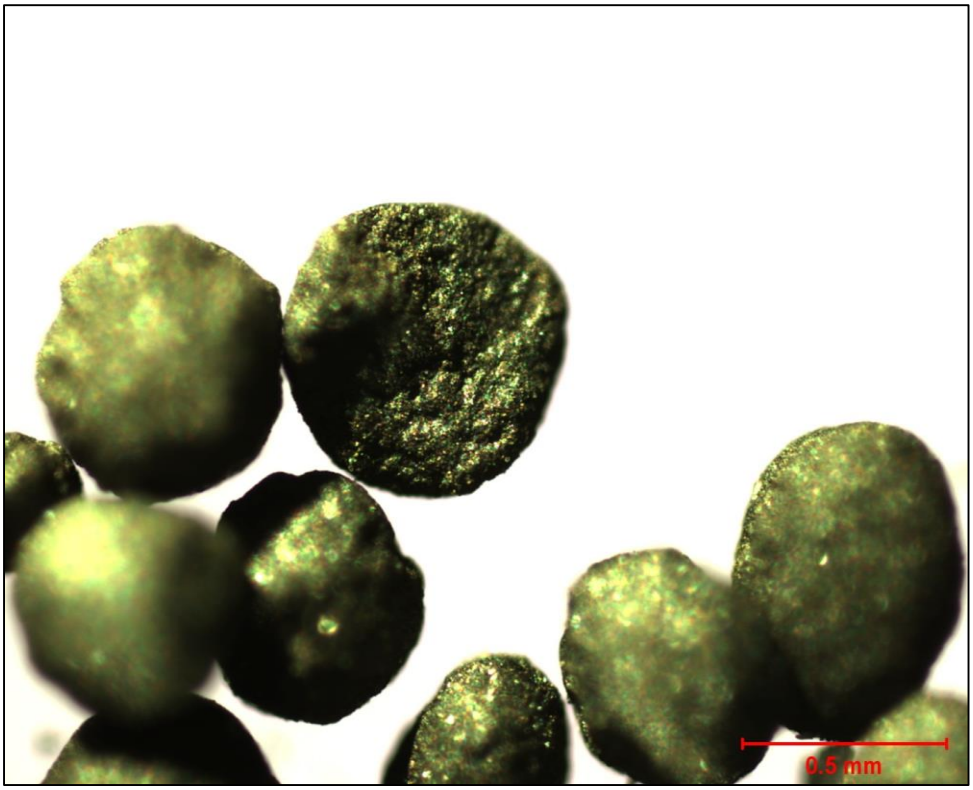

Figure 7.10. Fractured Proppant, 5x Magnification

Images from the optical microscope show that under the moderate stress scenario of 2000 psi, the proppant was crushed and the reservoir rock experienced some spalling. In addition, the addition of water at elevated temperature clumped the proppant pack to a certain extent, thereby lowering the permeability. Although the proppant crushing, rock spalling, and proppant clumping were not quantified, it is assumed that the extent of all was not great. These images indicate that such phenomena did occur, however, and give an explaination for lower than expected permeability values measured.

7.4 Proppant SEM Evaluations

Some scanning electron microscopy (SEM) analyses were done on the proppant packs from both the 1.5” diameter and 2.5” diameter samples. In both cases, characteristics that indicated dissolution were seen on the proppant surfaces. In addition

to the dissolutions observed, spheres of iron aluminum oxide, hypothesized to be hercynite, were also observed. Hercynite has the molecular formula $FeAl_2O_4$ and is classified as being in the spinel group of minerals. The spinels are any of a class of minerals with the general formula $A^{2+}B_2^{3+}O_4^{2-}$ which crystallize in a cubic crystal system. In the crystal system, the oxide anions arrange in a cubic close-packed lattice and the cations occupy some or all of the octahedral and tetrahedral sites in the lattice.

The hercynite formed at temperature and pressure created void filling spheres that reduced the porosity of the proppant pack over time and thereby contributed to diminishing the conductivity of the proppant pack over time. Additional dissolution and reprecipitation in the pore spaces is also hypothesized to have decreased the porosity through the proppant pack. Figure 7.11 shows hercynite on the proppant surface.

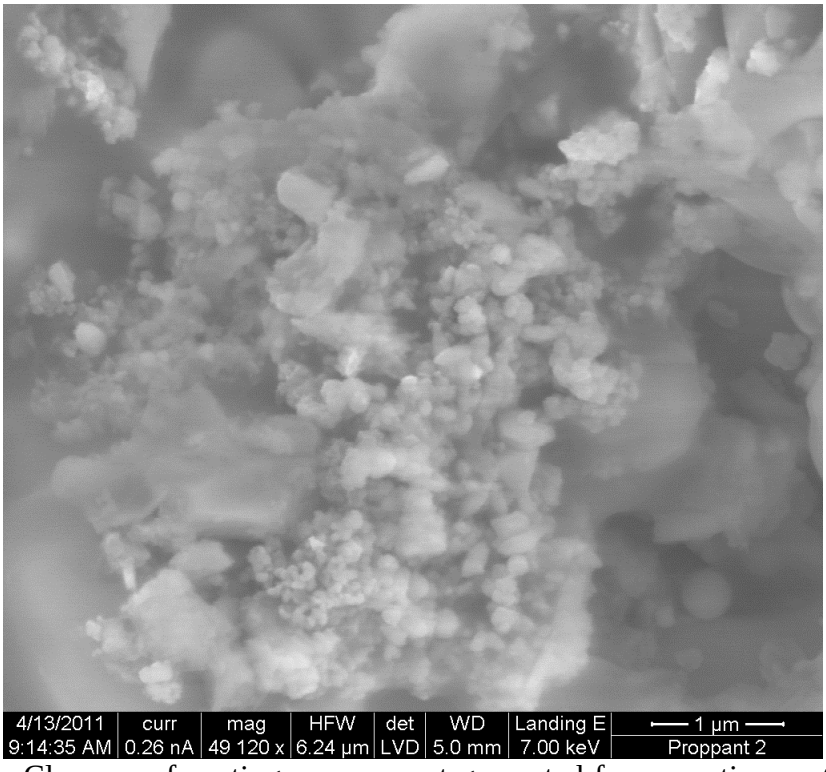

Figure 7.11. Close up of coating on proppant generated from reaction; note the sphere and glassy overlay

The overlay in Figure 7.11 was not attributed to charging but to a glassy imaging of a potential over lay of amorphous silica. On the bottom right hand side of the figure, a sphere was apparent. In the middle of the figure, granite chips are seen on the proppant sample, most with dissolution characteristics. Typical dissolution characteristics that were observed in SEM of all proppant samples are shown in Figure 7.12

Dissolution characteristics on the proppant face are characterized by the long clump groups of crystals shown in the above figures. These crystals were observed on proppant samples from all tested proppant packs. Figure 7.13 through Figure 7.15 depict some of the dissolved aluminosilicates on the proppant surfaces.

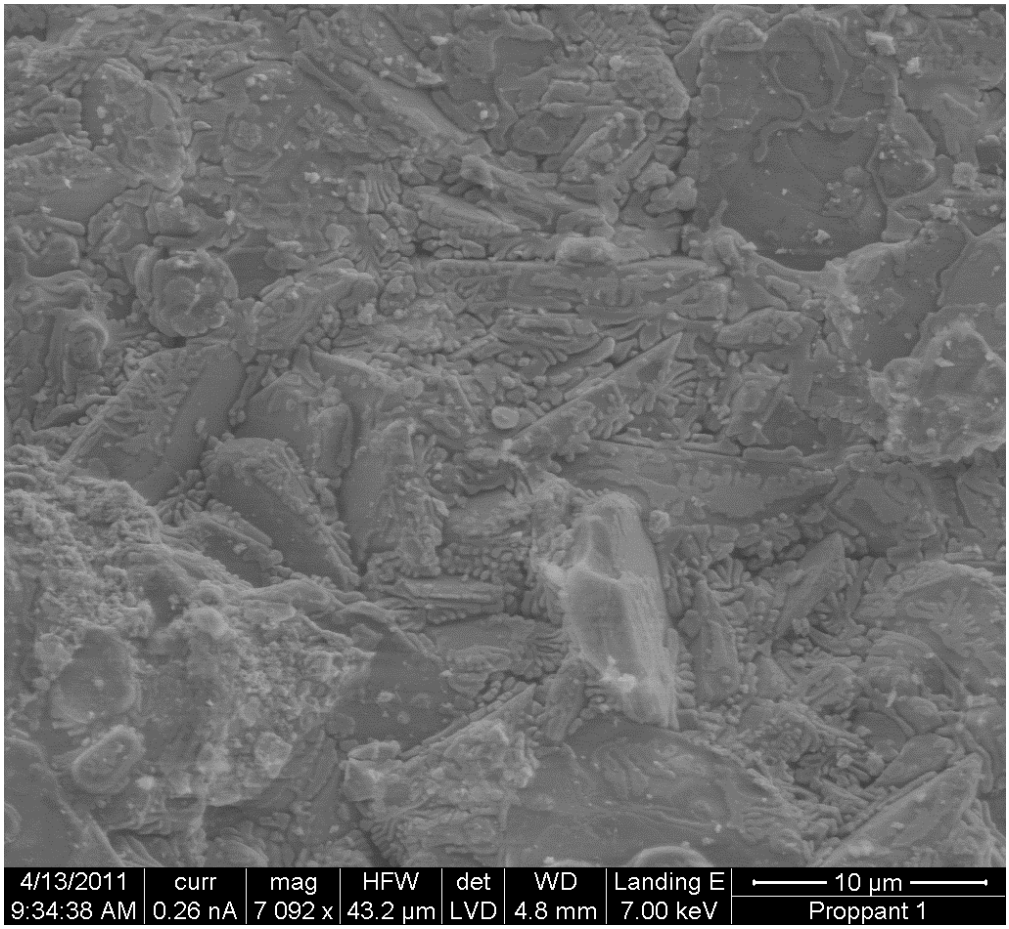

Figure 7.12. Dissolution of proppant, sample taken near rock face from 2.5" sample

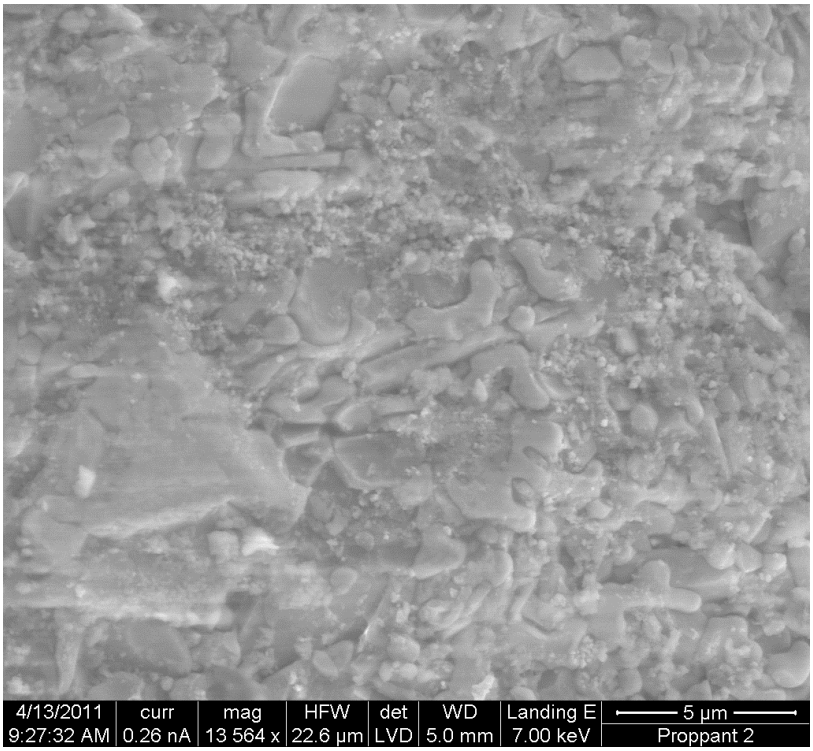

Figure 7.13. Reaction coating on proppant, dissolution, small sphere near the middle.

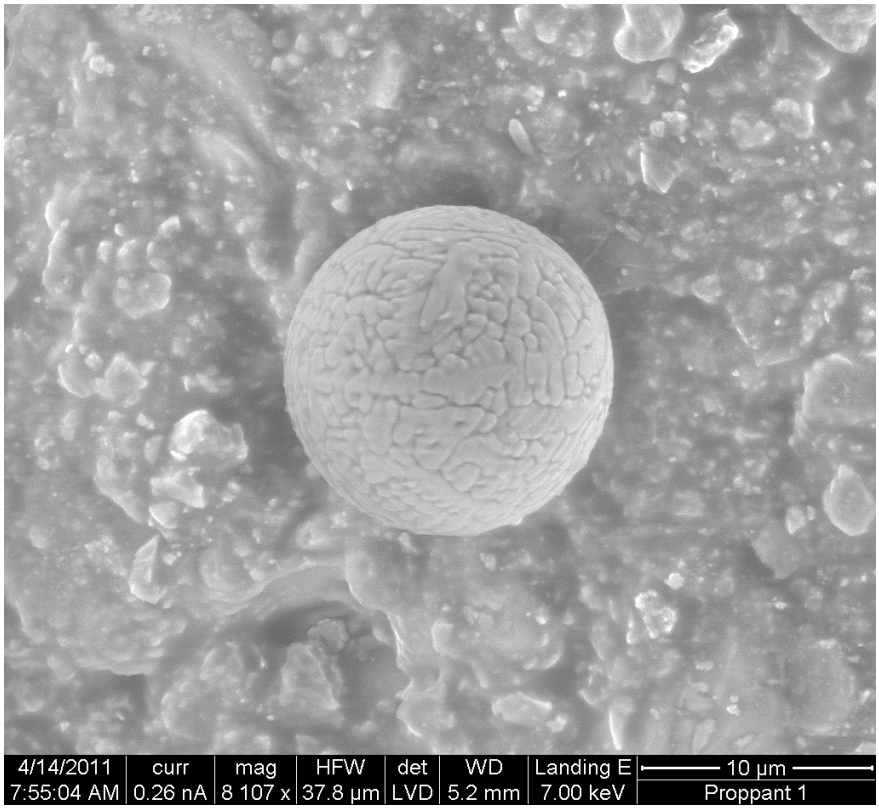

Figure 7.14. Coating on sphere and on proppant, iron rich

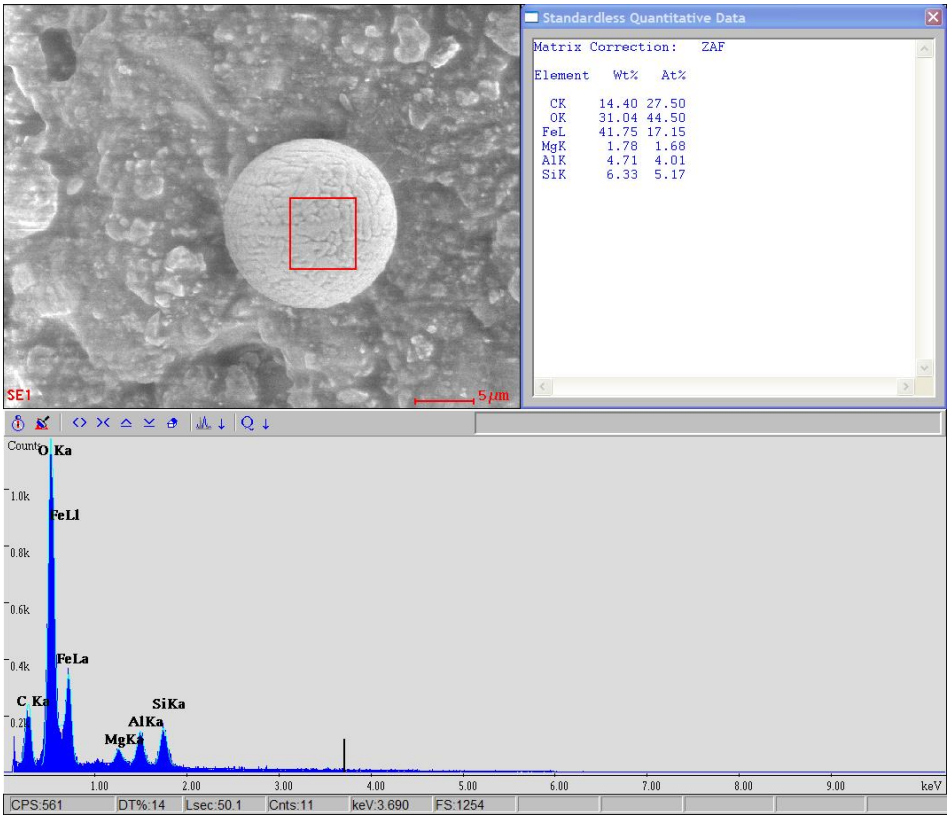

Figure 7.15. Refer to Figure 7.14

Alumina from the proppant was dissolved from the proppant and precipitated on the outside of the proppant sphere when oxygen and silica from the core sample created an aluminosilicate.

The ratio of Si+Al to oxygen given from the energy dispersive x-ray spectroscopy (EDX) on the sphere in Figure 7.15 indicates that the precipitated spheres correspond to the ½ ratio which are characteristic of zeolites (Byrappa and Yoshimura, 2011). To determine the composition of the sample using EDX, a high-energy beam of x rays is focused onto the sample. The atoms within the sample are in their ground state at discrete energy levels previous to excitation from the beam. As the electrons are excited, they are emitted, leaving a hole. An electron from the outer, higher-energy shell fills the

hole and the difference in energy between the excited and unexcited shells is measured and elemental composition is determined.

Figures 7.16 and 7.17 show that granite fines were generated during testing and stress from compression within the pressure vessel crushed some asperities from the sample face.

The embedment of the sphere on the surface of the agglomeration of granite and proppant pieces indicates that the spheres are formed through reprecipitation at locations where proppant and silica from the core sample become saturated, much as described by Weaver et al. (2006) in his pressure solution model for diagenesis.

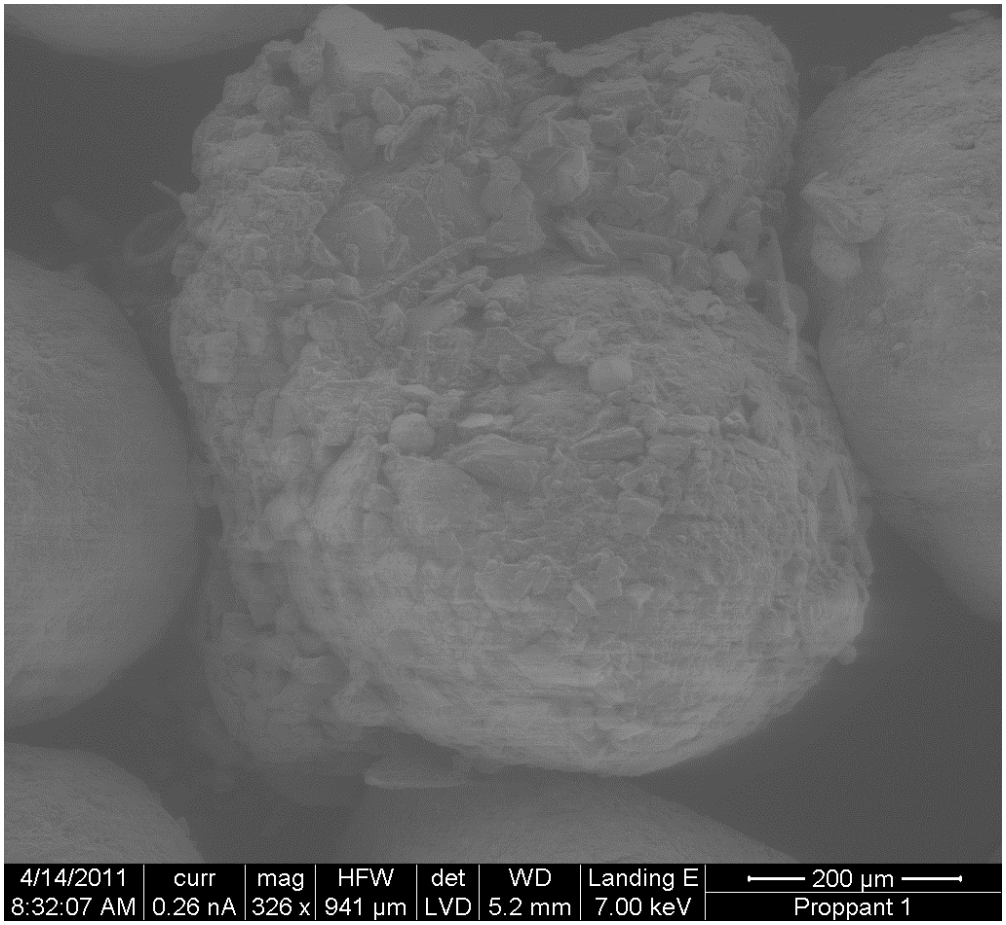

Figure 7.16. Agglomeration of poorly formed proppant particle(s) and granite

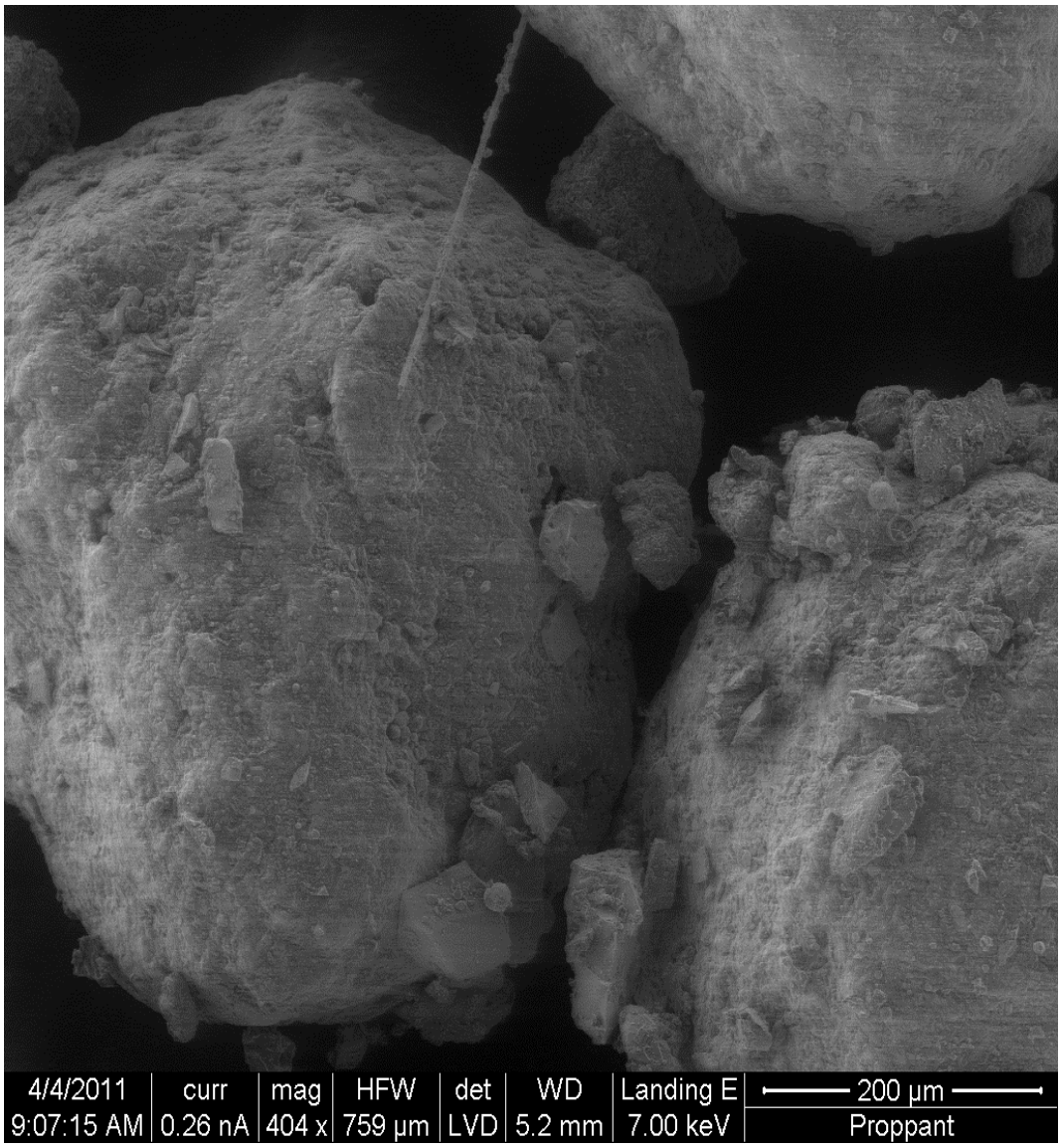

Figure 7.17. Proppant particle with small granite grains surrounding the surface; also of interest is the fiber in the top of the image.

The granite fines on the surface of the proppant particles analyzed by SEM validate that asperities of the sample faces were crushed during testing. These granite fines ultimately reduced the porosity of the proppant pack and lowered the conductivity of the fracture.

Figure 7.18 and 7.19 depict some of the other interesting observations from SEM analysis. Several of the objects may be from contamination.

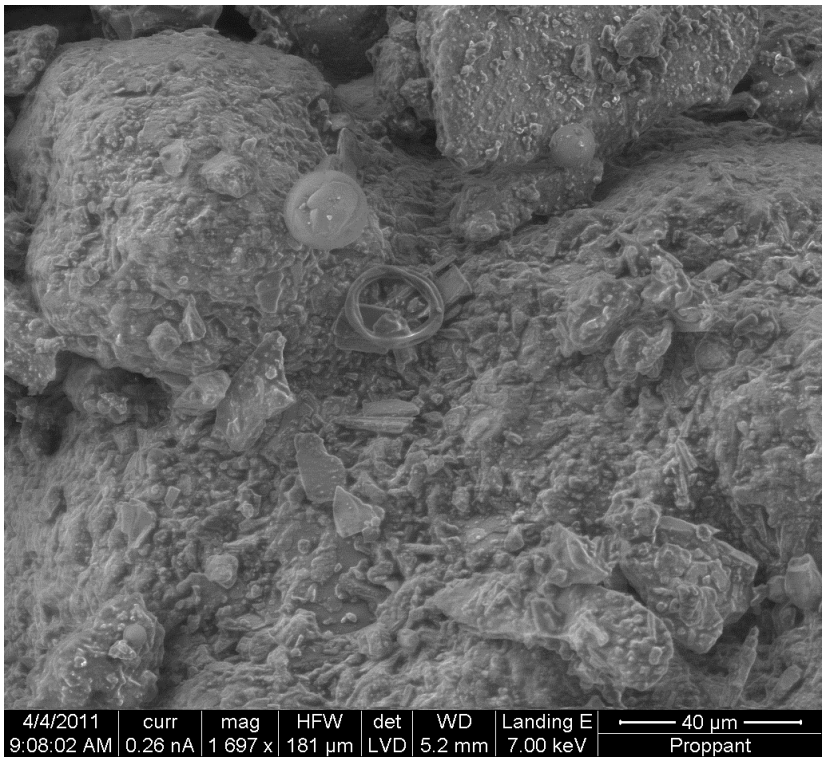

Figure 7.18. Interesting looped fiber in the center, also, two spheres on the sides.

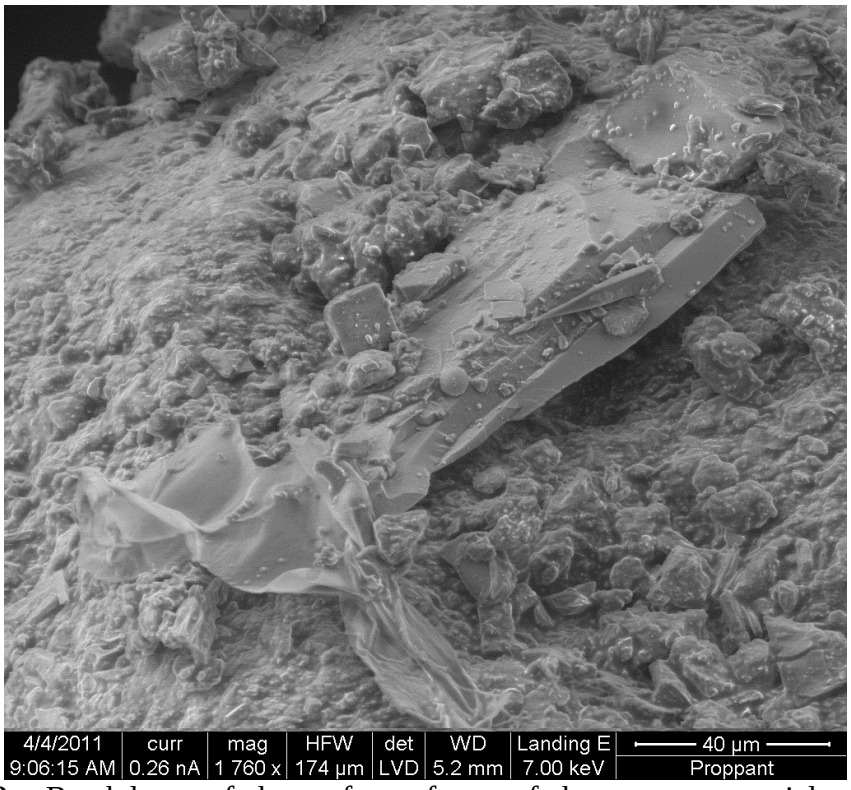

Figure 7.19. Breakdown of the surface of one of the proppant particles, large clay protrusion and some dissolution on the sides.

7.5 Core Sample SEM Evaluations

Limited embedment of the proppant may have created the indentions on the 1.5" core sample, as shown in Figures 7.20- 7.22. Compressed granite fines within valleys on the face of the core sample were observed, as shown in Figure 7.22. In addition to the compressed granite fines observed, there were limited observations of possibly precipitated zeolites that had precipitated from the proppant and attached themselves to the face of the core samples. These precipitates were observed primarily only within the proppant and were not found on the original untested granite core faces.

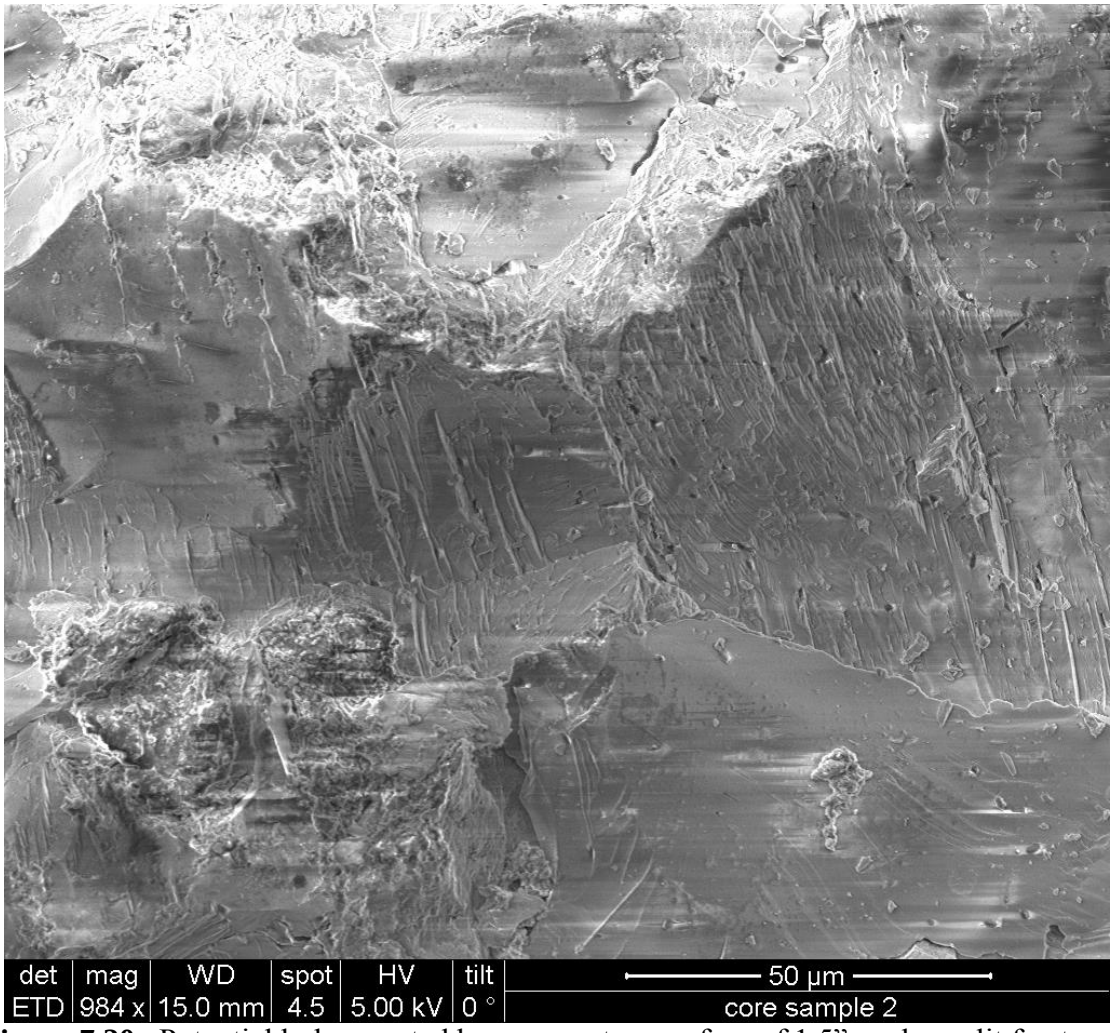

Figure 7.20. Potential holes created by proppant on surface of 1.5" wedge split fracture

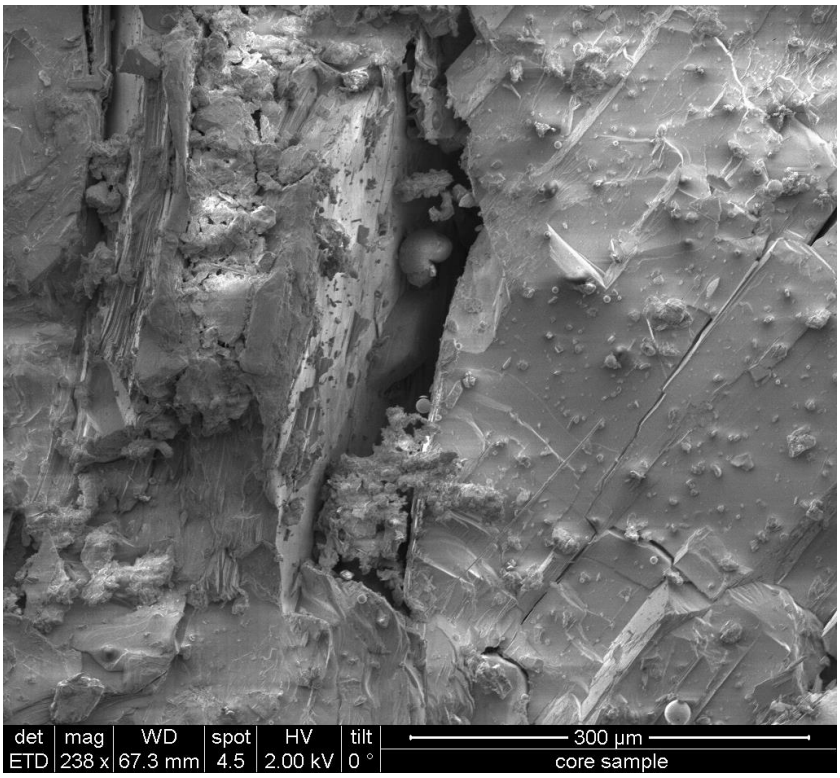

Figure 7.21. 2.5" wedge split fracture surface. Note the spheres on the surface and the large tree like structure in the middle.

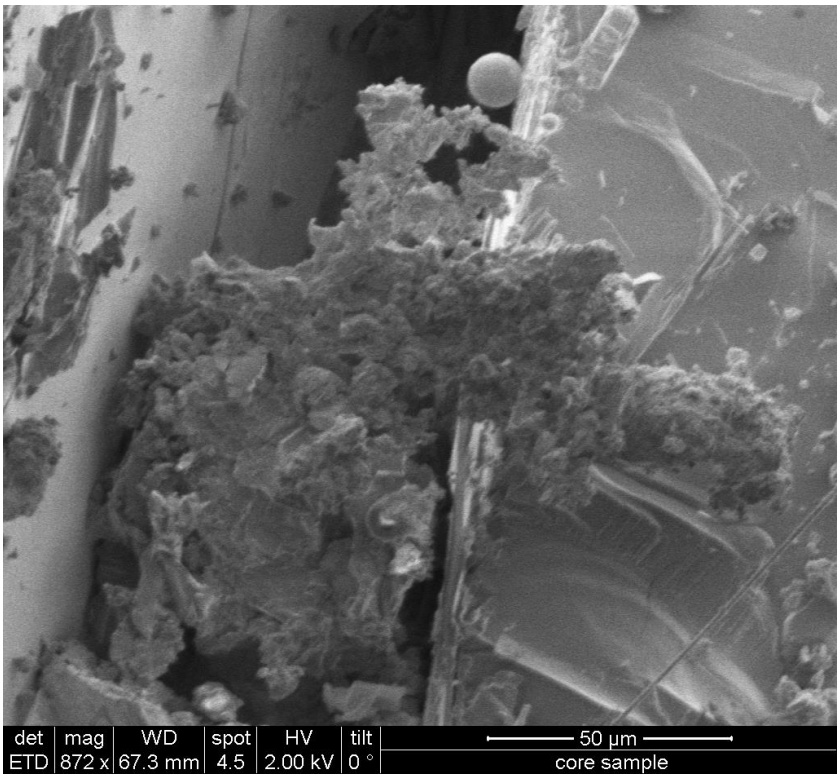

Figure 7.22. Potential granite fines compressed together.

CHAPTER 8

CONCLUSIONS

8.1 Conclusions and Recommendations

Limited testing completed on self-propped fractures indicates that under moderate stress scenarios, the conductivity of the fracture is compromised from asperity crushing. In addition to asperity crushing, elevated temperature fluid in the fracture facilitates dissolution of the asperities. The results from the self-propped experiments suggest that proppant is necessary for maintaining fracture conductivity in geothermal fractures for extended amounts of time.

Water at elevated temperature contacting the sintered bauxite proppant lowered the permeability through the fracture. Multiphase effects were the dominant permeability reducing mechanism as the water was not deoxygenated previous to flowing through the fracture. Some testing at 95°C was completed without a back pressure regulator and the back pressure applied was not adequate during the 200°C testing to ensure single phase flow through the fracture. Consequently, the values presented at temperature may be much lower than expected downhole without multiphase flow.

Conductivity values obtained at ambient temperature are representative of the literature conductivity values released by the manufacturer. Conductivity values obtained at temperature are within the realm of numbers obtained at elevated temperature within the scientific community, and indicate that temperature does influence proppant

permeability by decreasing ultimate conductivity of the fracture. Although the conductivity values presented for all experiments at temperature are adequate and represent effective production in a geothermal well, the calculated values are higher than expected due to the unstressed fracture width being used in the calculations. Pack rearrangement, crushing of proppant and asperities, or proppant embedment under stress would decrease the fracture width. Even after consideration of the proppant pack width decreasing, it is still concluded that at these proppant concentrations, downhole fractures will produce to desired expectations of EGS stimulation. At lower concentrations (e.g., if the proppant does not disperse well in the fractures downhole or if there is proppant flow back), it is shown that while initial conductivity will be orders of magnitude higher for the initial couple of days, the conductivity will diminish to ineffective values over a short amount of time.

Observations from optical microscopy indicate that to some extent, proppant crushing did occur and granite fines were generated from potential embedment or spalling of granite fines from the surface. Also, the optical microscope indicated clumping of the proppant to a small extent, which my indicate dissolution and reprecipitation of material at the contact points between proppant particles. Observations from SEM indicate that extensive proppant dissolution was observed in all tested proppant samples. Also, reactions at high temperature produced porosity filling materials, which ultimately aided granite fines and multiphase flow in the fracture in decreasing conductivity. SEM observations also showed limited embedment of proppant in the surface of the samples, even at the low confining stress of 2000 psi.

Recommendations for future testing would be to ensure that adequate back pressure is maintained on the system to ensure that multiphase flow does not occur within the fracture. In addition to this, the water that is used for flow through the fracture needs to be deoxygenated. The cooling grooves on the pressure vessel need to be utilized to ensure that the o-rings do not fail at elevated temperature.

The results presented indicate that caution must be used when applying proppant lab data at ambient temperature to scenarios where elevated temperature and stress will be observed, as permeability is decreased with an increase in temperature. Also, many other effects such as fines migration in the proppant pack and non-Darcy flow that are typically not observed in lab testing will reduce ultimate conductivity downhole in hydraulically fractured systems.

APPENDIX

EXPERIMENTAL EQUIPMENT

A.1 Small Vessel

The small vessel was designed to accommodate samples with a diameter of 1.5". The small vessel was an existing vessel donated by Dr. Milind Deo for initial testing at low temperature. The pressure vessel, endcaps, and one of the retaining rings are shown in Figure A.1.

On the endcaps of the rock sample (metallic pieces at the top of Figure A.1, with orange silicone tape wrapped around them), small fixtures extrude to facilitate tightening, with a 5/8" wrench. This action turns the endcap-rock package in order to either help it be snug within the vessel or to pull the rock out after a test. A 1/8" Swagelok to 1/8" NPT fittings on the sides of the vessel was used to apply radial, hydrostatic confining pressure to the sample in the vessel.

The maximum length of core that could be accommodated in the small vessel was 7 inches. This small pressure vessel was rated to 5000 psig.

The orange silicon tape was used on the extruded portion in contact with the rock of the endcap to help seal the ends of the Teflon jacket securing the rock from the confining fluid. Although an o-ring was placed in a groove under the silicon tape (about

Figure A.1. Small Vessel System.

adequately seal the rock off from the confining fluid. Once confining fluid intruded the fracture of the sample the test would need to be terminated and restarted. Hose clamps were used to try and tighten the silicon tape and jacket on the o-rings on the protruding portion of the endcaps, but this was only marginally successful. Although there were two grooves for o-rings and back up rings, only one ring/back up ring system was used to prevent an accumulation of pressure between the two rings and eventual failure of the o-ring system.

Initially, a confining pressure of 3000 psi was planned for the confining pressure. This was downgraded when it was determined that the o-rings in the vessel could typically only accommodate a maximum confining pressure of approximately 2300 psi.

To ensure the o-rings did not fail, the confining pressure for all future testing in this vessel was reduced to 2000 psig. In order to complete the tests at temperature, new Viton® o-rings and teflon back-up rings were obtained. Previously, leakage in the vessel had been attributed to rubber o-rings; however, sealing problems persisted as the transition to viton o-rings was made. Most of the o-rings that had been used to obtain data at temperature failed as this vessel was not obtained for high temperature testing. The problems with the jacket sealing on the rock can be attributed to installation protocol. It was necessary to push the endcaps through the entire length of the vessesl body to install and seal the fracture package. As the trailing endcap slides into the vessel, it loosens the jacket on the metal endcap and allows for confining fluid to enter under the jacket and into the sample (when the confining pressure is applied). The issue with the o-rings sealing is unresolved, as they were rated to much higher differential pressure. One possibility is that there is a surface blemish on the inside of the tubular body of the vessel or potentially multiple blemishes. With the installation methodology, a scratch in the body (perhaps with an endcap) could potentially cut the o-ring. In order to run tests at temperature, it was decided to manufacture another vessel with improved sealing capacity and easier installation. It was also decided that larger diameter core samples would be tested and a larger diameter vessel was designed and fabricated.

A.2 Large Vessel

The larger vessel was designed to prevent the failure of the sealing o-rings. A cooling groove was added to maintain the o-ring temperature below the rated value of 200°C (for the Viton o-rings). The new endcap design eliminated the unintentional loosening of the jacket while pushing the endcap and rock system through the small vessel. The endcaps were designed with sufficient diameter for future testing with LVDTs (Linear Variable Differential Transformers) or similar fixtures installed to measure the strain of the sample during testing. The machine drawings for the large vessel are given in Appendix A. Figure A.2 shows the endcaps designed for the large vessel.

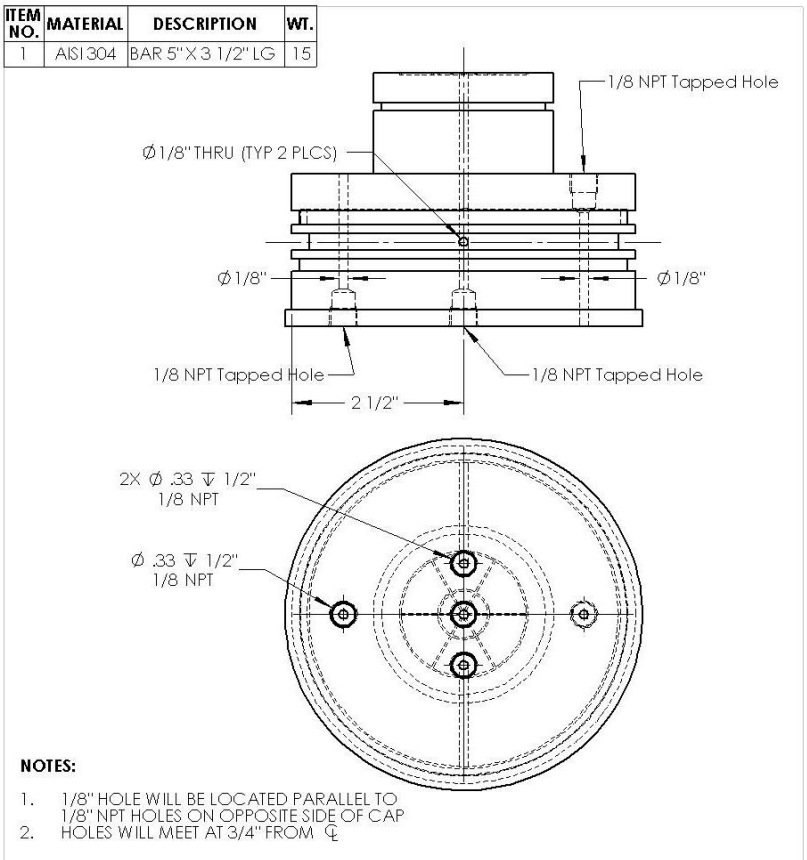

Figure A.2. Endcap Drawing

The endcaps that were installed at the upstream and downstream ends of the rock/proppant configuration were made from 316-stainless steel. As shown in Figure A.2, the 1/8" NPT tapped hole on the inside of the endcap (the side with the protruding face plate) was for a LVDT set up at some time in the future; this was not installed in the system for the measurements reported here. Two o-ring grooves were machined both above and below the center cooling groove with the hole drilled through it for cooling fluid flow. The outer o-ring was a safety precaution. The 1/8" NPT hole in the center of the endcap is for flow through the end cap and into the propped fracture. Tubing is connected to the end cap using a trheaded fitting. The other two 1/8" NPT holes were drilled so that cooling water could be pumped into the middle groove between the o-rings on the side of the endcap. One of the holes was connected to a tube which had cooling water flowing through it and the other hole was the outlet for the cooling groove. Finally, the last 1/8" NPT hole tapped was for confining fluid; the ISCO pump responsible for the confining pressure was connected to this through 1/8" Swaglok tubing. Figure A.3 is a photograph of the endcap/cooling goove assembly.

The groove on the protruding portion of the endcap is a tape groove, which is used instead of an o-ring groove. Silicon tape is placed in the groove and after the sample has been jacketed to the endcaps, tie wire is wrapped around the jacket and pinches it into the silicon tape, sealing the jacket from confining fluid.
Figure A.4 is a machine drawing of the endcaps. It shows the grooves on the faceplate. These grooves were similar to features in the smaller-diameter vessel. The two concentric circular grooves were connected by radial grooves. This ensured that

Figure A.3. Endcap, o-ring and cooling grooves

water is dispersed across the entire rock face, which allows for water to find the fracture even if the main source of flow (the hole in the center) is blocked - for any reason.

The floating endcap is the protruding portion of the stationary endcap. A 1/8" NPT hole was tapped in the opposite end of the partial sample. A 1/8" tube was connected with a threaded fitting. A central hole drilled through the stationary endcap (the 5" diameter portion) allowed a tube connected to the faceplate portion to be pushed through the hole in the 5" diameter portion and through a 1/8" NPT fitting. Figure A.5 presents a photograph of this endcap set up.

After core samples were placed on the endcaps they were placed within the pressure vessel. The floating endcap piece ensured that the entire core sample was unable to break away and rip the jacketing material holding the core sample in place.

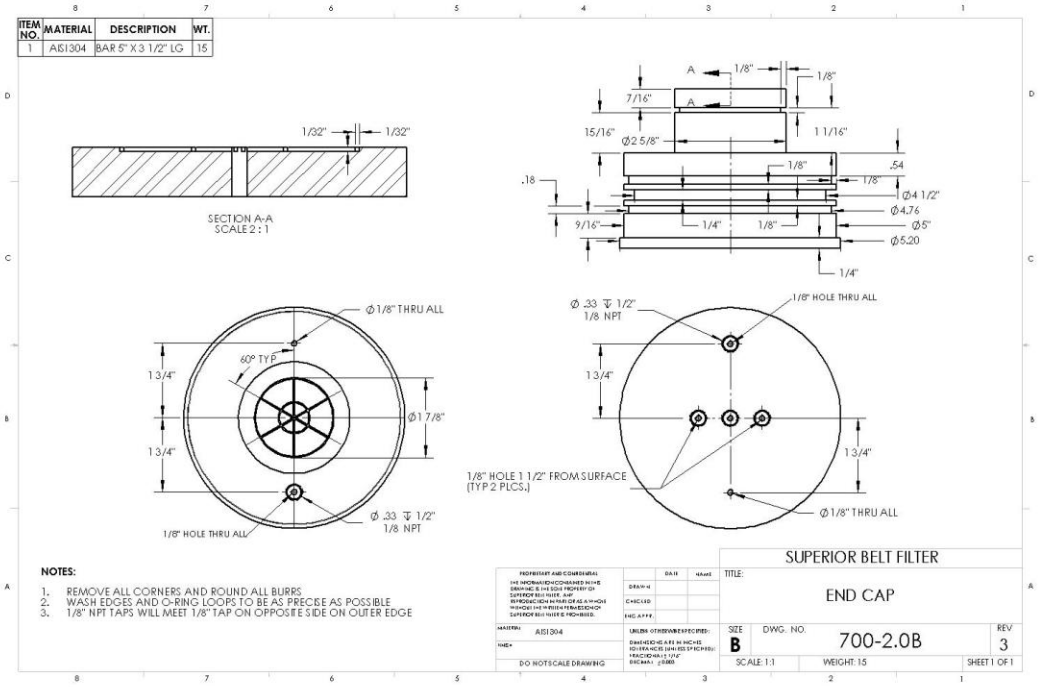

Figure A.4. Second Endcap Drawing

Figure A.5. Stationary and Floating Endcap in the Large Vessel Assembly

As shown in Figure A.5, the tape grooves were filled with silicon tape to seal the sample off from the confining fluid. After the sample was jacketed, tie wire was wrapped around those grooves. Tubing connected through the flow through portion of the endcaps was connected to a differential pressure transducer. Additional images of the endcap and floating endcap piece are shown in Figure A.6 through Figure A.8. The set up of both endcaps with a sample is presented in Figure A.8.

Figure A.6. Endcap with floating endcap piece.

Figure A.7. Back of the Endcaps, all holes are tapped for 1/8" NPT fittings

Figure A.8. Inside the vessel

Brass shim stock was used at the rock-endcap interface to prevent failure of the jacket at those points. The blue tape shown on the rock sample was used to similarly hold strips of brass shim stock in place along the sides of the fracture to prevent the confining stress from puncturing the jacket along the length of the propped fracture. After this sample preparation, tie-wire was wrapped around the jacket on top of the tape grooves, as covered by orange silicone tape in Figure A.8. Once the jacket had been wired on, the entire fixture (end caps, proppant sandwiched within granite half cores, jacketing, and tie wires) was placed in the pressure vessel and contained using the sealing end closures. Figure A.9 shows the machining diagram that the core sample was placed in for testing.

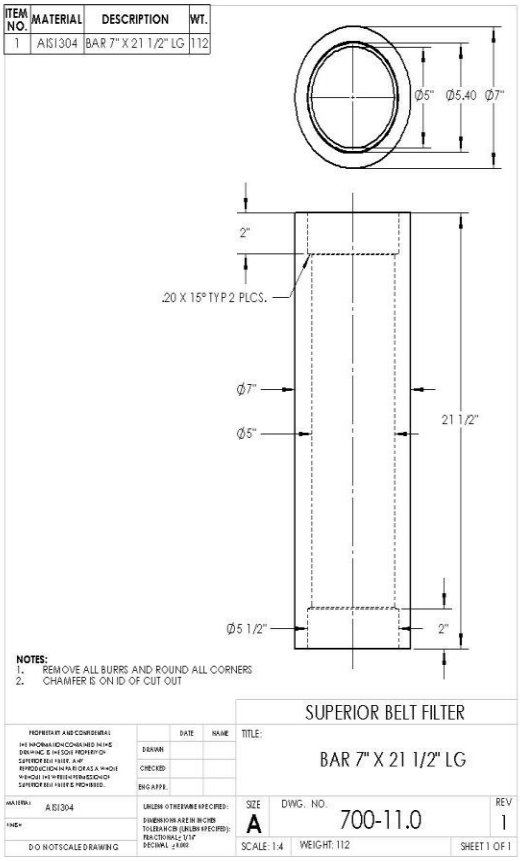

Figure A.9. Vessel

The body of the pressure vessel is made from 4140 heat treated stainless steel. The outer diameter is 7” and the inner diameter is 5”. Each end of the vessel body is internally threaded; the nominal diameter of the threaded section is 5.5”. These threads allow end closures to be threaded in. The threads are 0.2” in depth, 12 threads per inch. The end closures (Figure A.10) are doughnut shaped with an outer diameter of 5.5” and 4” outer diameter. These end closures are 2” in height. Each end closure has two slots on the outside flat face. These mate with a customized two-pronged wrench for tightening them down and isolating the confining pressure against the sample vessel. The sealing rings were also made from 316-stainless steel.

Figure A.10. Sealing Rings

REFERENCES

American Petroleum Institute: Recommended Practices for Evaluating Short Term Proppant Pack Conductivity. API RP 61, Oct. 1989

Andrews: Bauxite Proppant, United States Patent 4,713,203, December 15, 1987

Atteberry, R.D., Tucker, R.L., Ritz, J.W. 1979: Application of Sintered Bauxite Proppants to Stimulation of Low Permeability South Texas Gas Reservoirs. SPE Paper 7924 presented at the 1979 SPE symposium on Low-Permeability Gas Reservoirs. Denver, Colorado, May 20-22, 1979

Barree, R.D., et al.: 2003: Realistic Assessment of Proppant Pack Conductivity for Material Selection. SPE Paper 84306 presented at the 2003 Annual Technical Conference, Denver, CO, October 5-8

Campbell, D., Hanold, R., Sinclair, A., & Vetter, O. (1981). A Review of the Geothermal Well Stimulation Program. *International Geothermal D r i l l ing and Completion Techno1 ogy Conference.* Albuquerque, NM.

Cinco-Ley, H., & Samaniego V., F. (1977). Effect of Wellbore Storage and Damage on the Transient Pressure Behavior of Vertically Fractured Wells. *SPE Annual Fall Technical Conference and Exhibition.* Denver, CO.

Cobb, S.L, and Farrell, J.J 1986: Evaluation of Long-Term Proppant Stability. SPE paper 14133 presented at the International Meeting on Petroleum Engineering.

Cooke, C.E. 1973: Conductivity of Frature Proppants in Multilayers. Journal of Petroleum Technology. (September 1973) 1101-1107

Dueneckel, R., Conway, M.W., Eldred, B., Vincent, M.C. 2011. Proppant Diageneis-Integrated Analyses Provide New Insights into Origin, Occurrence, and Implications for Proppant Performance. Paper SPE 139875 presented at the SPE Hydraulic Fracturing Technology Conference, The Woodlands, Texas, USA, 24-26 January.

Fitzgibbon, J.J.,: Sintered Spherical Pellets Containing Clay as a Major Component Useful for Gas and Oil Well Proppants, United States Patent 4,427,068, January 24, 1984.

Fredd C.N., McConnell, S.B., Boney, C.L., England, K.W. 2000: Experimental Study of Hydraulic Fracture Conductivity Demonstrates the Benefits of Using Proppants. SPE Paper 60326 presented at the 2000 SPE Rocky Mountain Region/Low Permeability Reservoirs Symposium held in Denver, CO, 12-15 March.

Hanh, G., 1986: How Long Will it Prop? Drilling, the Wellsite Publication. Vol 47, No. 6, Issue 596, April 1986.

Heunges, E. (. (2010). *Geothermal Energy Systems - Exploration, Development, and Utilization.* Weinheim: WILEY-VCH Verlag GmbH & Co. KGaA,.

International Organization for Standardization: Completion fluids and Materials – Part 5: Procedures for measuring the long-term conductivity of proppants. ISO 13503-5 2006.

Knox, J.A. and Weaver, J.D. 1989: A Solution to Proppant Dissolution in Hydrothermal Environments. Proceedings of the Fourteenth Workshop on Geothermal Reservoir Engineering, Stanford University, Palo Alto, California, USA, January 24-26, 1989.

Legarth, B., Tischner, T., & Huenges, E. (2003). Stimulation Experiments in Sedimentary Low-Enthalpy Reservoirs for Geothermal Power Generation in Germany. *Geothermics, 32*((4-6)), 487-495.

Legarth, B., Huenges, E., & Zimmermann, G. (2005). Hydraulic fracturing in a sedimentary geothermal reservoir: Results and Implications. *International Journal of Rock Mechanics & Mining Sciences, 42*, 1028-1041.

Lunghofer, E.P.: Process for the Production of Sintered Bauxite Spheres, United States Patent No. 4,440,886, April 3, 1984.

Maurer Engineering Inc. Geothermal Fracture Stimulation Technology: Volume 4. Proppant Analysis at Geothermal Conditions; DOE/AL/10563-T8 (Vol. 4): US Department of Energy, January 1981.

McDaniel, B.W. 1986: Conductivity Testing of Proppants at High Temperature and Stress. SPE Paper 15067 presented at the 56th California Regional Meeting, Oakland, April 2-4

McDaniel, B.W. 1987: Realistic Fracture Conductivities of Proppants as a Function of Reservoir Temperature. SPE/DOE Paper 16453 presented at the SPE/DOE Low Permeability Reservoirs Symposium held in Denver, CO, May 18-19.

Montgomery, C.T. and Steanson, R.E. 1984: Proppant Selection – The Key to Successful Fracture Stimulation. SPE paper 12616 presented at the Deep Drilling and Production Symposium, Amarillo, TX April 1-3

Morris, C.W., and Sinclair, A.R. 1984: Evaluation of Bottomhole Treatment Pressure for Geothermal Well Hydraulic Fracture Stimulation. *Journal of PetroleumTechnology,* 36(5), 829-836

Palisch, T.T., Duenckel, R., Bazan, L., Heidt, H., and Turk, G., 2007: Determining Realistic Fracture Conductivity and its Impact on Well Performance—Theory and Field Examples. SPE Paper 106301 presented at the 2007 Hydraulic Fracturing Technology Conference, College Station, TX, Jan 29-31.

Reinicke, A., Zimmermann, G., Huenges, E., & Burkhardt, H. (2005). Estimation of Hydraulic Parameters after Stimulation Experiments in the Geothermal Reservoir Groß Schönebeck3/90 (North-German Basin). *International Journal of Rock Mechanics and Mining Sciences, 42*(7-8), 1082-1087.

Vincent , M.C. 2009: Examining our Assumptions – Have Oversimplifications Jeopardized Our Ability to Design Optimal Fracture Treatments? Paper SPE 119143 presented at the 2009 Hydraulic Fracturing Technology Conference, The Woodlands, Jan 19-21.

Weaver, J.D., Nguyen, P.D., Parker, M.A., and van Batenburg, D. 2005. Sustaining Fracture Conductivity. Paper SPE 94666 presented at the 6th SPE European Formation Damage Conference, Scheveningen, The Netherlands, 25-27 May.

Weaver, J., Parker, M., van Batenburg, D., and Nguyen, P. 2006. Sustaining Conductivity. Paper SPE 98236 presented at the SPE International Symposium on Formation Damage Control, Lafayette, LA., February.

Weaver, J., Parker, M., van Batenburg, D., and Nguyen, P. 2007. Fracture Related Diagenese May Impact Conductivity. SPEJ September: 272.

Weaver, J.D., Rickman, R., and Luo, H., 2008, Fracture Conductivity Loss Due to Geochemical Interactions. Paper SPE 118174 Presented at the Eastern Regional/AAPG Eastern Section Joint Meeting, Pittsburgh, Pennsylvania, 11-15 October.

Whitney, D.D. and Evans, R.D. 1989: The Influence of Temperature, effective stress and non-darcy flow on the fracture flow capacity of propped fractures. University of Oklahoma, USA.

Yasuhara, H., Elsworth, D., and Polak, A. 2003. A Mechanistic Model for Compaction of Granular Aggregates Moderated by Pressure Solution, Journal of Geophysical Research, Vol. 108, No. B11: 2530, November 18

Yasuhara, H., Polak, A., Mitani, Y., Grander, A.S., Halleck, P.M., Elsworth, D. 2006: Evolution of fracture permeability through fluid—rock reaction under hydrothermal conditions. Earth and Planetary Science Letters 244 (2006) 186-200